

DRIFT PERFORMANCE vs. OPERATING TEMPERATURE  
IN A LOW-COST STRAPDOWN GYROSCOPE

by

MIGUEL VICENTE GUERRERO

Captain, Argentine Air Force

Engineer in Electronics, School of Aeronautics

Engineering, Cordoba, ARGENTINA, 1972

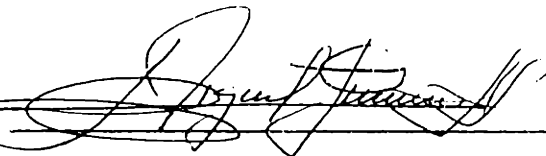
SUBMITTED IN PARTIAL FULFILLMENT OF  
THE REQUIREMENTS FOR THE DEGREE OF  
MASTER OF SCIENCE

at the

MASSACHUSETTS INSTITUTE OF TECHNOLOGY

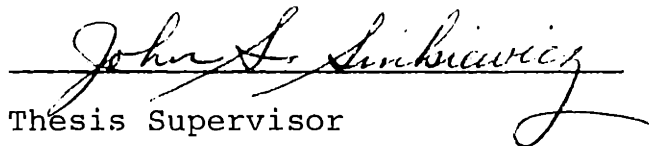
February 1977

Signature of Author



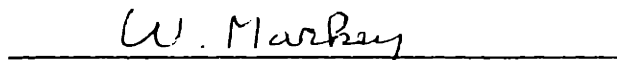
Department of Aeronautics and  
Astronautics, 1977

Certified by



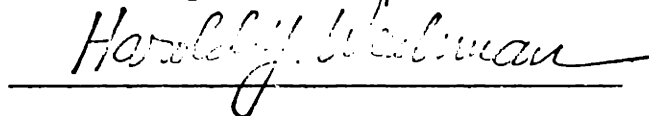
Thesis Supervisor

Certified by

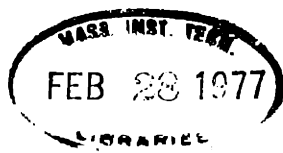


Thesis Supervisor

Accepted by



Chairman, Departmental Graduate  
Committee



DRIFT PERFORMANCE vs. OPERATING TEMPERATURE  
IN A LOW-COST STRAPDOWN GYROSCOPE

by

MIGUEL VICENTE GUERRERO

Submitted to the Department of Aeronautics and  
Astronautics in February 1977, in partial fulfillment  
of the requirements for the degree of Master of Science

ABSTRACT

An experimental investigation into the dependence  
of drift uncertainty coefficients on operating temperature,  
in a Hamilton Standard Mini RIG-30 single-degree-of-freedom,  
integrating gyroscope, is described and the results presented.

Thesis Supervisors:

John Sinkiewicz

Title: Lecturer, Department of Aeronautics and  
Astronautics.

Winston R. Markey, ScD.

Title: Professor of Aeronautics and Astronautics.

ACKNOWLEDGMENTS

I would like to express my sincerest appreciation to both Thesis Supervisors, Professor Winston R. Markey and Mr. John S. Sinkiewicz.

In addition to their collective service as Thesis Supervisors these two gentlemen each deserve special recognition.

Mr. Sinkiewicz, who as Lecturer in the Department of Aeronautics and Astronautics, personally took the responsibility for providing the technical knowledge and support for my research and also who ably guided me through an Internship training in the field of Test and Evaluation of inertial sensors. Indeed, without the technical contribution and constructive criticisms of Mr. Sinkiewicz, this work could not have been completed.

Professor Markey, who as Director of the Measurement Systems Laboratory, provided the environmental facility for this investigation and the gyroscope itself, and as advisor provided helpful suggestions and encouragement throughout the course of this work, and more importantly, he has served as my inspirational teacher during my years of study at M.I.T.

ACKNOWLEDGMENTS (continued)

Further, I would like to thank Hamilton Standard, who made the Mini RIG-30 available.

The opportunity and support to do this graduate work provided by the Argentine Air Force is deeply appreciated.

Last, but not least, I wish to express my deepest gratitude to my wife, Josefina, for her continuous encouragement and patience during the many long hours expended in this undertaking.

TABLE OF CONTENTS

	Page
CHAPTER I INTRODUCTION	12
1-1 Background	12
1-2 Objective	12
1-3 Organization	13
CHAPTER II INSTRUMENT DESCRIPTION	14
2-1 The Hamilton Standard Mini RIG-30 Subminiature Rate Integrating Gyroscope	14
CHAPTER III TEST FACILITY	22
3-1 Gyroscope Test Station	22
3-2 Gyroscope Alignment and Test Fixture	22
3-3 Two-axis Model D Type Turntable	28
3-4 Test Console	28
CHAPTER IV BACKGROUND THEORY	33
4-1 Definition	33
4-2 Hypothesis	33
4-3 Gyroscope Error Model Equation	34
CHAPTER V TEST RESULTS	36
5-1 Introduction	36
5-2 Multiple Revolution Servo-Turntable Tests	36
5-2-1 No Temperature Control	36
5-2-2 Temperature Controlled	41

TABLE OF CONTENTS (Cont.)

	Page
5-3 Multiple Revolution Tumbling Tests	45
5-3-1 No Temperature Control	45
5-3-2 Temperature Controlled	50
5-4 Tumbling Tests	54
CHAPTER VI CONCLUSIONS AND RECOMENDATIONS	60
6-1 Conclusions	60
6-2 Recomendations	61
APPENDIX I GYROSCOPE ERROR MODEL EQUATION	62
APPENDIX II GYROSCOPE TEST	70
REFERENCES	92

LIST OF ILLUSTRATIONS

Figure	Page
CHAPTER II	14
2-1-1 Mini RIG-30 Cutaway	15
2-1-2 Mini RIG-30 Outline Dimensions	16
2-1-3 Mini RIG-30 Schematic Diagram	17
CHAPTER III	22
3-1-1 Mini RIG-30 Gyroscope Test Station	23
3-1-2 Mini RIG-30 Gyroscope Test Station Layout	24
3-1-3 Mini RIG-30 Gyroscope Test Station Block Diagram	25
3-1-4 Mini RIG-30 Gyroscope Servo Control Loop	26
3-2-1 Mini RIG-30 Installed in the Alignment and Orientation Fixtures	27
3-2-2 Mini RIG-30 and Table Top Interfaces	29
3-3-1 Two-axis Model D Type Turntable	30
3-4-1 Test Console	32
CHAPTER V	36
5-2-1 Mini RIG-30 Overall Drift Performance IA Vertical Down, Without Temperature Control	39
5-2-2 Mini RIG-30 Drift Performance, IA Vertical Down, Without Temperature Control, Four Harmonics Removed	40

LIST OF ILLUSTRATIONS (Cont.)

Figure		Page
5-2-3	Mini RIG-30 Overall Drift Performance IA Vertical Down ,With Temperature Control	43
5-2-4	Mini RIG-30 Drift Performance IA Vertical Down,With Temperature Control, Four Harmonics Removed	44
5-3-1	Mini RIG-30 Overall Drift Coefficient Parameter Performance,IA Horizontal North,Without Temperature Control	48
5-3-2	Mini RIG-30 Drift Coefficient Parameter Performance,IA Horizontal North, Temperature Control,Four Harmonics Removed	49
5-3-3	Mini RIG-30 Overall Drift Coefficient Parameter Performance,IA Horizontal North,With Temperature Control	52
5-3-4	Mini RIG-30 Drift Coefficient Parameter Performance,IA Horizontal North, Temperature Control,Four Harmonics Removed	53
5-4-1	Mini RIG-30 BD vs. Temperature	56
5-4-2	Mini RIG-30 ADIA vs. Temperature	57
5-4-3	Mini RIG-30 ADSRA vs. Temperature	58
5-4-4	Mini RIG-30 ADOA vs. Temperature	59
APPENDIX I		62
I-1-1	Vector Representation of the Gyroscope	62
I-1-2	Right-Hand-Rule for the Gyroscope	63



LIST OF ILLUSTRATIONS (Cont.)

Figure		Page
APPENDIX II		70
II-2-1-a	Calibration FC-77 FEN WALL SN-58	
	Sensor Current 1.0 mA	71
II-2-1-b	Calibration FC-77 FEN WALL SN-58	
	Sensor Current 2.0 mA	72
II-2-1-c	Calibration FC-77 FEN WALL SN-58	
	Sensor Current 4.0 mA	73
II-3-1	Mini RIG-30 Servo Loop Block	
	Diagram	78
II-3-2	Gyroscope Orientation IA Vertical Down	81
II-3-3	Gyroscope Orientation IA Horizontal North	
	$\phi=0$ deg	83
II-3-4	Gyroscope Orientation IA Horizontal North	
	$\phi=180$ deg	84
II-3-5	Gyroscope Orientation IA Horizontal North	
	$\phi=90$ deg	85
II-3-6	Gyroscope Orientation IA Horizontal North	
	$\phi=270$ deg	86

LIST OF TABLES

Table	Page
CHAPTER II	14
2-1-I Hamilton Standard Mini RIG-30,Nominal Mechanical and Dynamic Characteristics	18
2-1-II Hamilton Standard Mini RIG-30,Nominal Performance Characteristics	20
CHAPTER V	36
5-2-I Mini RIG-30 Multiple Revolution Servo Turn-Table Test,IA Vertical Down,No Temperature Control for 72 hours	38
5-2-II Mini RIG-30 Multiple Revolution Servo Turn-Table Test,IA Vertical Down, No Temperature Control for 42 hours, Temperature Control for 30 hours	42
5-3-I Mini RIG-30 Multiple Revolution Turn-Table Test,IA Horizontal North,No Temperature Control	47
5-3-II Mini RIG-30 Multiple Revolution Turn-Table Test,IA Horizontal North,With Temperature Control	51

LIST OF TABLES (Cont.)

Table	Page
5-4-I Mini RIG-30 Drift Performance vs. Temperature	55
APPENDIX II	70
II-2-I Mini RIG-30 DC Resistance and Continuity Check	75

CHAPTER I

INTRODUCTION

1-1 Background

Manufacturers of low-cost gyroscopes, typically state in their specifications that certain single-degree-of-freedom, floated instruments can operate over a wide temperature range and maintain a particular level of performance. One such statement can be exemplified by Hamilton Standard's published specifications on a Mini RIG-30 subminiature gyroscope "The most salient feature of the Mini RIG-30 is its ability to operate over an extended temperature range without the use of heaters".

1-2 Objective

The objective of this thesis is to identify the particular level of performance and dependence of gravity insensitive and mass unbalance terms as a function of instrument operating temperature.

This test and evaluation of the drift coefficient dependence upon operating temperature in low-cost, strapdown gyroscopes is considered useful in applications where the system environmental temperature varies over a wide temperature range.

If mass unbalance shifts, float time constant changes, and other operating temperature dependent parameters could be minimized without the use of temperature control, then system cost would also tend to be minimized.

1-3 Organization

A description of the instrument and the test facility precede the discussion of the test results.

The results and conclusions are based upon a sequence of tests performed on one instrument ,they do not attempt to categorize all low-cost,strapdown instruments or the Mini RIG-30 family.

(\*)

(\*)

(For the reader who is not familiar with the test and evaluation of gyroscopic instruments,Appendix I shows the development of the gyroscope error model equation and Appendix II describes how the test and evaluation was performed).

CHAPTER II

INSTRUMENT DESCRIPTION

2-1 The Hamilton Standard Mini RIG-30 Subminiature Rate Integrating Gyroscope

The Hamilton Standard Mini RIG-30 is a floated, single-degree-of-freedom, strapdown instrument. A cutaway view of the Mini RIG-30 gyroscope is shown in Fig. 2-1-1. Fig. 2-1-2 shows the outline dimensions, Fig 2-1-3 shows its schematic diagram, and Tables 2-1-I and 2-1-II list a number of its operational and performance parameters as quoted by Hamilton Standard (Publishing of this performance data does not infer author verification except as indicated in the text).

The ball-bearing wheel rotates at 24,000 rpm, developing an angular momentum of 30,000 gm-cm<sup>2</sup>/s.

A four-pole, 800 Hz, two-phase synchronous motor drives the wheel. The wheel and motor structure are mounted in an hermetically-sealed, cylindrical float surrounded by high density fluid.

The float assembly which is neutrally bouyant at operating temperature is centered in the housing by a low friction, low radial clearance suspension.

The signal generator (SG) consists of a differential transformer that is excited with 10 V (rms) at 4800 Hz.

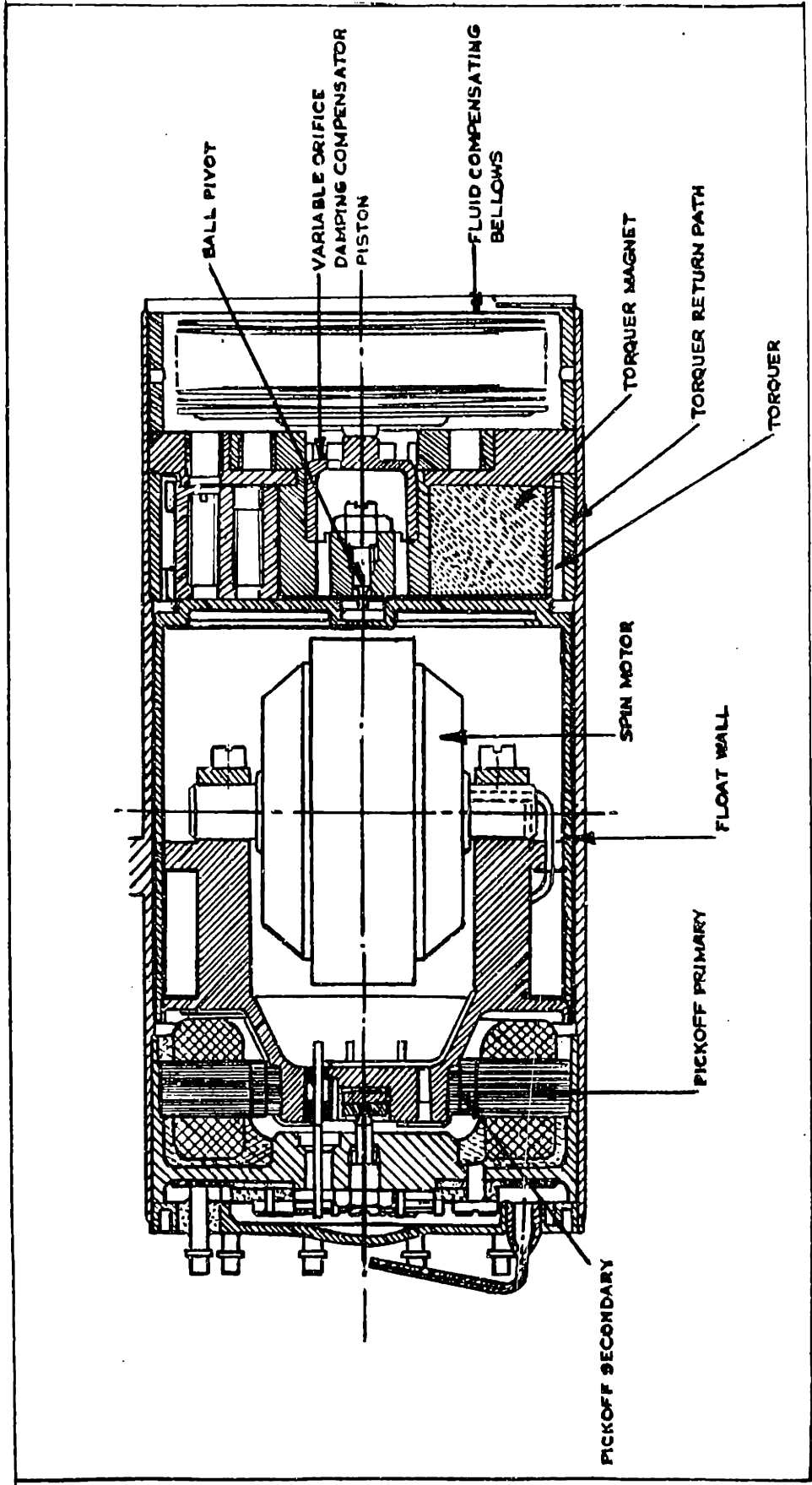


Fig. 2-1-1 Mini RIG-30 Cutaway

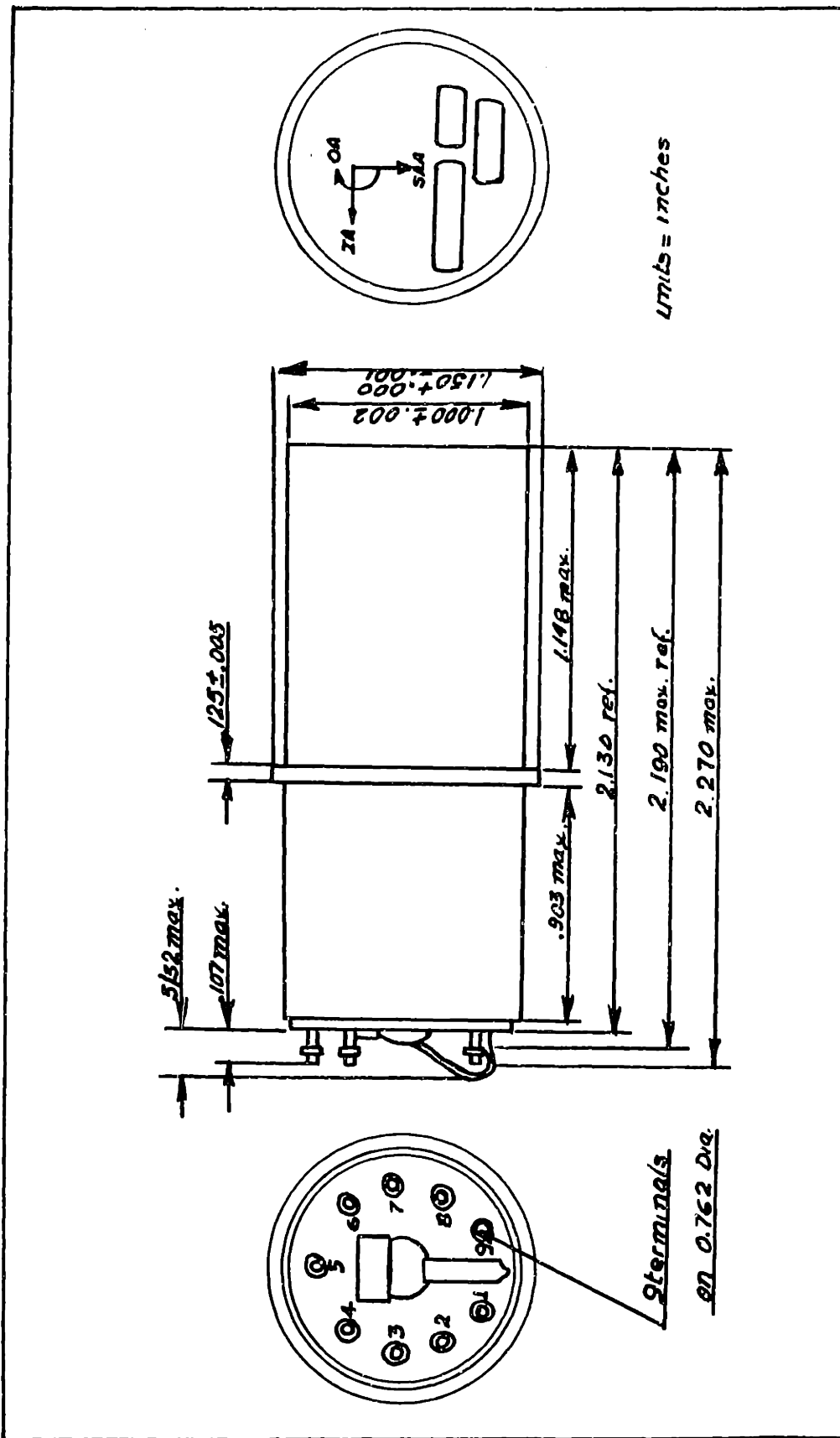


Fig. 2-1-2 Mini RIG-30 Outline Dimensions



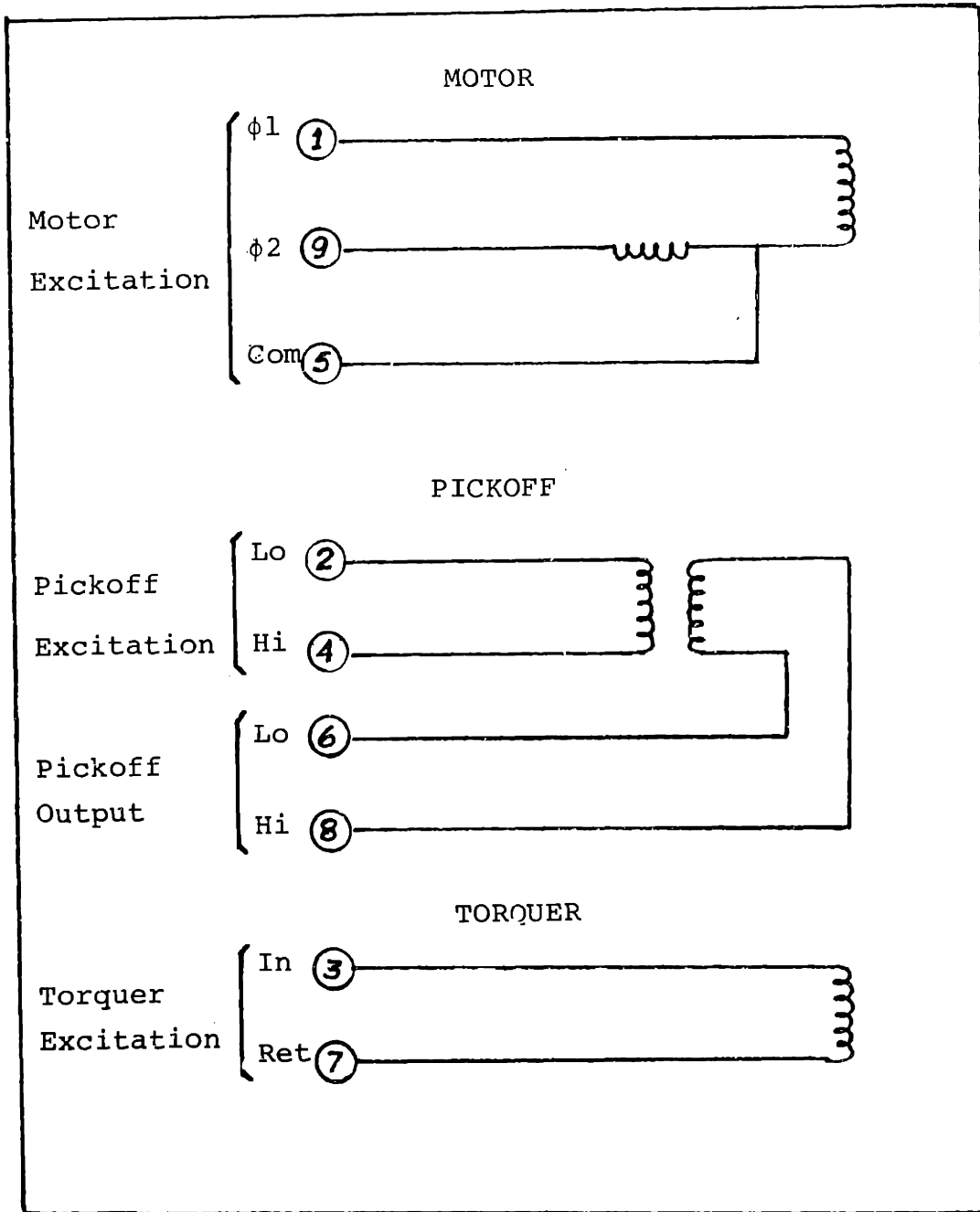


Fig.2-1-3 Mini RIG-30 Schematic Diagram

Table 2-1-I  
Hamilton Standard Mini RIG-30, Nominal Mechanical and  
Dynamic Characteristics \*\*\*

Parameter	Mini RIG-30
Angular Momentum (H)	30,000 gm-cm <sup>2</sup> /s
Gimbal Inertia (J)	24 gm-cm <sup>2</sup>
Damping Coefficient (C)	15,000 dyne-cm-s (*)
Characteristic Time	1.6 ms (*)
Gyro Gain (H/C)	2.0 (*)
Input Angle	1.5 deg (*)
Pickoff	
-Frequency	4800 Hz
-Voltage	10 V (rms)
-Current	15 mA
-Scale Factor	20 mV/mR
-Load	10 Kohms
-Phase Shift	0 ± 5 deg
-Null	5 mV (rms max.)
Spin Motor	
-Frequency	800 Hz
-Voltage	26 V (rms)
-Power	3 W running (max.) 5 W starting (max.)
-Activation Time	30 s (**)

\*\*\* As published by Hamilton Standard

\*\* Shorter with overvoltage

\* ± 20 % Through 180 °F temperature range about  
specified set point

Table 2-1-I ( Cont. )

Parameter	Mini RIG-30
Torquer	
-Resistance DC	350 Ohms
-Scale Factor	0.8 deg/s/mA (max.)
-Maximum Rate	70 continuous deg/s
	140 intermittent deg/s
Temperature Operating	0 to 180 °F
Altitude	Unlimited
Weight	4.5 ounces (max.)

\*\*\* As published by Hamilton Standard

Table 2-1-II

Hamilton Standard Mini RIG-30, Nominal Performance

Characteristics \*\*\*

Parameter	Mini RIG-30
Drift Performance	
-G-sensitive Drift	10 deg/h/g
-Non G-sensitive Drift	10 deg/h
-Anisoelastic	0.3 deg/h/g <sup>2</sup>
Enviromental Capability	
-Acceleration	250 g's
-Vibration-Sinusoidal	25 g's from 20 to 2500 Hz
-Vibration-Random	0.2 g/Hz 20 to 2500 Hz
-Shock	300 g's -5 ms (Half-sinepulse) 150 g's - 11 ms (Half-sinepulse)

\*\*\* As published by Hamilton Standard

Its output is proportional in magnitude and phase to the angular position of the float about the output axis.

The Mini RIG-30 uses a moving coil D'Arsonval type permanent magnet torquer which incorporates high energy alloy to provide maximum torque capability at minimum power levels and is fully stabilized to insure minimum variations of torquer scale factor with temperature or external magnetic fields.

The most salient feature of the Mini RIG-30 is its ability to operate over an extended temperature range without the use of heaters.

CHAPTER III

TEST FACILITY

3-1 Gyroscope Test Station

The test facility consists of a gyroscope alignment and test fixture, a two-axis Model D type turntable and an electronic support console (Figs. 3-1-1, 3-1-2 and 3-1-3).

Fig. 3-1-4 shows a conceptual block diagram of the gyroscope as connected in an inertial reference servo control loop.

3-2 Gyroscope Alignment and Test Fixture

The gyroscope fixture is the interface between the gyroscope, the turntable and the rest of the test station.

The fixture used consists of a two main parts:

- a) A three sided orientation fixture, which allows rotation of the instrument about three orthogonal axes.
- b) An alignment fixture, which is mounted on the orientation fixture that houses the gyroscope. This fixture is supported by three adjustable screws which provide alignment capability of the instrument's input axis about both the output and spin reference axis.

Both fixtures are made of type 256 aluminum casting which is stress-relieved for long-term stability

Fig. 3-2-1 shows the instrument installed in the alignment and orientation fixtures.

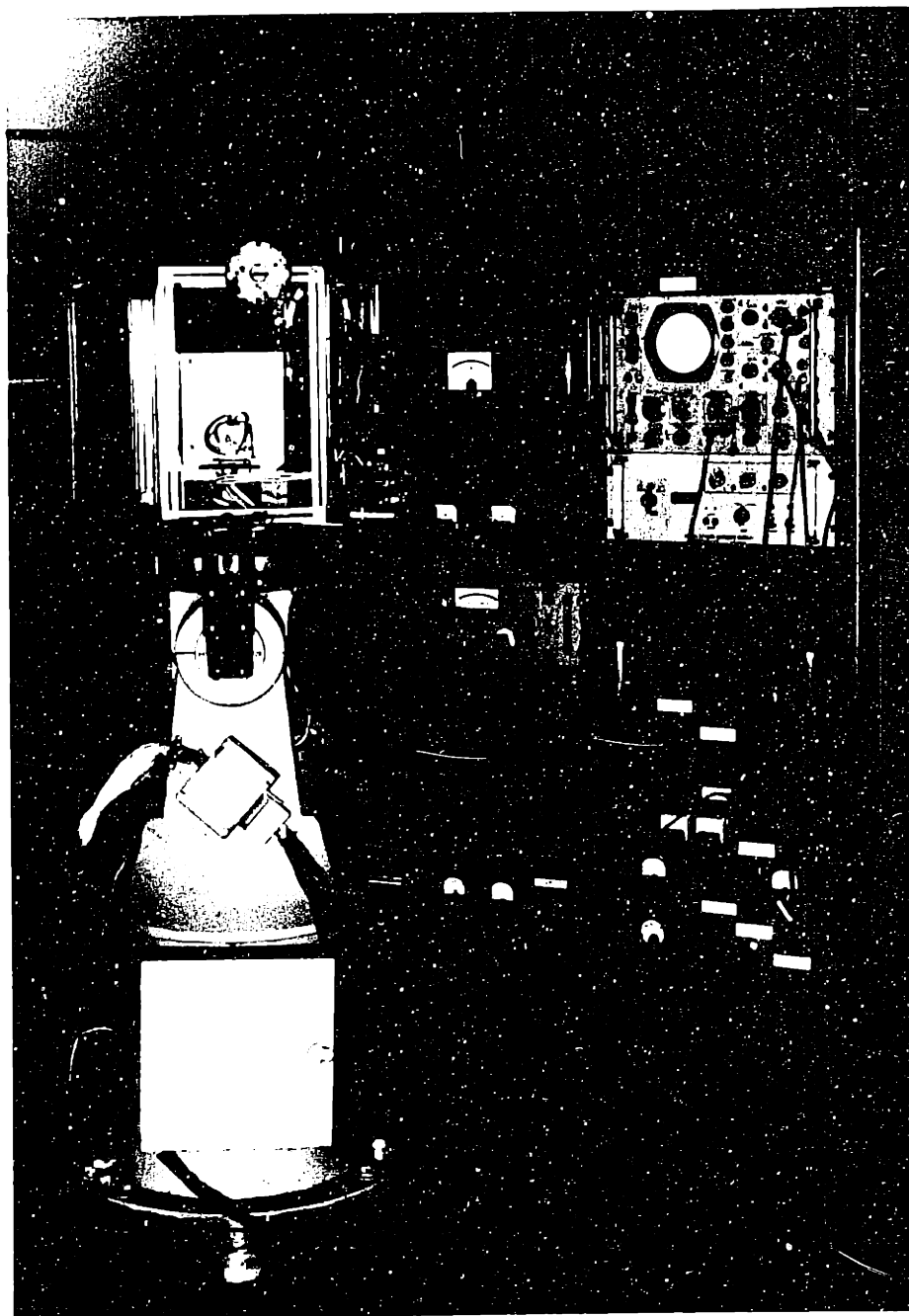


Fig.3-1-1 Mini RIG-30 Gyroscope Test Station

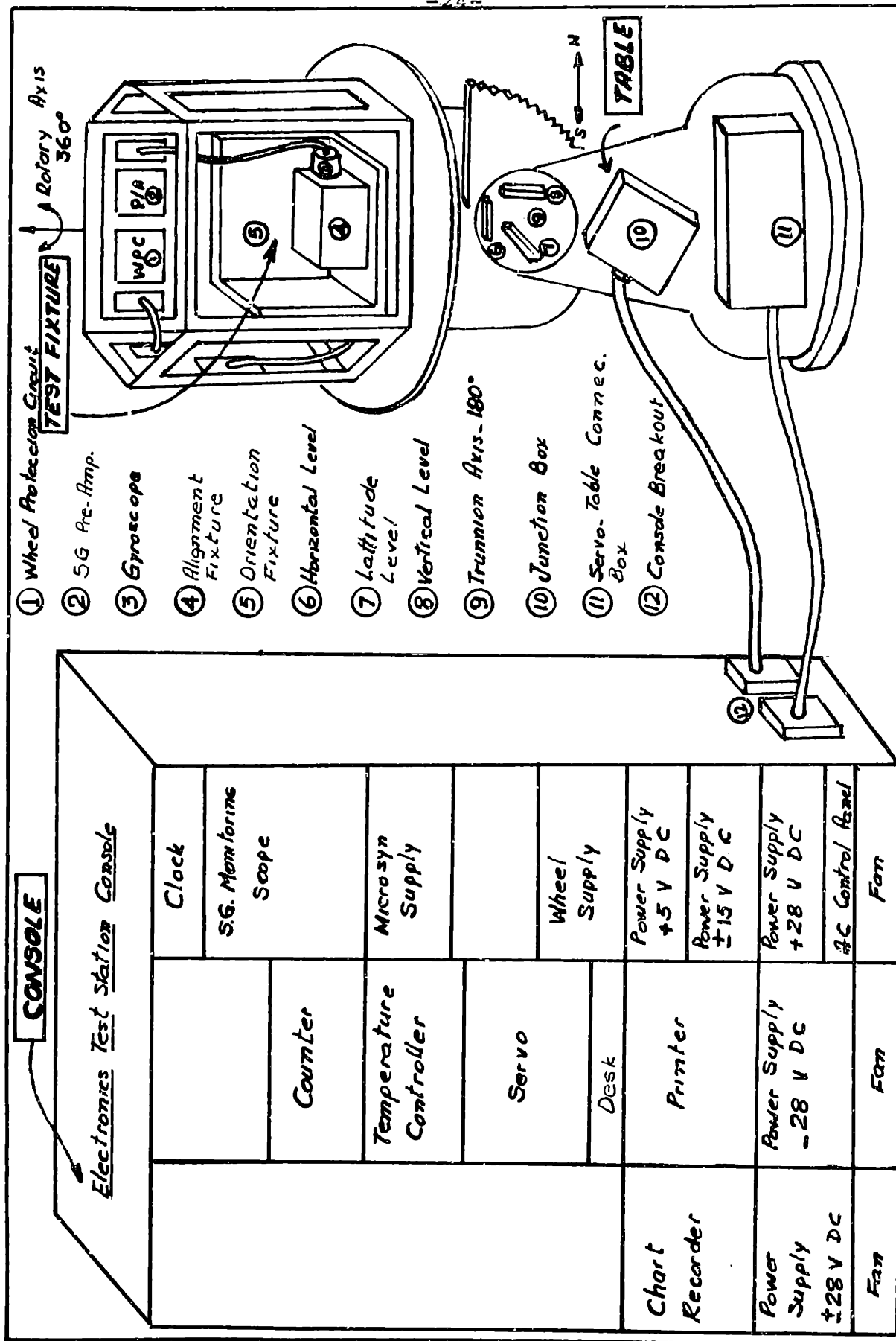


Fig. 3-1-2 Mini RIG-30 Gyroscope Test Station Layout



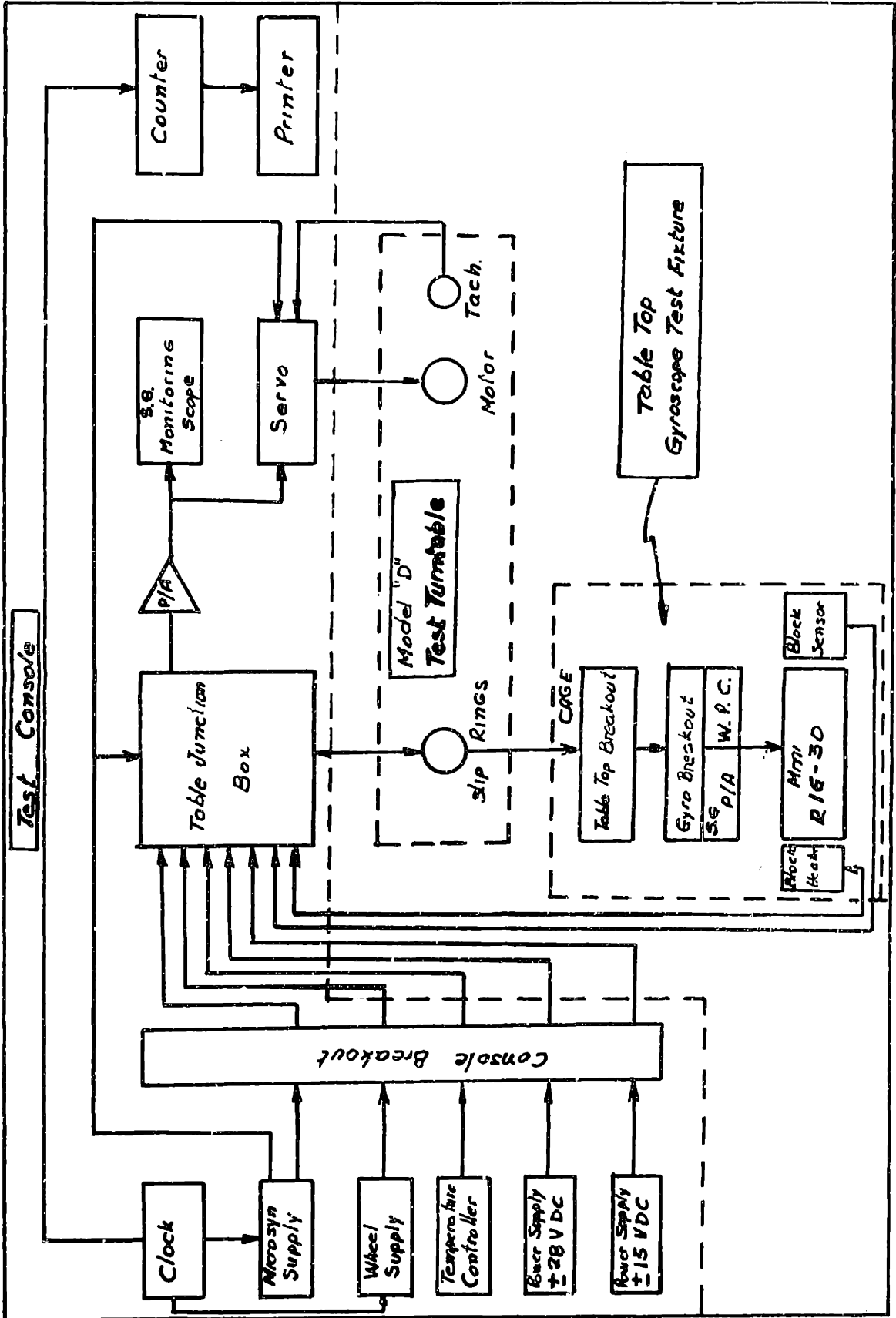


Fig. 3-1-3 Mini RIG-30 Gyroscope Test Station Block Diagram

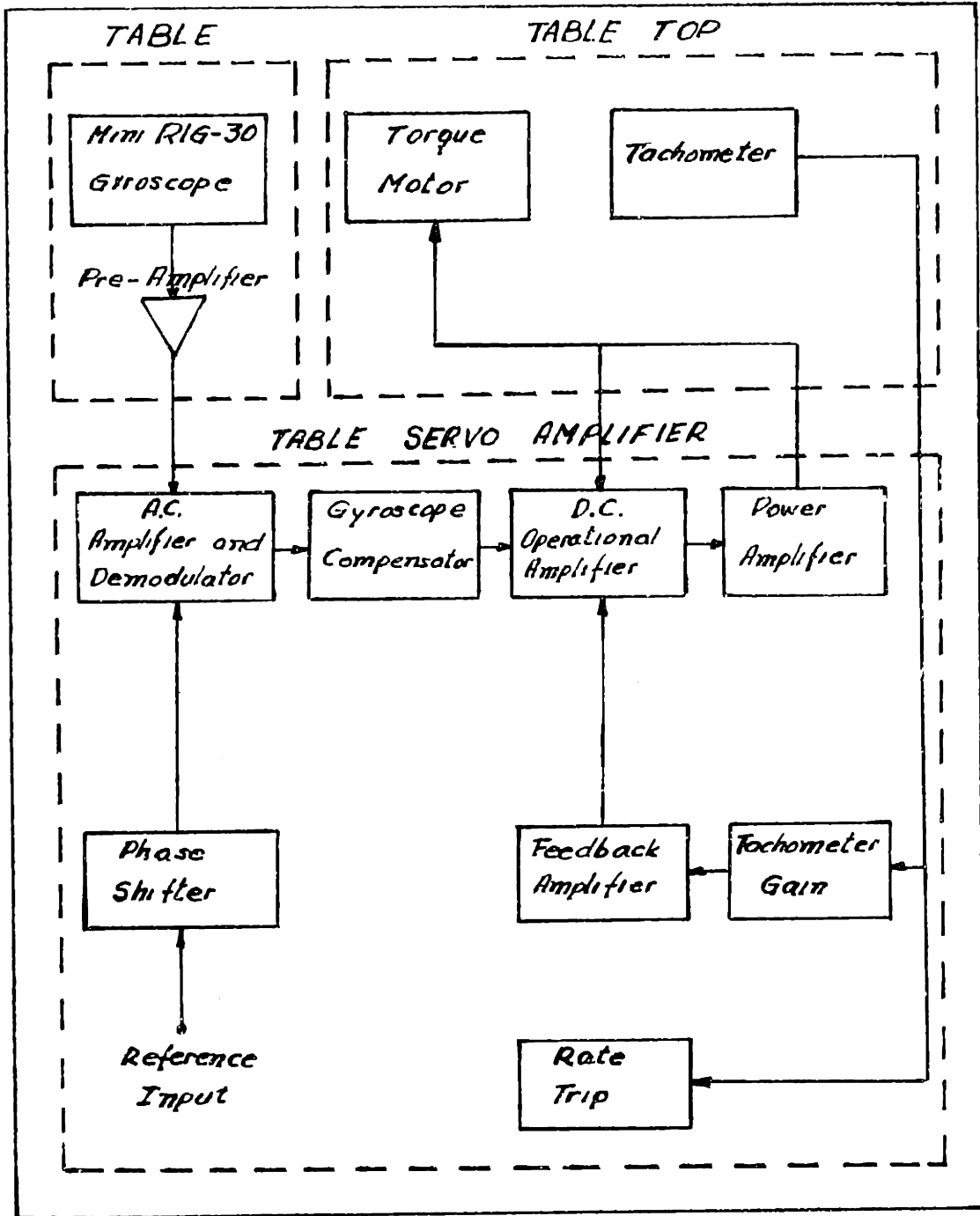


Fig.3-1-4 Mini RIG-30 Gyroscope Servo Control Loop

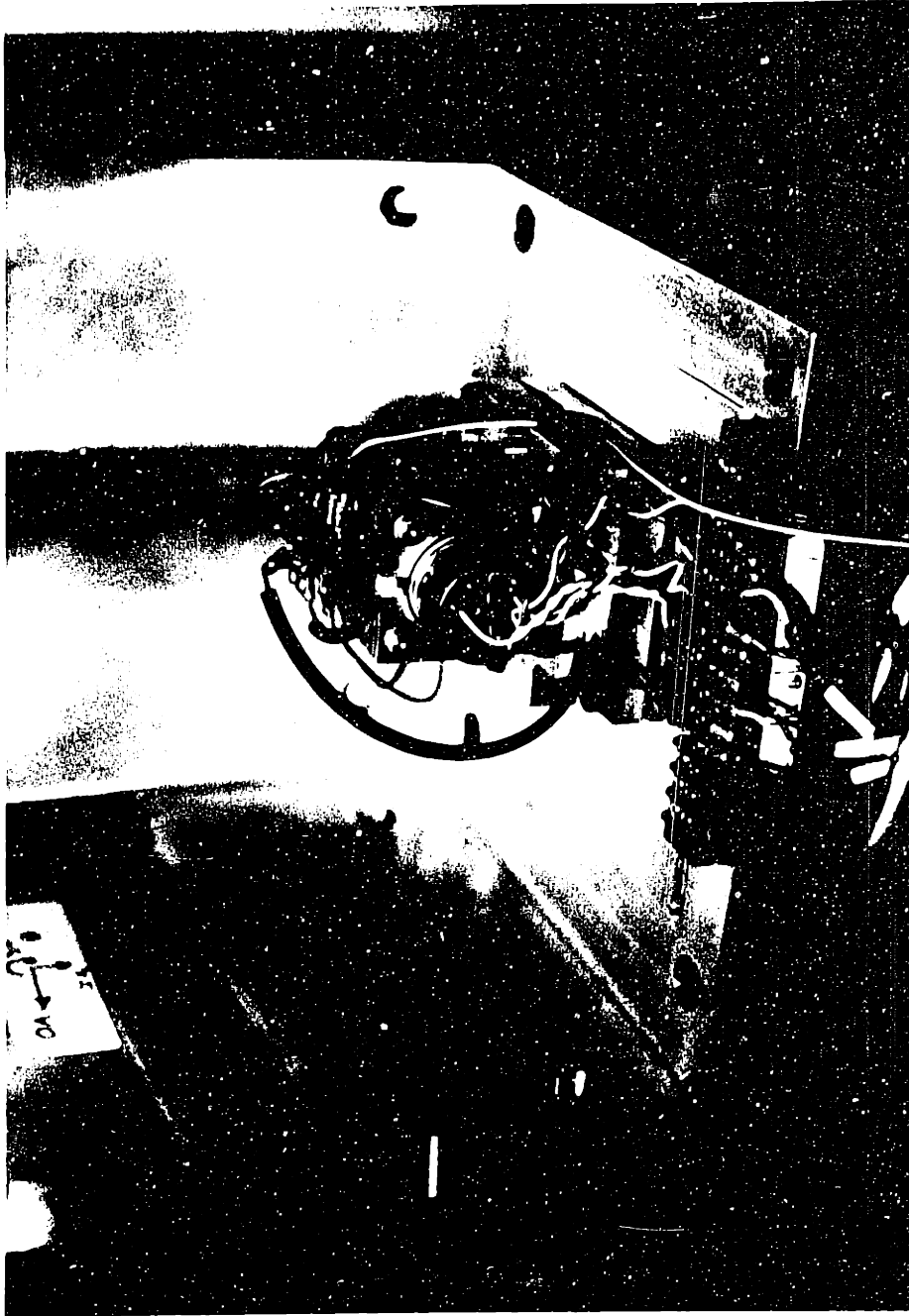


Fig. 3-2-1 Mini RIG-30 Installed in the Alignment and Orientation Fixture

Fig.3-2-2 shows all of the interfaces between the gyroscope and the table top (ie, mechanical, electrical and thermal).

### 3-3 Two-axis Model D Type Turntable

The Model D table (Fig.3-3-1) uses precision tapered roller bearings to support the table rotary axis, and an electro-optical (photo-cell) pickoff system for measuring table rotational angle.

The optical system is comprised of a scanning device that generates a pulse each time the ruled lines of a precision circular scale pass over a light source at an index point. The etched lines are spaced at one degree intervals so that 360 pulses are generated per revolution of the table rotary axis.

The elapsed time required for predetermined angular increments of table rotation is determined by counting the output of a highly precision clock. By use of a counter or computer the angular velocity of the table can be measured when counting clock pulses per table angle pulses.

The table is driven by a DC torque motor.

### 3-4 Test Console

The basic functions of the test console are:

- a) Excitation
- b) Control
- c) Monitoring

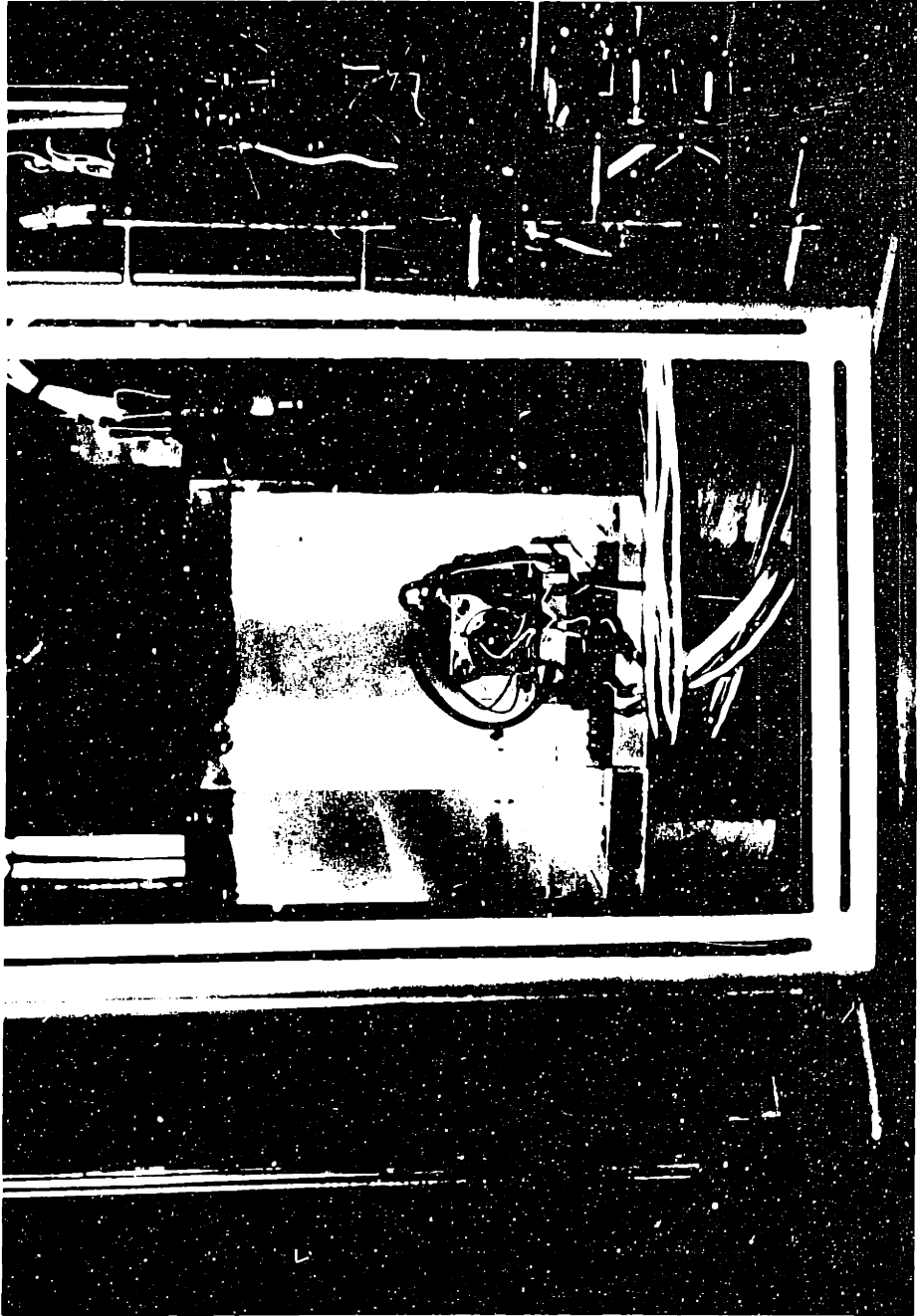


Fig. 3-2-2 Mini RIG-30 and Table Top Interfaces

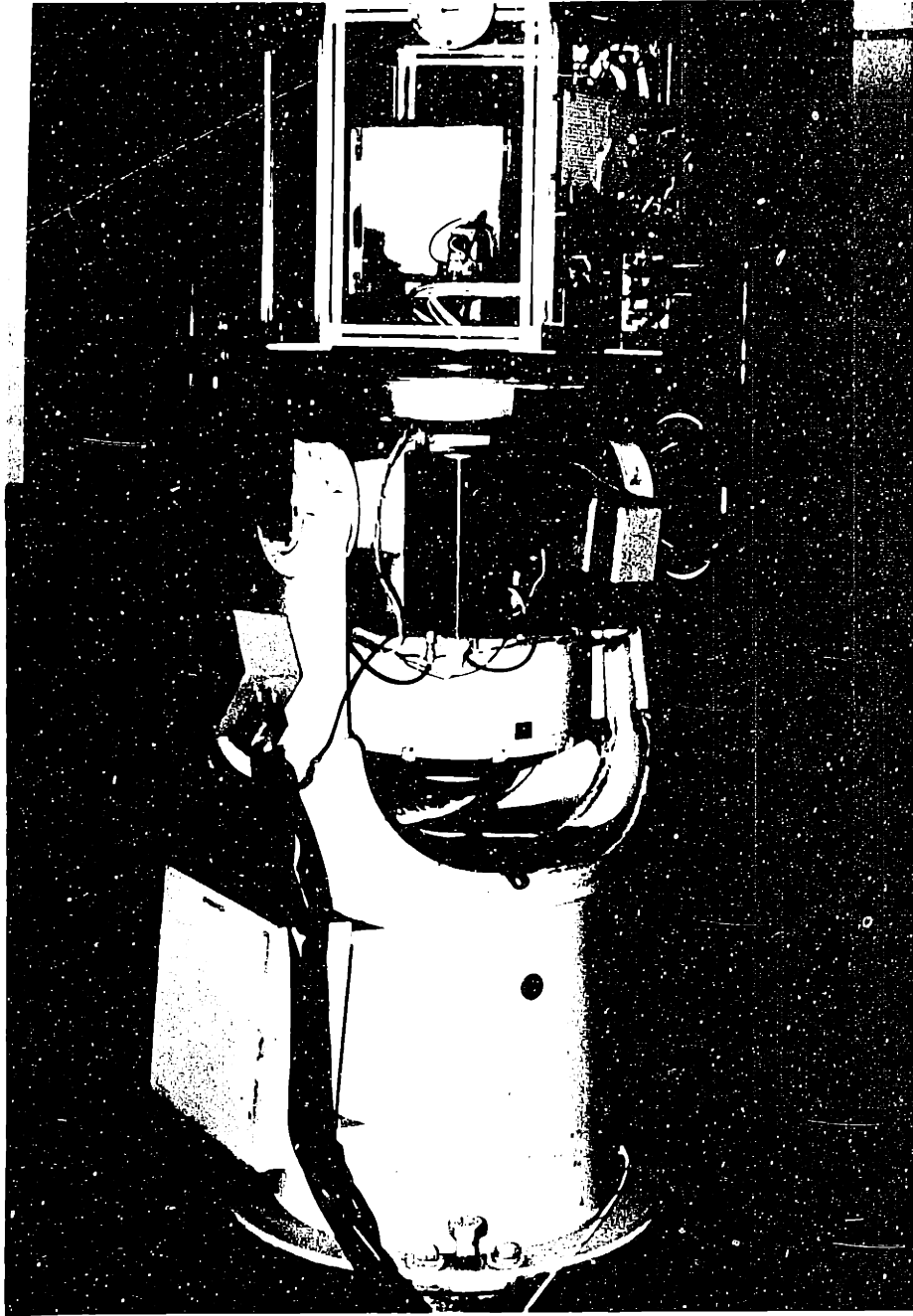


Fig.3-3-1 Two-axis Model D Type Turntable

The first a) includes electrical excitation of the gyroscope wheel, signal generator, temperature controller logic, etc.

The second b) includes the rate-feedback and servo control loops.

The third c) includes the data acquisition and monitoring of the signal-generator output and other gyroscope parameters.

Fig. 3-4-1 shows the actual console as used in the test.

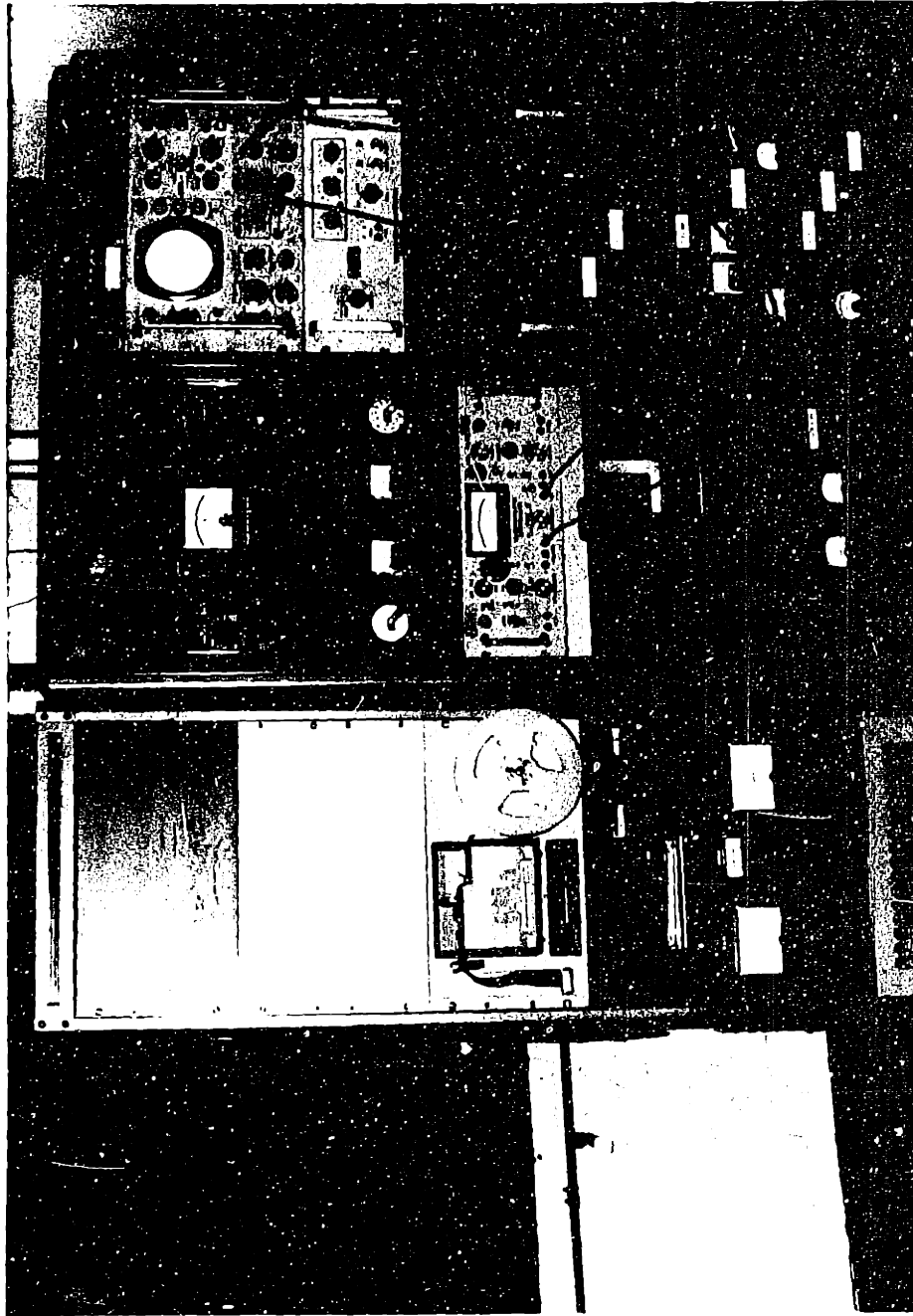


Fig.3-4-1 Test Console



CHAPTER IV

BACKGROUND THEORY

4-1 Definition

The steady-state error model equation of a single degree-of-freedom, floated, integrating gyroscope is assumed to have the form:

$$(1) \text{ Drift} = \pm \Sigma \text{ Nonacceleration sensitive drifts} \\ \pm \Sigma \text{ Acceleration sensitive drifts} \\ \pm \Sigma \text{ Acceleration squared sensitive drifts}$$

(all other terms are assumed to be negligible).

4-2 Hypothesis

Since it is not possible to perfectly match the thermal coefficients of expansion of all the materials in the construction of gyroscopic instruments it is hypothesized that changes in the various physical relationships between the piece parts would result, when a change in the operating temperature occurred. Namely, mass shifts would result from differential expansion between unmatched parts during unit operating temperature changes.

These mass shifts would result in drift coefficient instabilities as a function of unit temperature.

Even if the differential expansions were minimized, as in the design of the Mini RIG-30, to avoid mechanical shifting between parts, some drift performance instabilities would result from instrument temperature changes.

These particular drift instabilities vs. operating temperatures, for the Mini RIG-30, are summarized in the results.

It is further hypothesized that acceleration squared or compliance terms change insignificantly with operating temperature and thereby are also neglected resulting in an error model equation of:

$$(2) \text{ Drift} = \pm BD \pm \sum \epsilon g$$

where:

$$(3) \text{ BD} = \text{gravity insensitive bias drift (deg/h)}$$

$$(4) \epsilon g = \text{gravity sensitive drift (deg/h/g)}$$

#### 4-3 Gyroscope Error Model Equation

Rewriting the gyroscope error model equation:

$$(5) \text{ Drift} = \pm BD \pm ADIA \pm ADSRA \pm ADOA$$

where:

ADIA= acceleration sensitive drift along IA  
(deg/h/g)

ADSRA= acceleration sensitive drift along SRA  
(deg/h/g)

ADOA= acceleration sensitive drift along OA  
(deg/h/g)

Considering operating temperature dependence

$$(6) \text{ Drift} = \pm BD(1 + \Delta T_b) \pm ADIA(1 + \Delta T_I) \pm ADSRA(1 + \Delta T_S) \\ \pm ADOA(1 + \Delta T_O)$$

where:

$\Delta T_b$  = gyroscope drift sensitivity to a temperature change (deg/h/g/°F)

$\Delta T_I$  ,  $\Delta T_S$  ,  $\Delta T_O$  = gyroscope sensitivity to a temperature change along IA ,SRA and OA respectively (deg/h/g/°F)

CHAPTER V

TEST RESULTS

5-1 Introduction

The performance tests on a Hamilton Standard Mini RIG-30 single-degree-of-freedom, floated gyroscope are described in this section. The measurements include:

- a) Multiple Revolution Servo-Turntable Tests  
(IA vertical, inertial reference mode)
  - 1- No temperature control
  - 2- Temperature controlled
- b) Multiple Revolution Tumbling Tests  
(IA horizontal)
  - 1- No temperature control
  - 2- Temperature controlled
- c) Tumbling Tests  
(IA vertical, IA horizontal cardinal positions)
  - 1- Temperature controlled in the range of 100 to 160 °F in 10 °F intervals

5-2 Multiple Revolution Servo-Turntable Tests

5-2-1 No Temperature Control

a) This test measured the instrument's drift performance without instrument temperature control, the room temperature was held at  $72^{\circ}\text{F} \pm 2^{\circ}\text{F}$  and the unit was enclosed by a plexi-glass cover.

The average or constant drift for the unit in continuous operation (table direction ccw) for 72 hours was:

$$|\text{Drift}|_{\text{ave}} = | -BD + ADIA |_{\text{ave}} = +24.3 \text{ deg/h} \approx 1621.1 \text{ meru}$$

where:

$$1 \text{ meru} \approx 0.015 \text{ deg/h}$$

(see Table 5-2-I)

b) The test showed a misalignment of IA to the table rotary axis. (ie, The IA travelled in a cone about the table rotary axis for one revolution of the table)

The cosine and the sine terms indicate the magnitude of misalignment (see Table 5-2-I) the misalignment is equivalent to 0.7 deg of IA about OA and 1.5 deg of IA about SRA.

c) The point-to-point drift stability with the unit in continuous operation for 72 hours was approximately 0.6 deg/h.

d) For this test the gyroscope drift shows a single discontinuity of approximately 3 deg/h.

Fig.5-2-1 shows the overall drift performance (-BD+ADIA) of the Hamilton Standard Mini RIG-30 for IA vertical down without temperature control.

Fig.5-2-2 shows the drift performance with four harmonics removed. (ie, IA misalignment error, etc.)

Table 5-2-I

Mini RIG-30 Multiple Revolution Servo Turn-Table Test, IA  
 Vertical Down, No Temperature Control for 72 hours

R SERVO RUN, HS MINI-RIG 30, 180076  
 R IA VERT. DOWN, 1 DEGREE PRINTS, CLOCK=80CHZ.  
 R TABLE DIRECTION=CCW, NO TEMP CONTROL, TEMP=72 DEG F.  
 R FIRST PRINT=0 DEG., OA WEST @ 0 DEG.  
 R GYRO ON 15 MINS PRIOR TO FIRST PRINT.

	THREE PARAMETER BEST FIT	FIVE PARAMETER BEST FIT	SEVEN PARAMETER BEST FIT	NINE PARAMETER BEST FIT
CONSTANT (ERROR)	+1621.144 ( 1.164)	+1620.327 ( 1.133)	+1620.567 ( 1.105)	+1620.451 ( 1.099)
COS(X) (ERROR)	- 19.294 ( 1.620)	- 19.906 ( 1.578)	- 20.411 ( 1.540)	- 20.636 ( 1.534)
SIN(X) (ERROR)	- 36.831 ( 1.672)	- 36.968 ( 1.526)	- 37.071 ( 1.585)	- 37.118 ( 1.576)
COX(2 X) (ERROR)	+ 0.000 ( 0.000)	+ 10.543 ( 1.589)	+ 10.081 ( 1.551)	+ 9.875 ( 1.544)
SIN(2 X) (ERROR)	+ 0.000 ( 0.000)	- 0.569 ( 1.514)	- 0.765 ( 1.574)	- 0.855 ( 1.565)
COX(3 X) (ERROR)	+ 0.000 ( 0.000)	+ 0.000 ( 0.000)	+ 9.535 ( 1.561)	+ 9.359 ( 1.553)
SIN(3 X) (ERROR)	+ 0.000 ( 0.000)	+ 0.000 ( 0.000)	+ 2.039 ( 1.563)	+ 1.915 ( 1.555)
COX(4 X) (ERROR)	+ 0.000 ( 0.000)	+ 0.000 ( 0.000)	+ 0.000 ( 0.000)	+ 2.638 ( 1.557)
SIN(4 X) (ERROR)	+ 0.000 ( 0.000)	+ 0.000 ( 0.000)	+ 0.000 ( 0.000)	+ 2.758 ( 1.549)

CONSTANT	+1621.144	+1620.327	+1620.567	+1620.451
(ERROR)	( 1.164)	( 1.133)	( 1.105)	( 1.099)
COS(X)	- 19.294	- 19.906	- 20.411	- 20.636
(ERROR)	( 1.620)	( 1.578)	( 1.540)	( 1.534)
SIN(X)	- 36.831	- 36.968	- 37.071	- 37.118
(ERROR)	( 1.672)	( 1.526)	( 1.585)	( 1.576)
COX(2 X)	+ 0.000	+ 10.543	+ 10.081	+ 9.875
(ERROR)	( 0.000)	( 1.589)	( 1.551)	( 1.544)
SIN(2 X)	+ 0.000	- 0.569	- 0.765	- 0.855
(ERROR)	( 0.000)	( 1.514)	( 1.574)	( 1.565)
COX(3 X)	+ 0.000	+ 0.000	+ 9.535	+ 9.359
(ERROR)	( 0.000)	( 0.000)	( 1.561)	( 1.553)
SIN(3 X)	+ 0.000	+ 0.000	+ 2.039	+ 1.915
(ERROR)	( 0.000)	( 0.000)	( 1.563)	( 1.555)
COY(4 X)	+ 0.000	+ 0.000	+ 0.000	+ 3.638
(ERROR)	( 0.000)	( 0.000)	( 0.000)	( 1.557)
SIN(4 X)	+ 0.000	+ 0.000	+ 0.000	+ 2.758
(ERROR)	( 0.000)	( 0.000)	( 0.000)	( 1.549)

FIRST 0 POINTS IGNORED IN COEFFICIENT CALCULATION  
SERVO POSITION IS IA VERT DOWN

$$\text{CONSTANT } (-B^2 + ADIA + KSI(G))^2$$

$$\text{SIN(X) = SIN(A) } W \text{ , COS(X) = - (SIN(A) ) W}$$

SRA IEH                      OR IEH

RMS OF REVOLUTION DIFFERENCE  
RMS13 = 13.254    NO. OF PTS. = 29  
RMS23 = 198.403    NO. OF PTS. = 29  
RMS12 = 56.007    NO. OF PTS. = 360

RMS OF DEVIATION FROM BEST FIT  
THREE            FIVE            SEVEN            NINE            PTS  
31.841            30.945            30.163            29.980            749

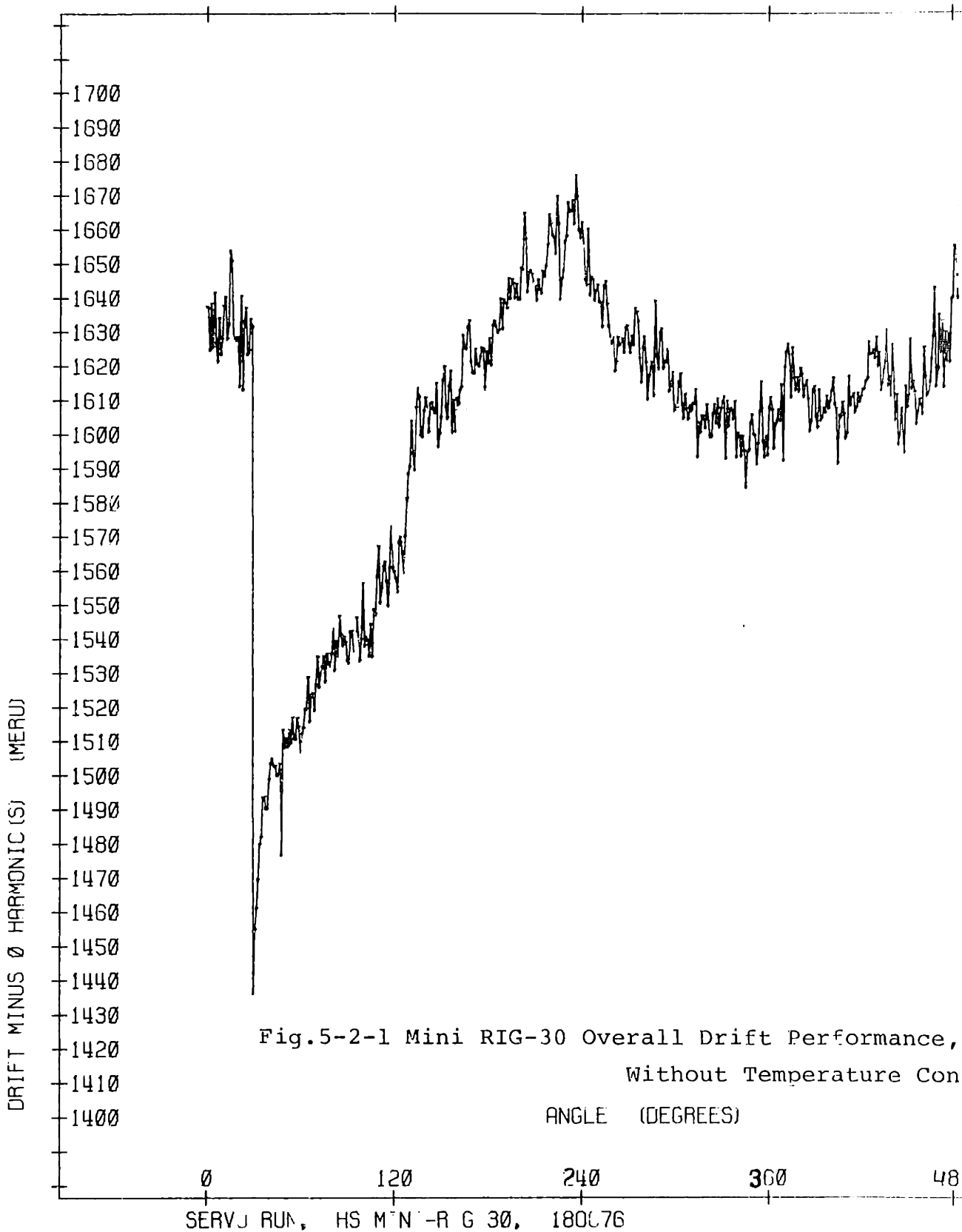
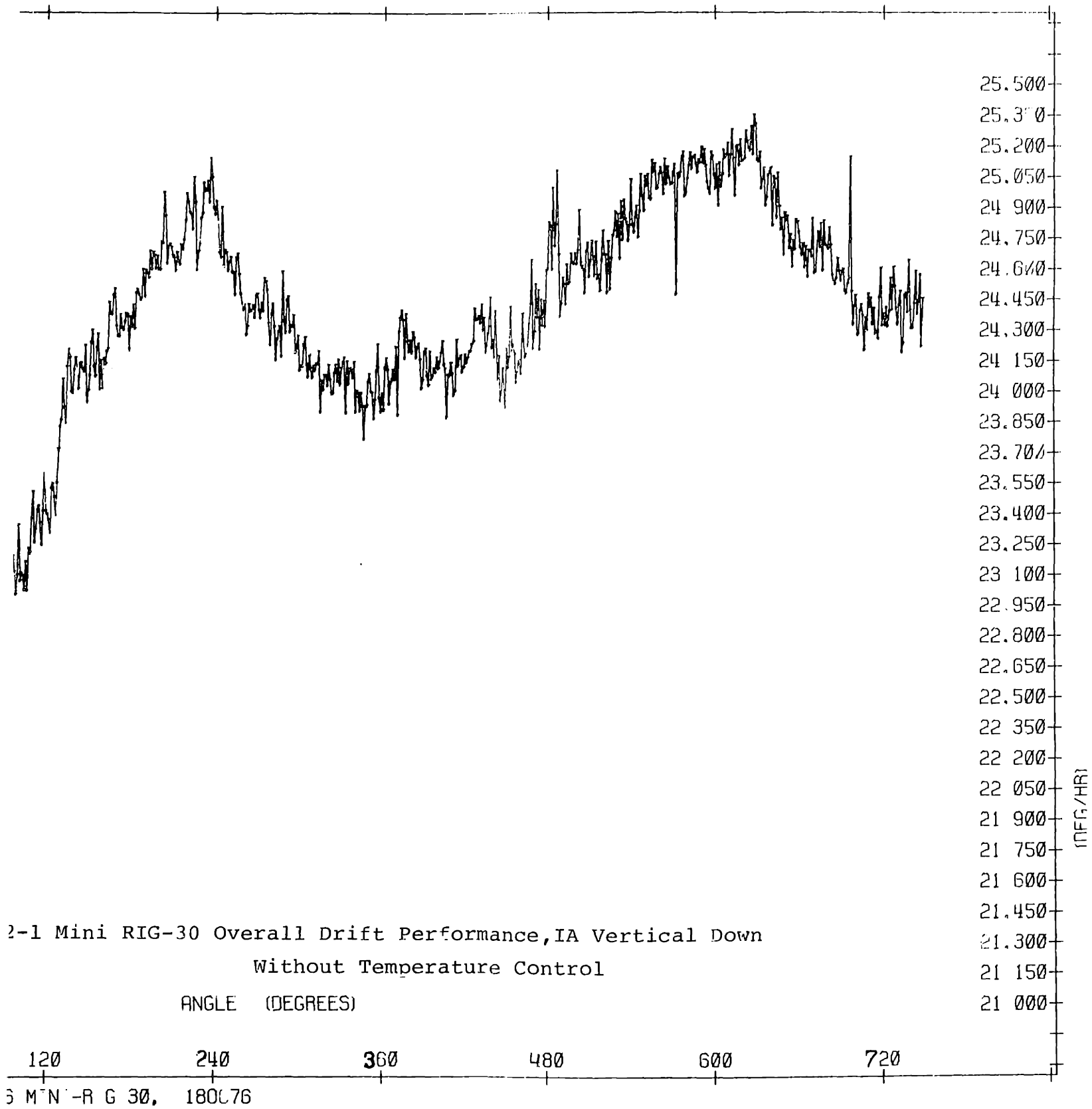


Fig.5-2-1 Mini RIG-30 Overall Drift Performance,  
Without Temperature Con





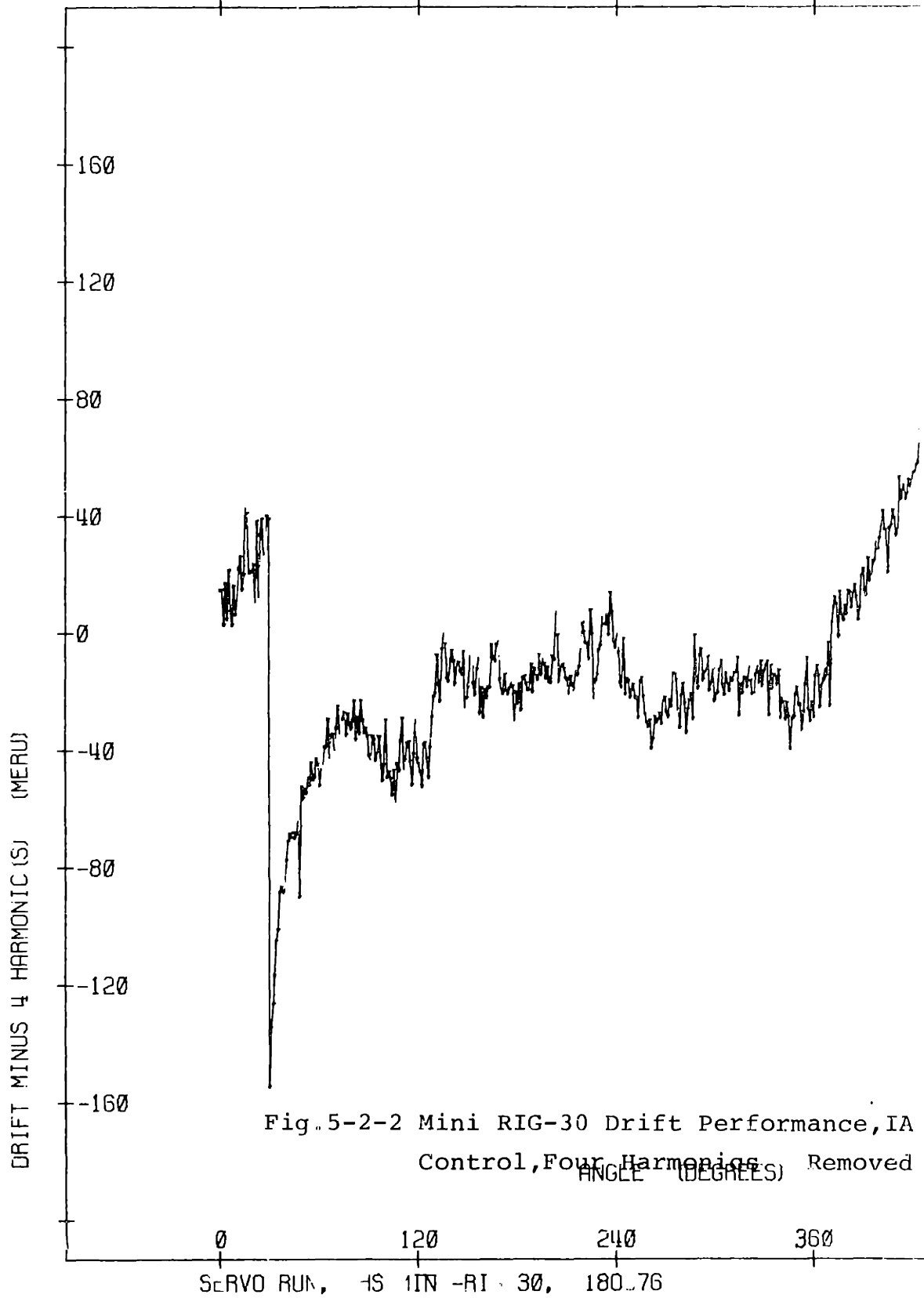
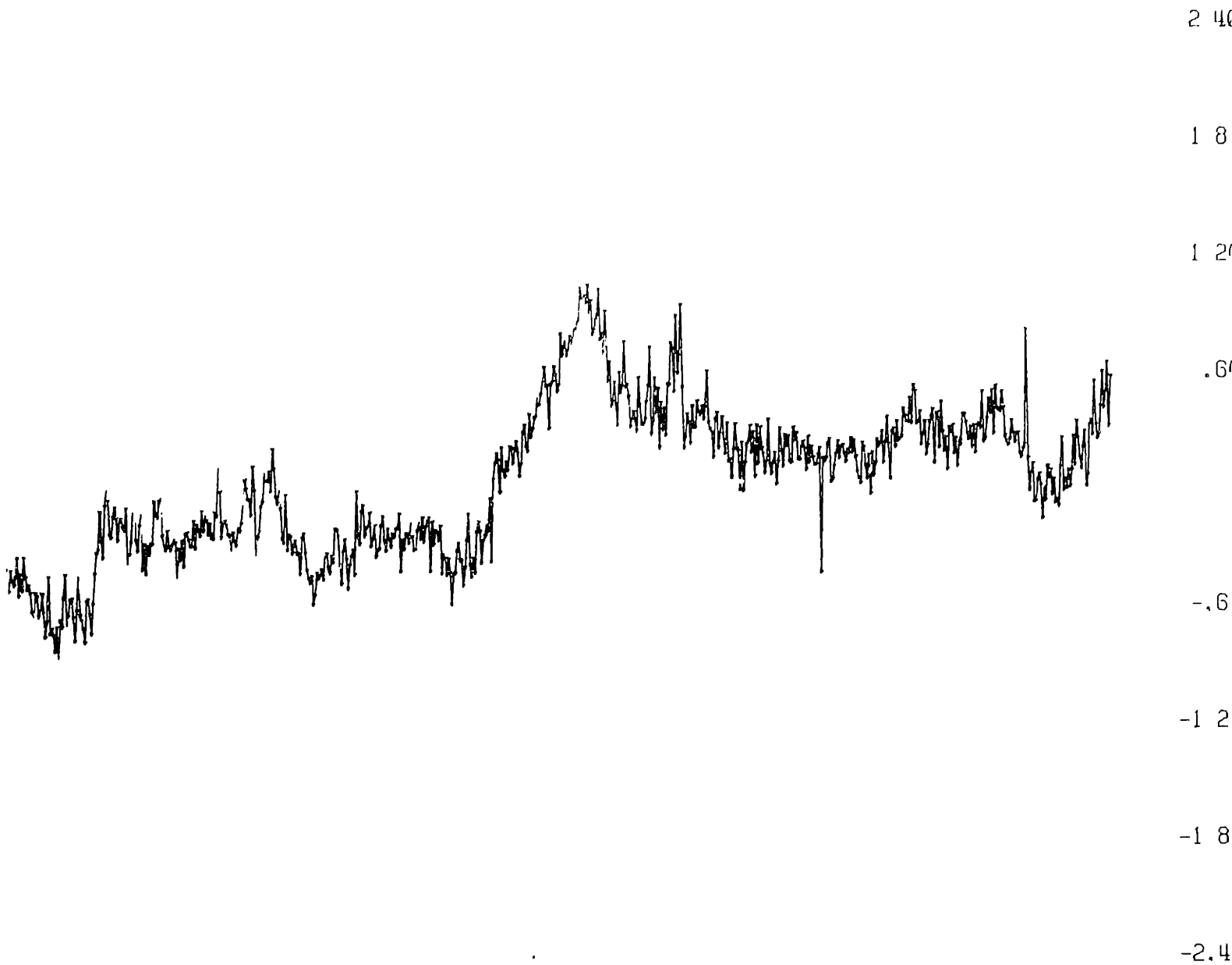


Fig. 5-2-2 Mini RIG-30 Drift Performance, IA Control, Four Harmonics Removed



-2-2 Mini RIG-30 Drift Performance, IA Vertical Down, Without Temperature Control, Four Harmonics Removed

ANGLE (DEGREES)

120 240 360 480 600 720  
-S 1IN -RI . 30, 180.76

5-2-2 Temperature Controlled

a) This test measured the instrument's drift performance with instrument temperature control. The room temperature was held at  $72^{\circ}\text{F} \pm 2^{\circ}\text{F}$  and the gyroscope was covered and initially run in this condition for 30 hours. The temperature controller was then connected and the instrument was temperature controlled at  $130^{\circ}\text{F} \pm 0.1^{\circ}\text{F}$  for 42 hours.

The average or constant drift, (Table 5-2-II) for the unit in continuous operation (table direction ccw) for 72 hours was:

$$|\text{Drift}|_{\text{ave}} = | -\text{BD} + \text{ADIA} |_{\text{ave}} = +26.4 \text{ deg/h} \approx 1760 \text{ meru}$$

b) Again the sine and cosine waves in the drift performance plot are a result of gyroscope misalignment with respect to the table rotary axis.

This IA misalignment shifted slightly (1.8deg) when the temperature of the unit and fixturing was changed, as expected.

c) The point-to-point drift stability with the unit in continuous operation for 72 hours was approximately 0.6 deg/h.

d) When the instrument operating temperature was changed ( $\Delta T \approx 60^{\circ}\text{F}$ ) it causes a  $\Delta | -\text{BD} + \text{ADIA} |_{\text{ave}}$  of approximately 3 deg/h

Fig.5-2-3 shows the drift performance (-BD+ADIA) of the gyroscope with temperature control and Fig.5-2-4 shows the same drift performance with four harmonics removed.

Table 5-2-II

PSS

Mini RIG-30 Multiple Revolution Servo Turn-Table Test, IA Vertical Down

No Temperature Control for 42 hours, Temperature Control for 30 hours

SERVO RUN, HS MINI-RIG 30, 220C76  
 IA VERT. DOWN, 1 DEGREE PRINTS, CLOCK=800HZ.  
 TABLE DIRECTION=CCW, NO TEMP CONTROL, TEMP=72 DEG F.  
 FIRST PRINT=0 DEG., OA WEST @ 0 DEG.  
 GYRO ON 15 MINS PRIOR TO FIRST PRINT.

R  
 R  
 R  
 R  
 R

	THREE PARAMETER BEST FIT	FIVE PARAMETER BEST FIT	SEVEN PARAMETER BEST FIT	NINE PARAMETER BEST FIT
CONSTANT (ERROR)	+1750.713 ( 2.295)	+1760.668 ( 2.267)	+1760.657 ( 2.256)	+1760.663 ( 2.242)
COS(X) (ERROR)	- 14.612 ( 3.232)	- 14.703 ( 3.193)	- 14.724 ( 3.177)	- 14.712 ( 3.159)
SIN(X) (ERROR)	- 12.360 ( 3.259)	- 12.364 ( 3.219)	- 12.364 ( 3.203)	- 12.363 ( 3.183)
COX(2 X) (ERROR)	+ 0.000 ( 0.000)	+ 6.706 ( 3.193)	+ 6.685 ( 3.178)	+ 6.697 ( 3.159)
SIN(2 X) (ERROR)	+ 0.000 ( 0.000)	- 11.359 ( 3.219)	- 11.860 ( 3.202)	- 11.859 ( 3.183)
COX(3 X) (ERROR)	+ 0.000 ( 0.000)	+ 0.000 ( 0.000)	+ 2.411 ( 3.178)	+ 2.423 ( 3.159)
SIN(3 X) (ERROR)	+ 0.000 ( 0.000)	+ 0.000 ( 0.000)	- 8.341 ( 3.202)	- 8.338 ( 3.183)
COX(4 X) (ERROR)	+ 0.000 ( 0.000)	+ 0.000 ( 0.000)	+ 0.000 ( 0.000)	+ 0.392 ( 3.159)

(ERROR) ( 2.295) ( 2.267) ( 2.256) ( 2.242)

COS (X) - 14.612 - 14.703 - 14.724 - 14.712  
(ERROR) ( 3.232) ( 3.193) ( 3.177) ( 3.159)

SIN (X) - 12.360 - 12.364 - 12.364 - 12.363  
(ERROR) ( 3.259) ( 3.219) ( 3.203) ( 3.183)

COX (2 X) + 0.000 + 6.706 + 6.685 + 6.697  
(ERROR) ( 0.000) ( 3.193) ( 3.178) ( 3.159)

SIN (2 X) + 0.000 - 11.359 - 11.860 - 11.858  
(ERROR) ( 0.000) ( 3.219) ( 3.202) ( 3.183)

COX (3 X) + 0.000 + 0.000 + 2.411 + 2.423  
(ERROR) ( 0.000) ( 0.000) ( 3.178) ( 3.159)

SIN (3 X) + 0.000 + 0.000 - 9.341 - 8.338  
(ERROR) ( 0.000) ( 0.000) ( 3.202) ( 3.183)

COX (4 X) + 0.000 + 0.000 + 0.000 + 0.392  
(ERROR) ( 0.000) ( 0.000) ( 0.000) ( 3.160)

SIN (4 X) + 0.000 + 0.000 + 0.000 - 0.437  
(ERROR) ( 0.000) ( 0.000) ( 0.000) ( 3.182)

FIRST 0 POINTS IGNORED IN COEFFICIENT CALCULATION  
SERVO POSITION IS IA VERT DOWN

$$\text{CONSTANT } (-BD+ADIA+KSI(G))$$

$$\text{SIN}(X) = \text{SIN}(A) \cdot W \cdot \text{SPA} \cdot \text{IEH} \cdot \text{COS}(X) = -(\text{SIN}(A)) \cdot W \cdot \text{OE} \cdot \text{IEH}$$

RMS OF REVOLUTION DIFFERENCE  
RMS13 = 196.469 NO. OF PTS. = 5  
RMS23 = 999.787 NO. OF PTS. = 5  
RMS12 = 117.422 NO. OF PTS. = 360

RMS OF DEVIATION FROM BEST FIT  
THREE FIVE SEVEN NINE PTS  
61.836 61.084 60.777 60.409 725

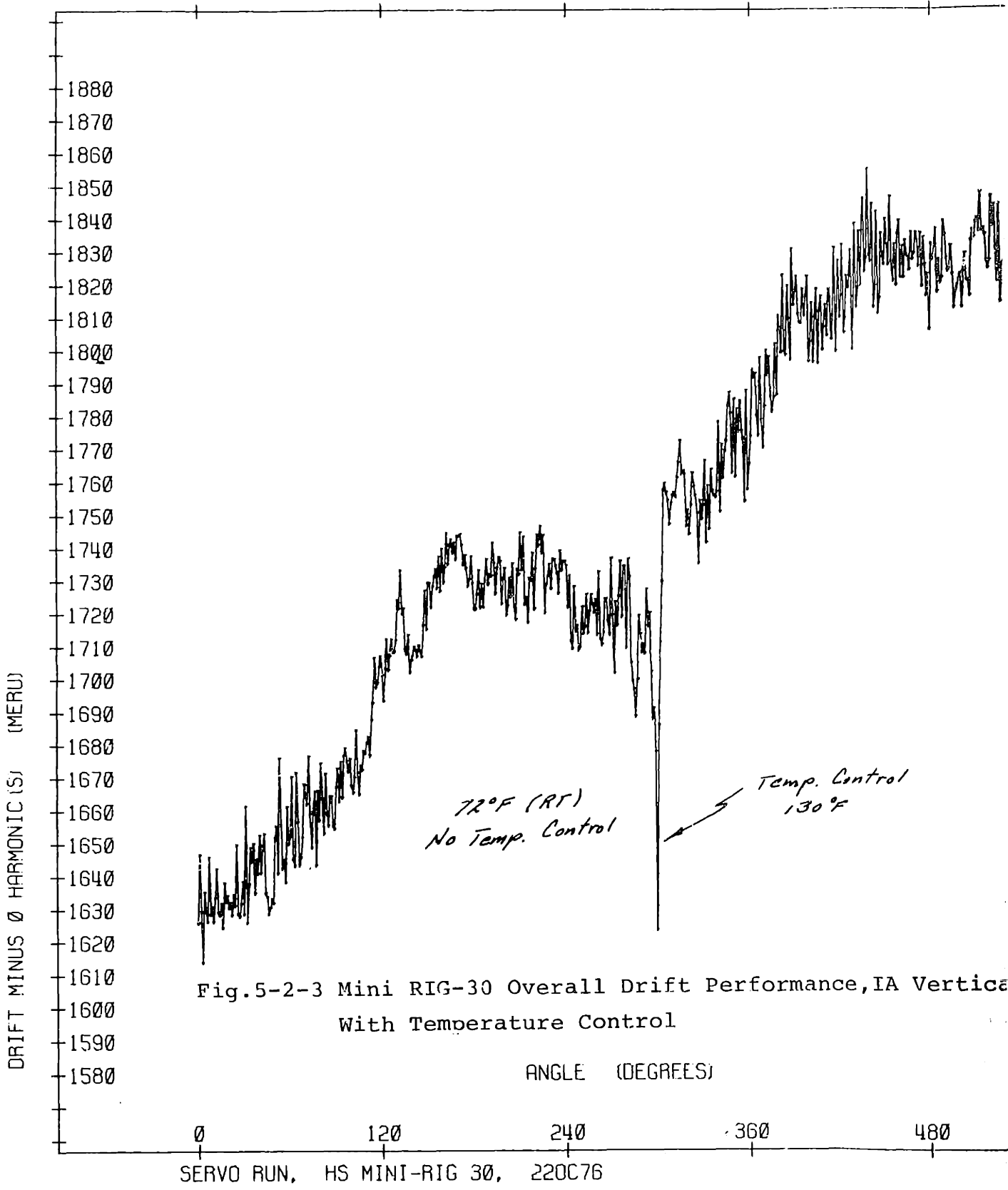
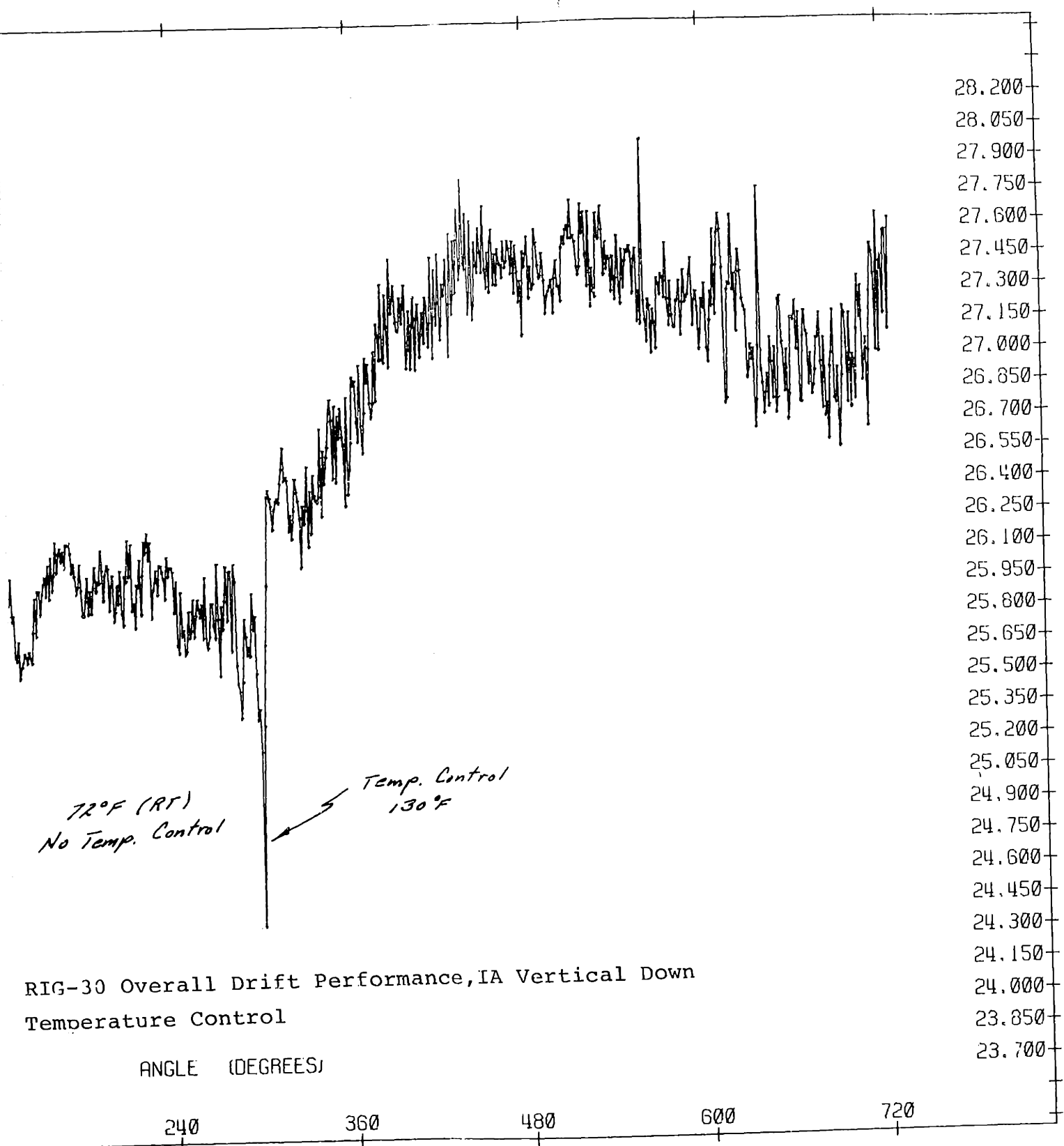


Fig.5-2-3 Mini RIG-30 Overall Drift Performance, IA Vertical  
With Temperature Control

SERVO RUN, HS MINI-RIG 30, 220C76



RIG-30 Overall Drift Performance, IA Vertical Down  
 Temperature Control

ANGLE (DEGREES)

240

360

480

600

720

I-RIG 30, 220C76

28.200  
 28.050  
 27.900  
 27.750  
 27.600  
 27.450  
 27.300  
 27.150  
 27.000  
 26.850  
 26.700  
 26.550  
 26.400  
 26.250  
 26.100  
 25.950  
 25.800  
 25.650  
 25.500  
 25.350  
 25.200  
 25.050  
 24.900  
 24.750  
 24.600  
 24.450  
 24.300  
 24.150  
 24.000  
 23.850  
 23.700

(DEG/HR)



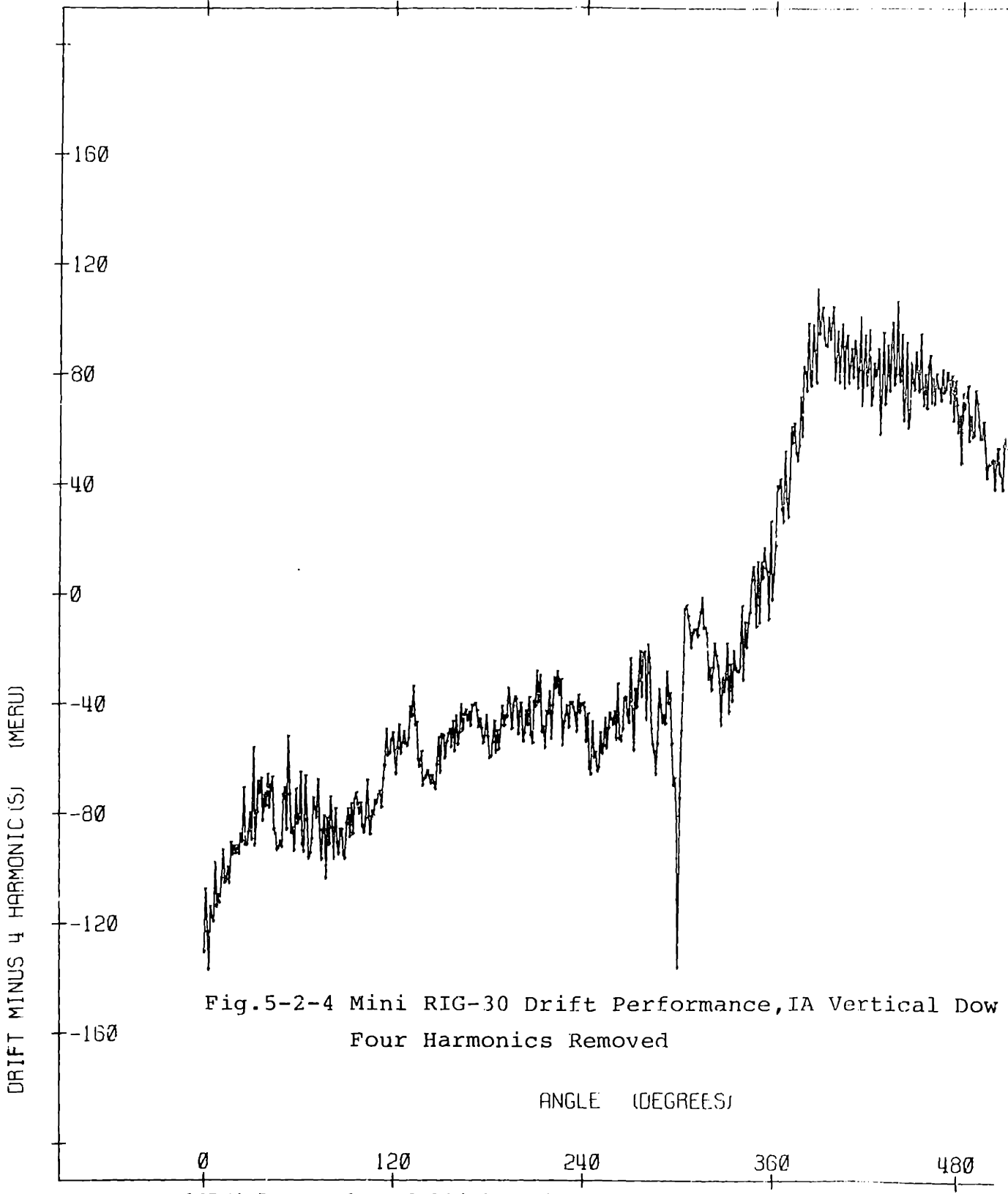
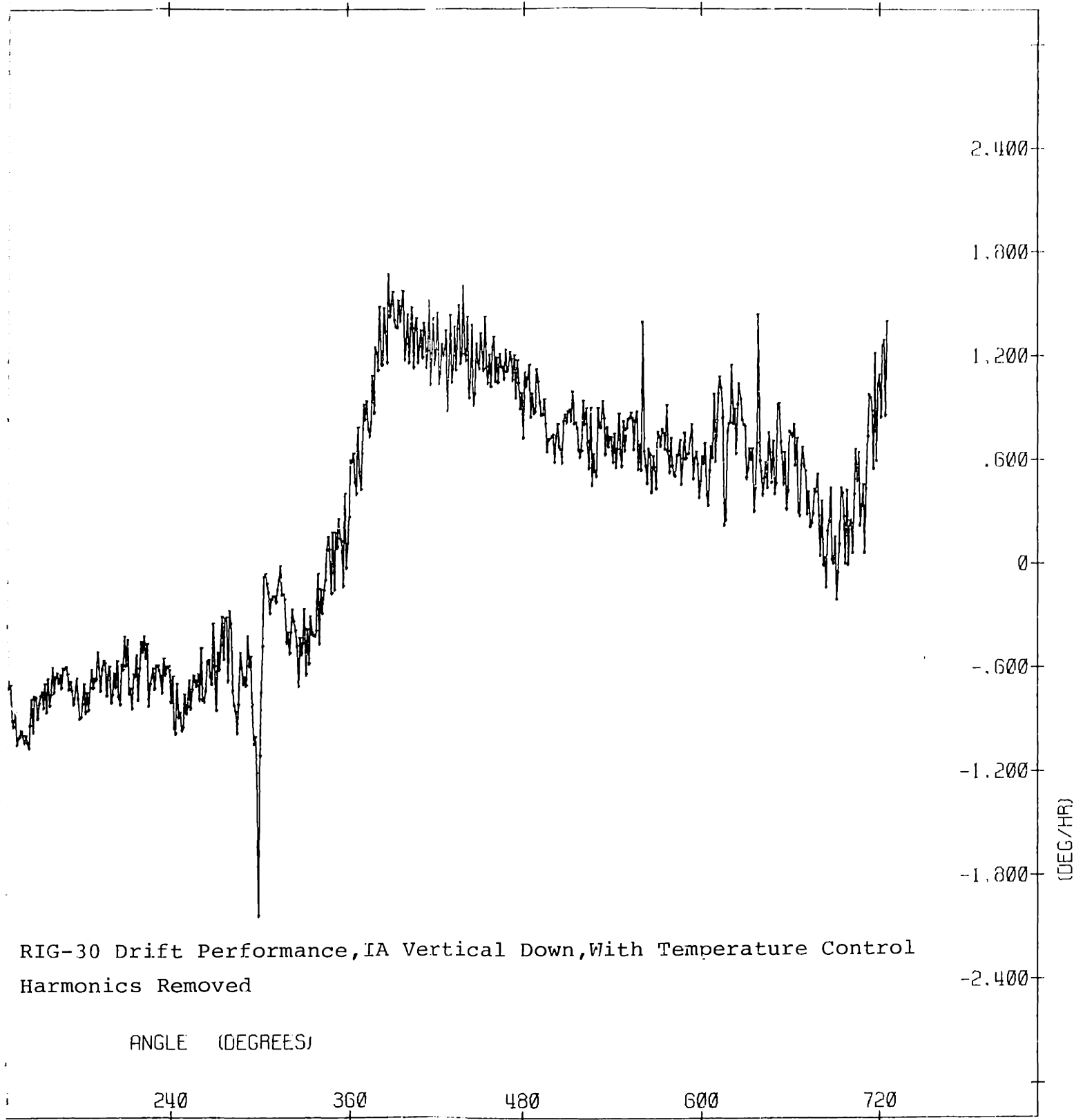


Fig.5-2-4 Mini RIG-30 Drift Performance, IA Vertical Dow  
Four Harmonics Removed

SERVO RUN, HS MINI-RIG 30, 220C76



RIG-30 Drift Performance, IA Vertical Down, With Temperature Control  
Harmonics Removed

ANGLE (DEGREES)

240

360

480

600

720

5-3 Multiple Revolution Tumbling Test

5-3-1 No Temperature Control

a) This test measured the instrument drift performance with no temperature control. The room temperature was held at  $72^{\circ}\text{F} \pm 2^{\circ}\text{F}$ .

The drift rates (table direction ccw) obtained from multiple revolution testing are evaluated by Fourier Analysis; the constant term being BD, the cosine term being ADSRA and the sine term being ADOA. Table 5-3-I shows the results of this test.

b) The average acceleration insensitive term, BD, for the unit in continuous operation for 72 hours was:

$$|BD|_{\text{ave}} \cong 34.87 \text{ deg/h} \cong 2325.21 \text{ meru}$$

c) The average ADSRA term was:

$$|ADSRA|_{\text{ave}} \cong 5.278 \text{ deg/h} \cong 351.896 \text{ meru}$$

d) The average ADOA term was:

$$|ADOA|_{\text{ave}} \cong 0.849 \text{ deg/h} \cong 56.66 \text{ meru}$$

e) The point-to-point drift stability with the unit in continuous operation for 72 hours was approximately 0.6 deg/h.

f) The drift performance plot during the 72-hour run, shows two discontinuities which are believed to be a result of table friction.

Fig.5-3-1 shows the overall drift coefficient parameter performance of the gyroscope for IA horizontal North. Fig.5-3-2 shows the drift coefficient parameter performance of the instrument with four harmonics removed.

Table 5-3-I  
Mini RIG-30 Multiple Revolution Turn-Table Test, IA Horizontal

North, No Temperature Control  
SERVO RUN, HS MINI-RIG 30, 01N076  
1 DEGREE PRINTS, CLOCK=800HZ. IA=HORIZ. NORTH.  
TABLE DIRECTION=CCW, NO TEMP CONTROL, TEMP=72 DEG F.  
FIRST PRINT=0 DEG., OA WEST @ 0 DEG.

R  
R  
R  
R

	THREE PARAMETER BEST FIT	FIVE PARAMETER BEST FIT	SEVEN PARAMETER BEST FIT	NINE PARAMETER BEST FIT
CONSTANT (ERROR)	+2325.212 ( 1.680)	+2325.223 ( 1.209)	+2324.798 ( 0.920)	+2324.953 ( 0.678)
COS(X) (ERROR)	+ 351.895 ( 2.352)	+ 351.922 ( 1.693)	+ 351.079 ( 1.288)	+ 351.386 ( 1.230)
SIN(X) (ERROR)	- 56.664 ( 2.400)	- 56.687 ( 1.726)	- 56.780 ( 1.313)	- 56.733 ( 1.253)
COX(2 X) (ERROR)	+ 0.000 ( 0.000)	- 12.232 ( 1.695)	- 13.052 ( 1.290)	- 12.759 ( 1.232)
SIN(2 X) (ERROR)	+ 0.000 ( 0.000)	+ 43.527 ( 1.724)	+ 43.343 ( 1.311)	+ 43.436 ( 1.251)
COX(3 X) (ERROR)	+ 0.000 ( 0.000)	+ 0.000 ( 0.000)	+ 28.116 ( 1.293)	+ 28.388 ( 1.234)
SIN(3 X) (ERROR)	+ 0.000 ( 0.000)	+ 0.000 ( 0.000)	- 10.721 ( 1.309)	- 10.587 ( 1.249)
COX(4 X) (ERROR)	+ 0.000 ( 0.000)	+ 0.000 ( 0.000)	+ 0.000 ( 0.000)	- 4.241 ( 1.237)
SIN(4 X) (ERROR)	+ 0.000 ( 0.000)	+ 0.000 ( 0.000)	+ 0.000 ( 0.000)	- 9.639 ( 1.246)

COS(X) (ERROR)	+ 351.896 ( 2.352)	+ 351.922 ( 1.693)	+ 351.079 ( 1.288)	+ 351.386 ( 1.230)
SIN(X) (ERROR)	- 56.664 ( 2.400)	- 56.687 ( 1.726)	- 56.780 ( 1.313)	- 56.733 ( 1.253)
COY(2 X) (ERROR)	+ 0.000 ( 0.000)	- 12.232 ( 1.695)	- 13.052 ( 1.290)	- 12.759 ( 1.232)
SIN(2 X) (ERROR)	+ 0.000 ( 0.000)	+ 43.527 ( 1.724)	+ 43.343 ( 1.311)	+ 43.436 ( 1.251)
COX(3 X) (ERROR)	+ 0.000 ( 0.000)	+ 0.000 ( 0.000)	+ 28.116 ( 1.293)	+ 28.388 ( 1.234)
SIN(3 X) (ERROR)	+ 0.000 ( 0.000)	+ 0.000 ( 0.000)	- 10.721 ( 1.309)	- 10.587 ( 1.249)
COY(4 X) (ERROR)	+ 0.000 ( 0.000)	+ 0.000 ( 0.000)	+ 0.000 ( 0.000)	- 4.241 ( 1.237)
SIN(4 X) (ERROR)	+ 0.000 ( 0.000)	+ 0.000 ( 0.000)	+ 0.000 ( 0.000)	- 9.639 ( 1.246)

FIRST 0 POINTS IGNORED IN COEFFICIENT CALCULATION  
SERVO POSITION IS IA HORIZ NORTH

$$\text{CONSTANT (BD+KIS(G) / 2)}$$

$$\text{SIN(X) = -ADDA, COS(X) = +ADSRA}$$

$$\text{SIN(2X) = -KIO(G) / 2, COS(2X) = KIS(G) / 2}$$

RMS OF REVOLUTION DIFFERENCE  
RMS13 = 37.084 NO. OF PTS. = 15  
RMS23 = 187.482 NO. OF PTS. = 15  
RMS12 = 38.076 NO. OF PTS. = 360

RMS OF DEVIATION FROM BEST FIT  
THREE FIVE NINE PTS  
45.572 32.778 24.930 23.788 735

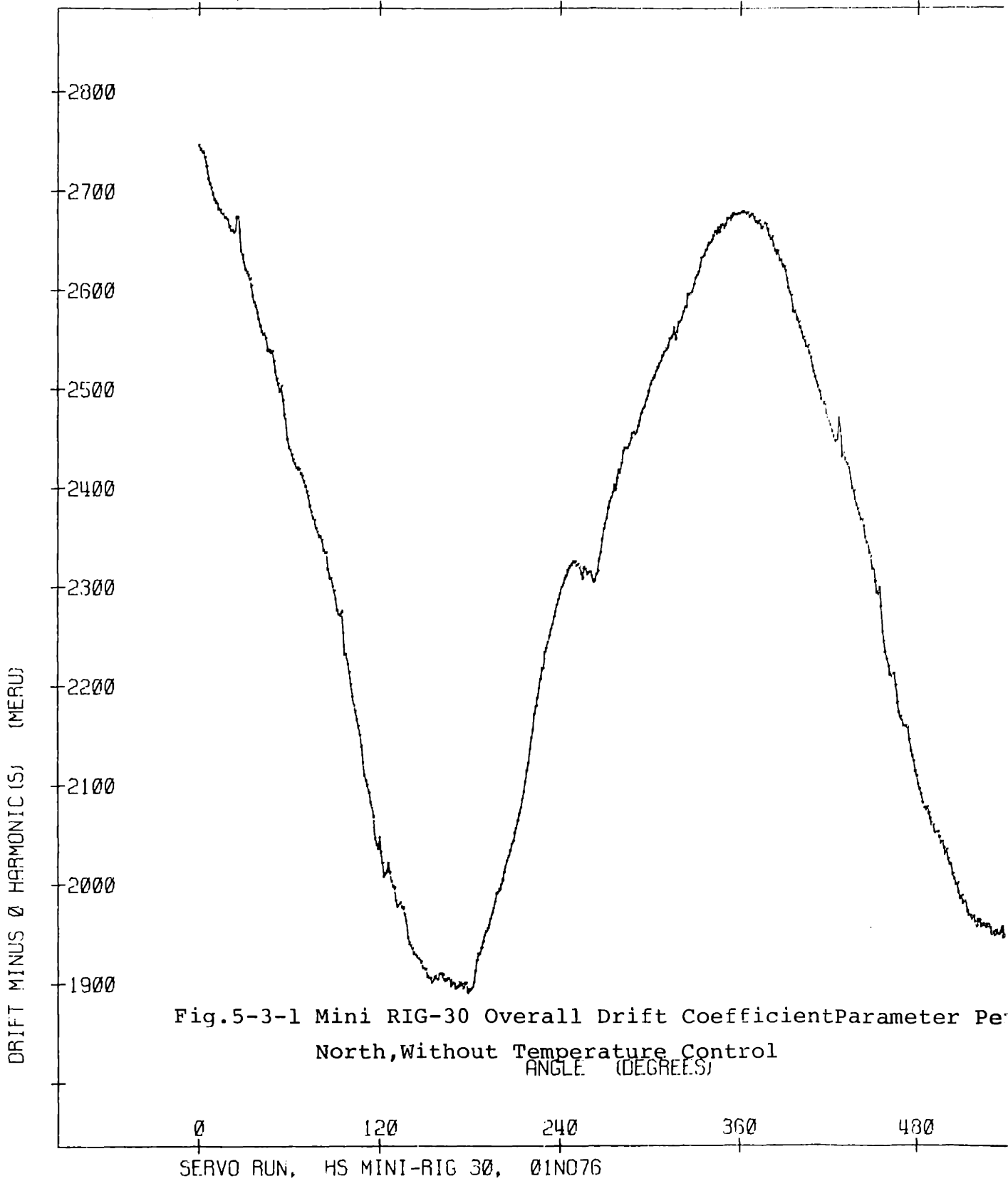
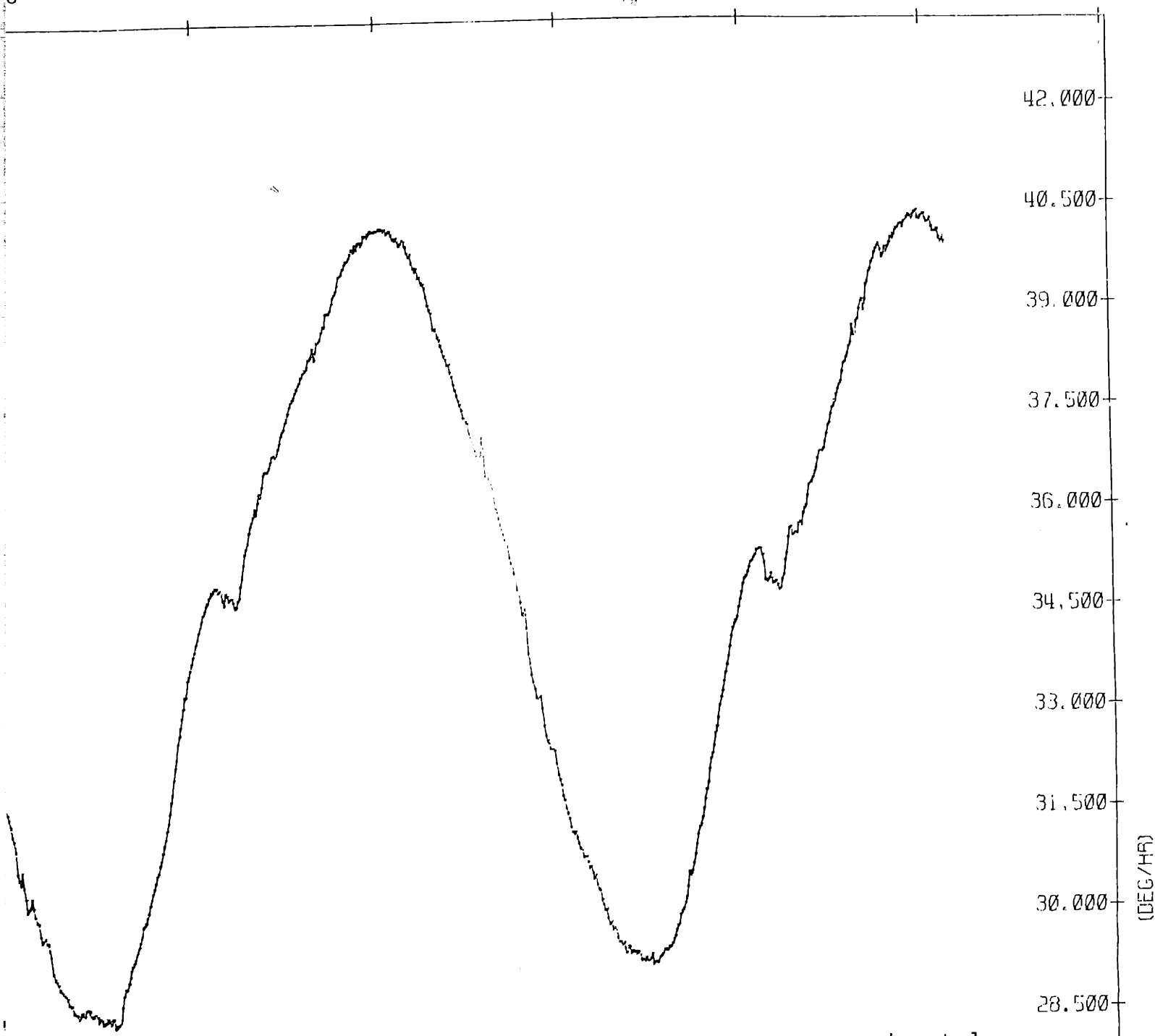


Fig.5-3-1 Mini RIG-30 Overall Drift Coefficient Parameter Per North, Without Temperature Control

SERVO RUN, HS MINI-RIG 30, 01N076



MINI-RIG-30 Overall Drift Coefficient Parameter Performance, IA Horizontal  
with, Without Temperature Control

ANGLE (DEGREE.S)

120 240 360 480 600 720

MINI-RIG 30, 01N076



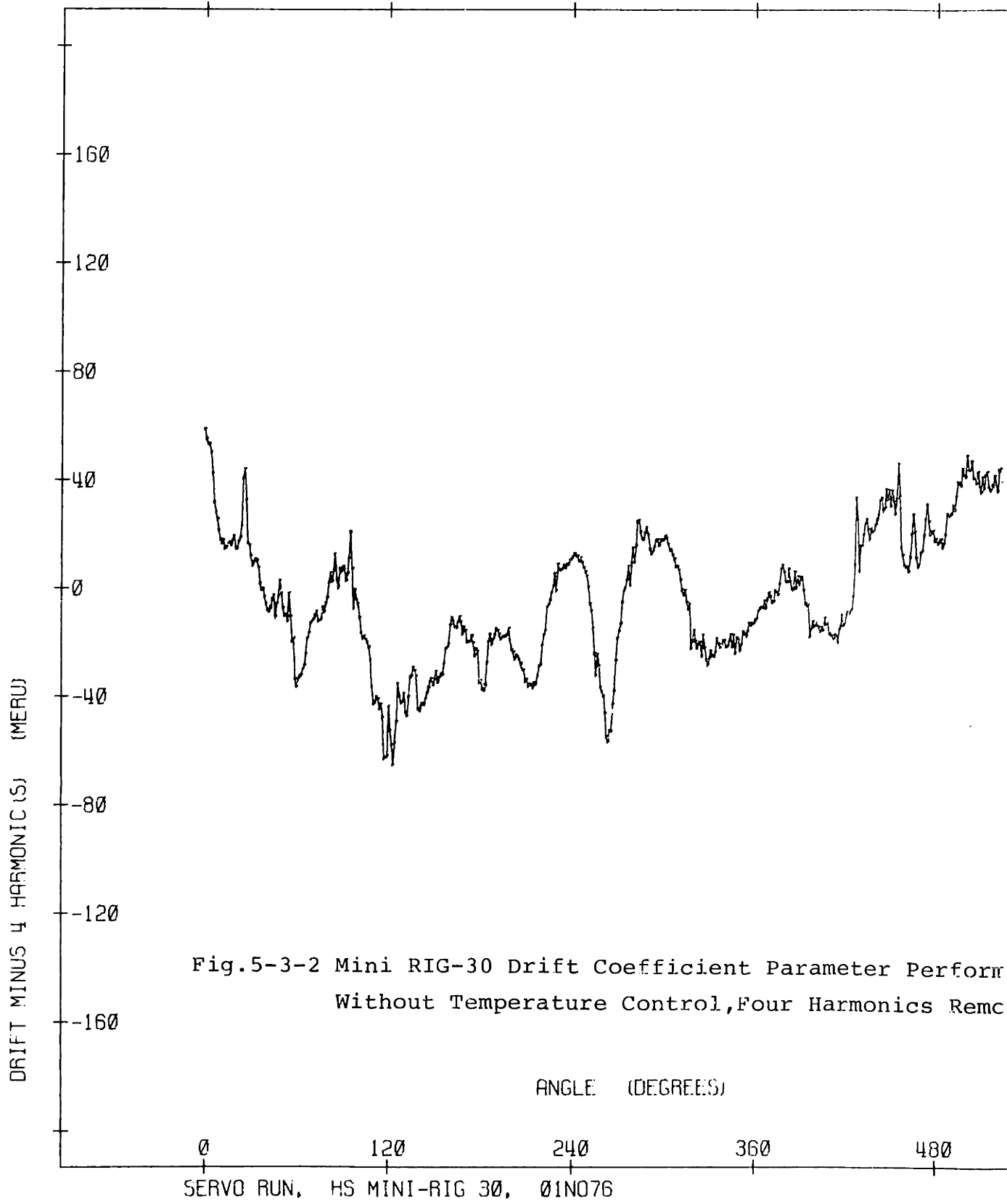
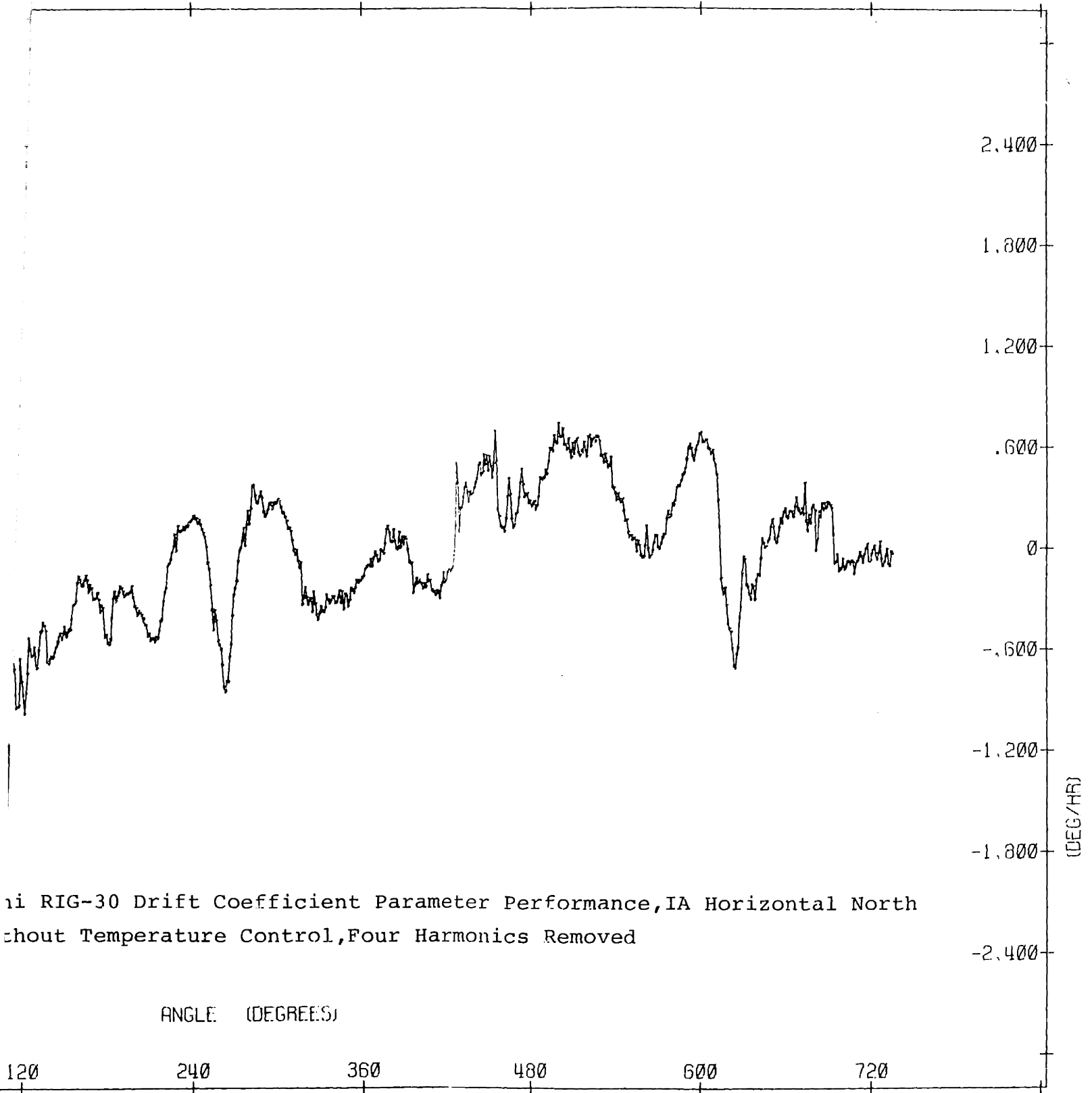


Fig.5-3-2 Mini RIG-30 Drift Coefficient Parameter Perform  
Without Temperature Control, Four Harmonics Remc

SERVO RUN, HS MINI-RIG 30, 01N076



ii RIG-30 Drift Coefficient Parameter Performance, IA Horizontal North  
without Temperature Control, Four Harmonics Removed

MINI-RIG 30, 01N076

5-3-2 Temperature Controlled

a) This test measured the instrument drift performance with unit temperature controlled at  $130^{\circ}\text{F} \pm 0.1^{\circ}\text{F}$

The room temperature was held at  $72^{\circ}\text{F} \pm 2^{\circ}\text{F}$ . Table 5-3-II shows the results for this test.

b) The average acceleration insensitive term (BD) for the unit in continuous operation (table direction ccw) for 72 hours was:

$$|\text{BD}|_{\text{ave}} \cong 34.93 \text{ deg/h} \cong 2329.92 \text{ meru}$$

c) The average ADSRA term for this test was:

$$|\text{ADSRA}|_{\text{ave}} \cong 5.31 \text{ deg/h} \cong 354.571 \text{ meru}$$

d) The average ADOA was:

$$|\text{ADOA}|_{\text{ave}} \cong 0.55 \text{ deg/h} \cong 37.04 \text{ meru}$$

e) The point-to-point drift stability with the unit in continuous operation for 72 hours was approximately 0.6 deg/h.

Fig. 5-3-3 shows the overall drift coefficient parameter performance of the gyroscope for IA horizontal North.

Fig. 5-3-4 shows the drift coefficient parameter performance of the instrument with four harmonics removed.

Table 5-3-II  
 Mini RIG-30 Multiple Revolution Turn-Table Test, IA Horizontal North  
 With Temperature Control

SERVO RUN, HS MINI-RIG 30, 05N076  
 6:30 PM

1 DEGREE PRINTS, CLOCK=800HZ. I<sub>A</sub>=HORIZ. NORTH.  
 TABLE DIRECTION=CCW, NTEMPERATURE CONTROLLED AT 130 DEG F.  
 FIRST PRINT=0 DEG., OA WEST @ 0 DEG.

R  
 R  
 R  
 R  
 R

	THREE	FIVE	SEVEN	NINE
	PARAMETER	PARAMETER	PARAMETER	PARAMETER
	BEST FIT	BEST FIT	BEST FIT	BEST FIT

CONSTANT	+2329.927	+2330.077	+2329.837	+2329.959
(ERROR)	( 0.974)	( 0.956)	( 0.643)	( 0.630)
COS(X)	+ 354.277	+ 354.571	+ 354.087	+ 354.321
(ERROR)	( 1.358)	( 1.333)	( 0.897)	( 0.879)
SIN(X)	- 37.047	- 36.996	- 37.009	- 36.951
(ERROR)	( 1.398)	( 1.370)	( 0.921)	( 0.902)
COX(2 X)	+ 0.000	- 6.760	- 7.257	- 7.049
(ERROR)	( 0.000)	( 1.340)	( 0.901)	( 0.884)
SIN(2 X)	+ 0.000	+ 3.242	+ 3.210	+ 3.321
(ERROR)	( 0.000)	( 1.363)	( 0.916)	( 0.898)
COX(3 X)	+ 0.000	+ 0.000	+ 22.666	+ 22.836
(ERROR)	( 0.000)	( 0.000)	( 0.906)	( 0.888)
SIN(3 X)	+ 0.000	+ 0.000	- 15.698	- 15.546
(ERROR)	( 0.000)	( 0.000)	( 0.911)	( 0.893)
COX(4 X)	+ 0.000	+ 0.000	+ 0.000	- 2.013
(ERROR)	( 0.000)	( 0.000)	( 0.000)	( 0.801)
SIN(4 X)	+ 0.000	+ 0.000	+ 0.000	- 4.565
(ERROR)	( 0.000)	( 0.000)	( 0.000)	( 0.889)

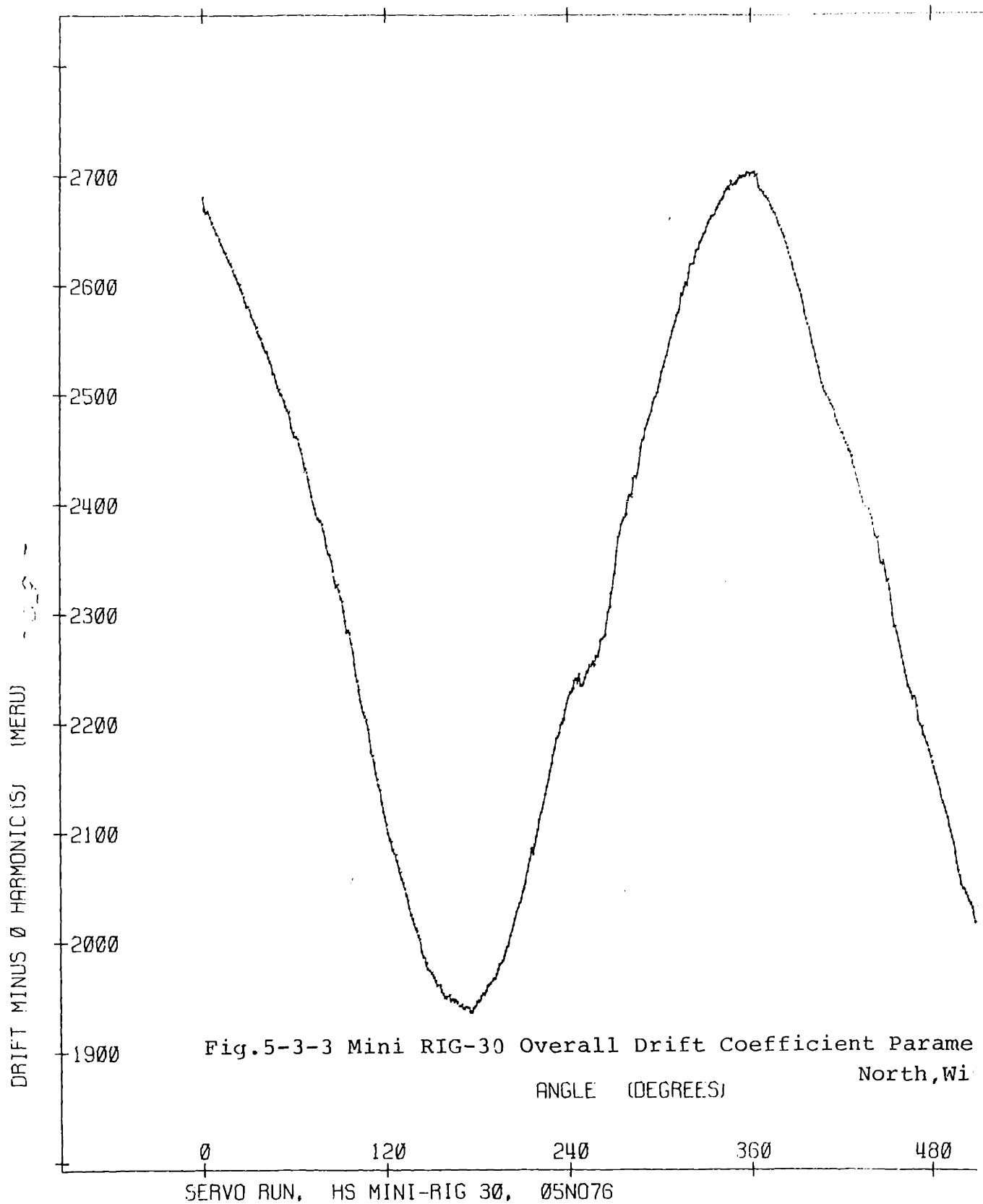
COS(X)	+ 354.277	+ 354.571	+ 354.087	+ 354.321
(ERROR)	( 1.358)	( 1.333)	( 0.897)	( 0.879)
SIN(X)	- 37.047	- 36.996	- 37.009	- 36.951
(ERROR)	( 1.398)	( 1.370)	( 0.921)	( 0.902)
COX(2 X)	+ 0.000	- 6.760	- 7.257	- 7.049
(ERROR)	( 0.000)	( 1.340)	( 0.901)	( 0.884)
SIN(2 X)	+ 0.000	+ 3.242	+ 3.210	+ 3.321
(ERROR)	( 0.000)	( 1.363)	( 0.916)	( 0.898)
COX(3 X)	+ 0.000	+ 0.000	+ 22.666	+ 22.836
(ERROR)	( 0.000)	( 0.000)	( 0.906)	( 0.888)
SIN(3 X)	+ 0.000	+ 0.000	- 15.698	- 15.546
(ERROR)	( 0.000)	( 0.000)	( 0.911)	( 0.893)
COX(4 X)	+ 0.000	+ 0.000	+ 0.000	- 2.013
(ERROR)	( 0.000)	( 0.000)	( 0.000)	( 0.891)
SIN(4 X)	+ 0.000	+ 0.000	+ 0.000	- 4.565
(ERROR)	( 0.000)	( 0.000)	( 0.000)	( 0.889)

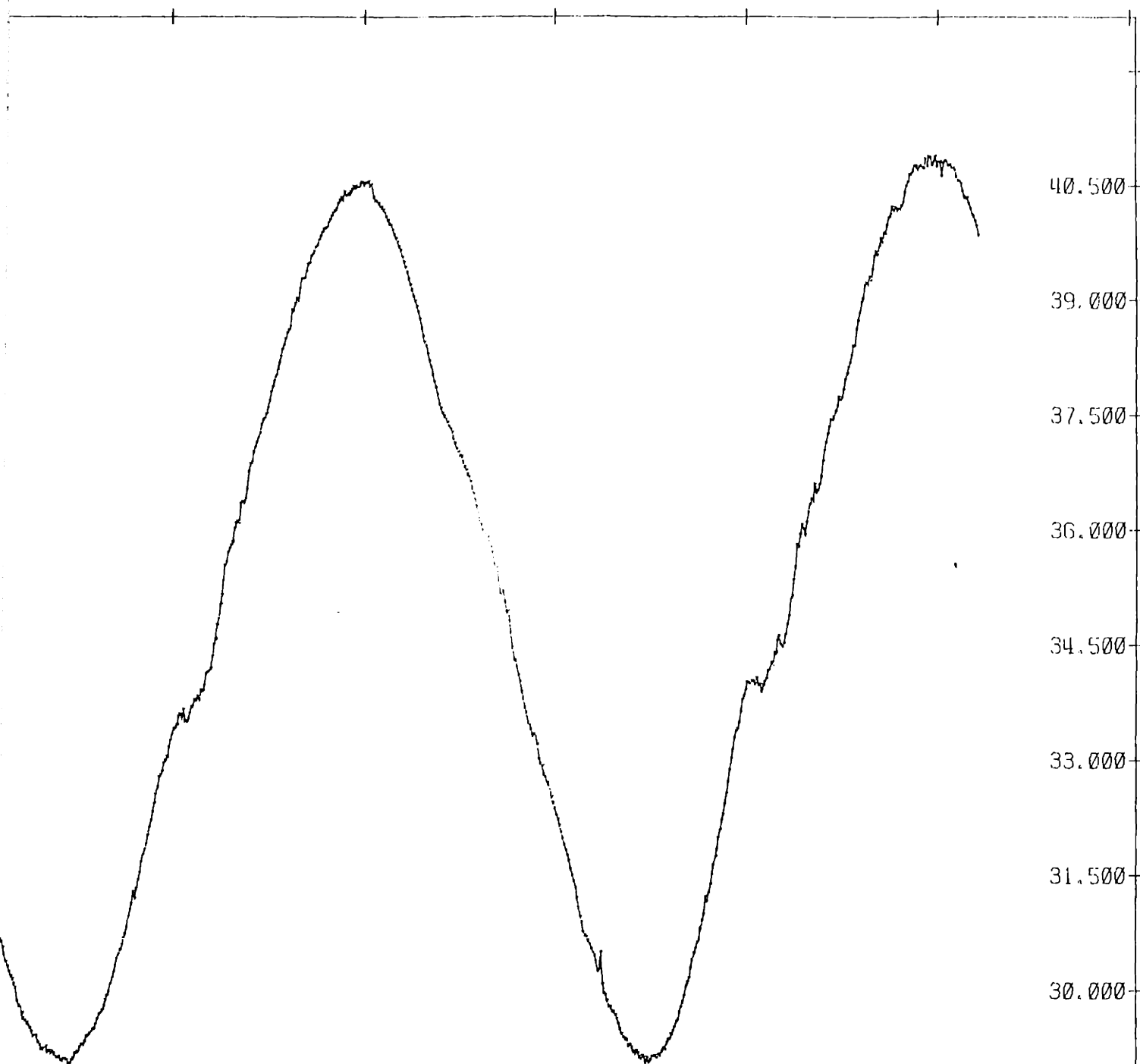
FIRST 0 POINTS IGNORED IN COEFFICIENT CALCULATION  
SERVO POSITION IS IA HORZ NORTH

CONSTANT (BD+KIS(G) / 2)
SIN(X) = -ADOA, COS(X) = +ADSRA
SIN(2X) = -KIO(G) / 2, COS(2X) = KIS(G) / 2

RMS OF REVOLUTION DIFFERENCE  
RMS13 = 63.316 NO. OF PTS. = 25  
RMS23 = 99.274 NO. OF PTS. = 25  
RMS12 = 24.987 NO. OF PTS. = 360

RMS OF DEVIATION FROM BEST FIT  
THREE FIVE SEVEN NINE PTS  
26.593 26.063 17.514 17.152 745





RIG-30 Overall Drift Coefficient Parameter Performance, IA Horizontal North, With Temperature Control

ANGLE (DEGREES)

240

360

480

600

720

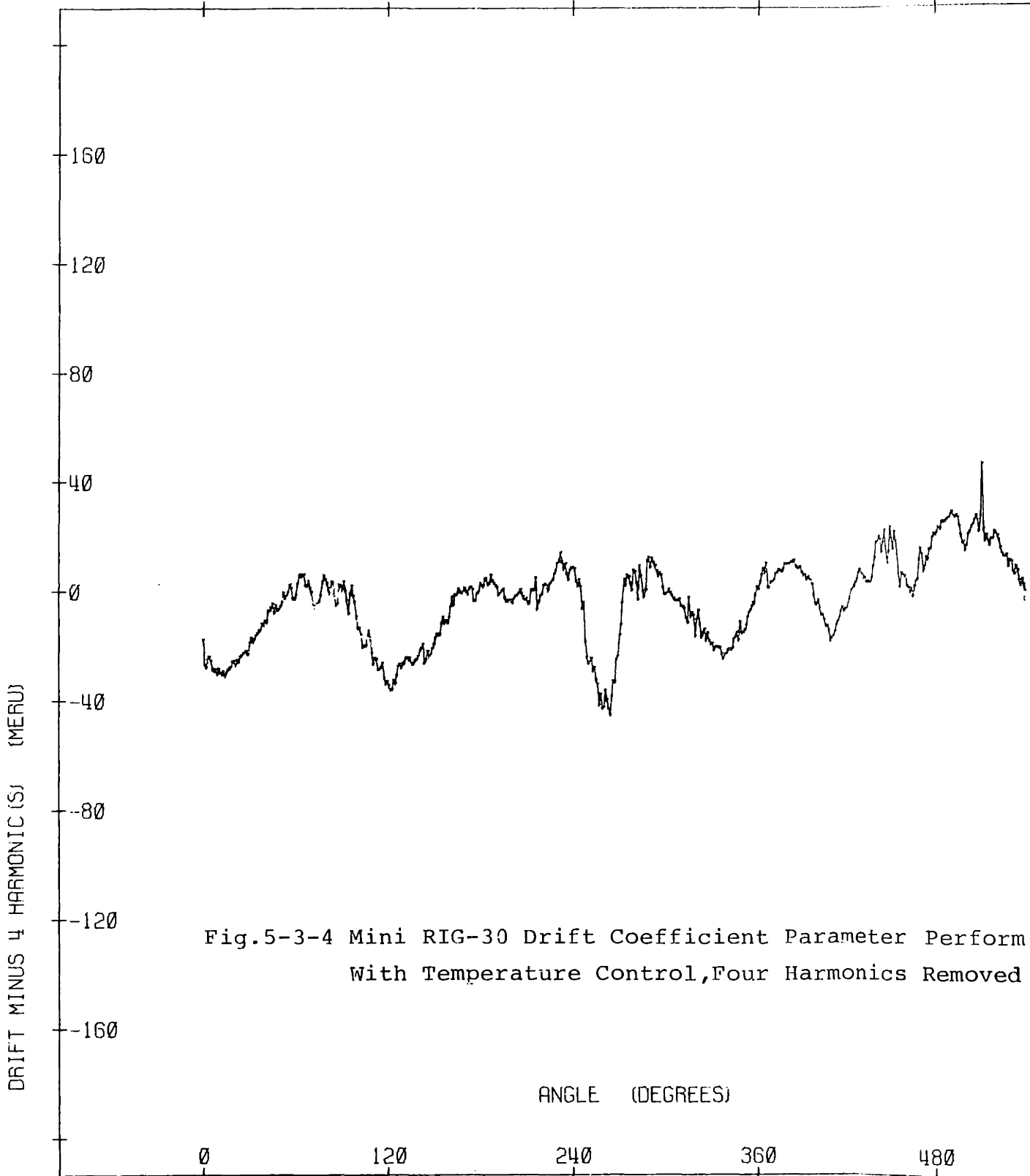
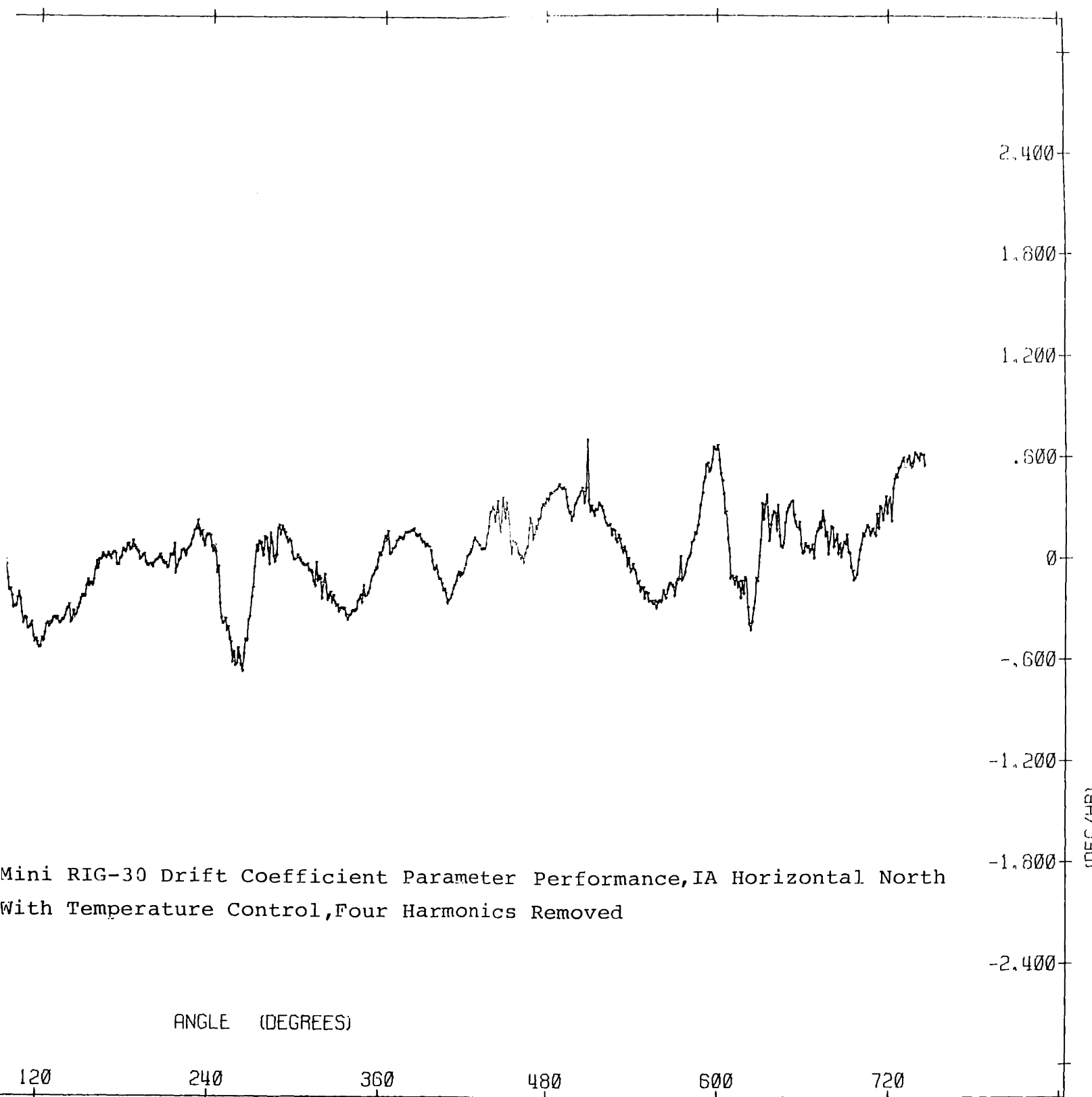


Fig.5-3-4 Mini RIG-30 Drift Coefficient Parameter Perform With Temperature Control, Four Harmonics Removed

SERVO RUN, HS MINI-RIG 30, 05NC76





Mini RIG-30 Drift Coefficient Parameter Performance, IA Horizontal North  
With Temperature Control, Four Harmonics Removed

5 MINI-RIG 30, 05N076

5-4 Tumbling Test

a) These tests measured the drift coefficient parameters as a function of instrument operating temperature, over a range of 60°F.

The measurements were performed at 100,110,120,130,140, 150 and 160°F ±1°F.

The room temperature was held at 72°F±2°F. The entire set of tests was performed in a continuous sequence. Between tests, the wheel was not turned off and the unit was not cooled down.

b) The acceleration insensitive drift (BD) and the drifts due to an acceleration along the spin reference axis (ADSRA) the input axis (ADIA) and the output axis (ADOA) are tabulated in Table 5-4-I for data obtained in these tests.

c) Figs 5-4-1, 5-4-2, 5-4-3 and 5-4-4 show the drift coefficient parameters of the Mini RIG-30 vs. temperature within a range of 60°F.

d) The change in acceleration insensitive drift (BD) for a  $\Delta T$  of 60 °F was 0.6 deg/h

e) The change in ADIA and ADSRA for a  $\Delta T$  of 60°F was: 2.91 deg/h/g and 0.27 deg/h/g, respectively.

f) ADOA showed no apparent change in magnitude and remained within the previously measured stability for  $\Delta T$  of 60°F.

Table 5-4-I

Mini RIG-30 Drift Performance vs. Temperature

Drift Coefficient Parameters (deg/h )	Temperature (°F±1°F)						
	100	110	120	130	140	150	160
BD	37.25	37.34	37.43	37.71	37.75	37.82	37.85
Drift Coefficient Parameters (deg/h/g)	Temperature (°F±1°F)						
	100	110	120	130	140	150	160
ADIA	68.89	69.25	69.74	70.58	71.06	71.51	71.80
ADSRA	7.10	7.20	7.28	7.31	7.32	7.34	7.37
ADOA	0.19	0.17	0.21	0.18	0.20	0.20	0.19



Fig. 5-4-1 Mini RIG-30 BD vs. Temperature

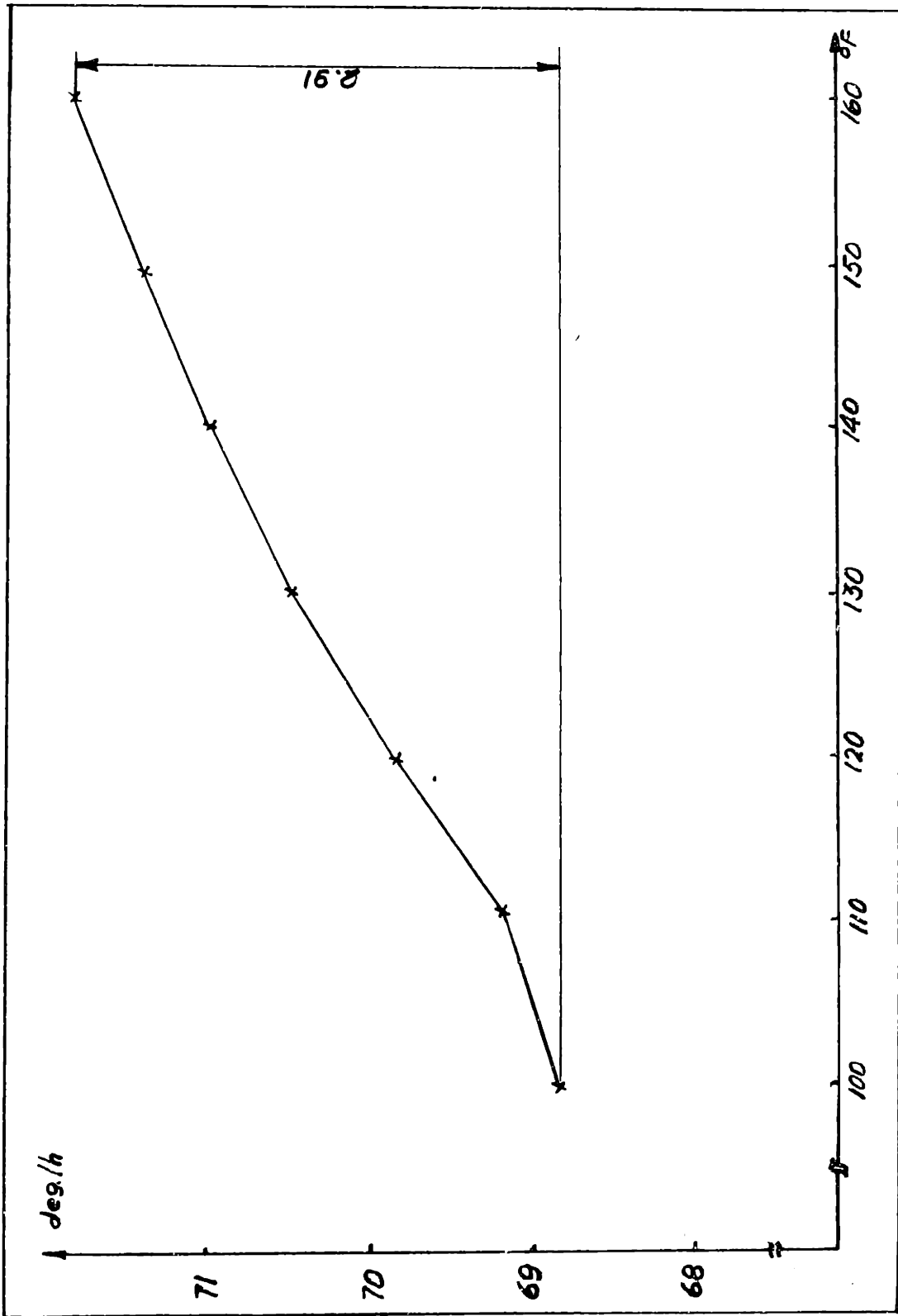


Fig. 5-4-2 Mini RIG-30 ADIA vs. Temperature

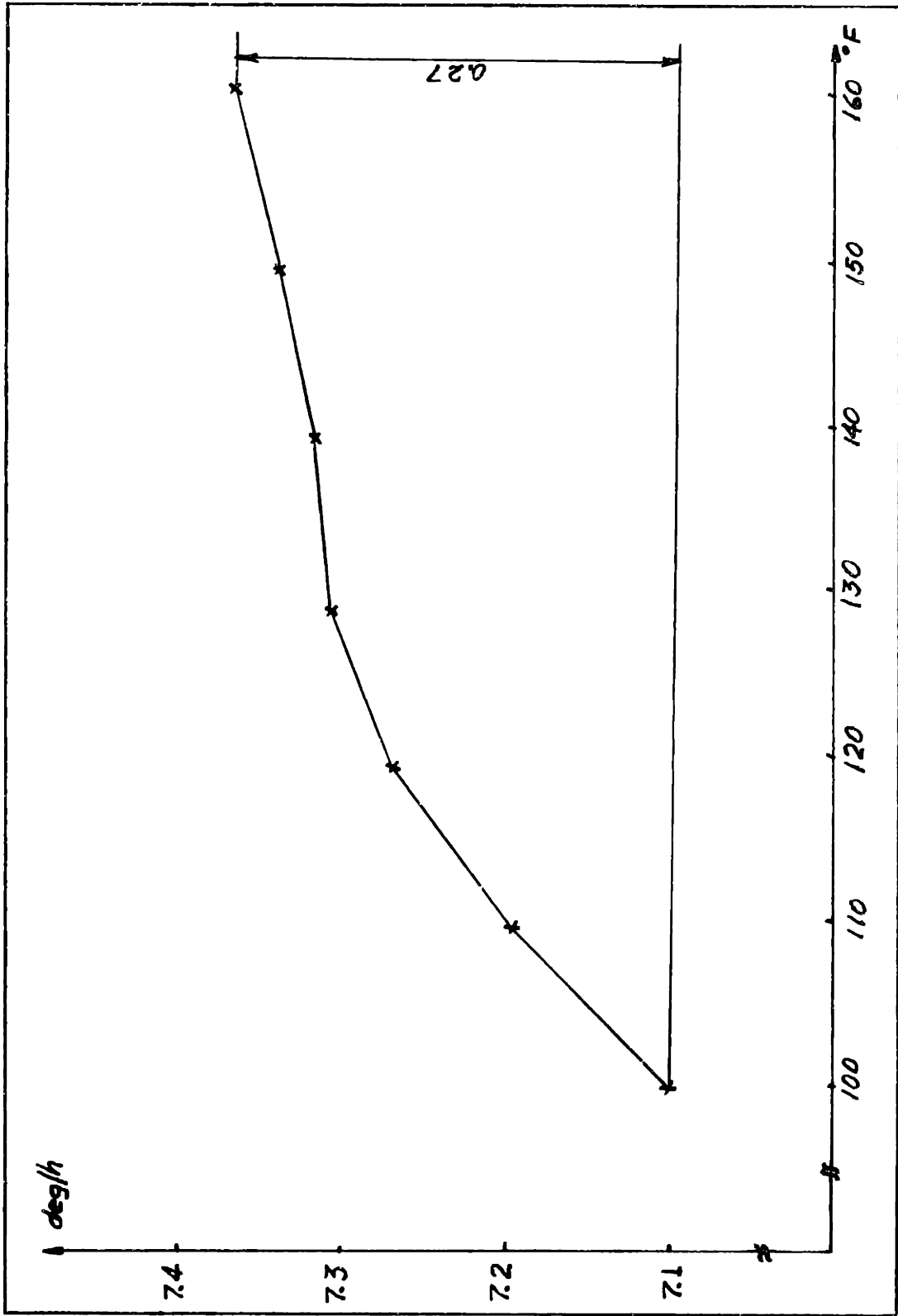


Fig. 5-4-3 Mini RIG-30 ADSRA vs. Temperature

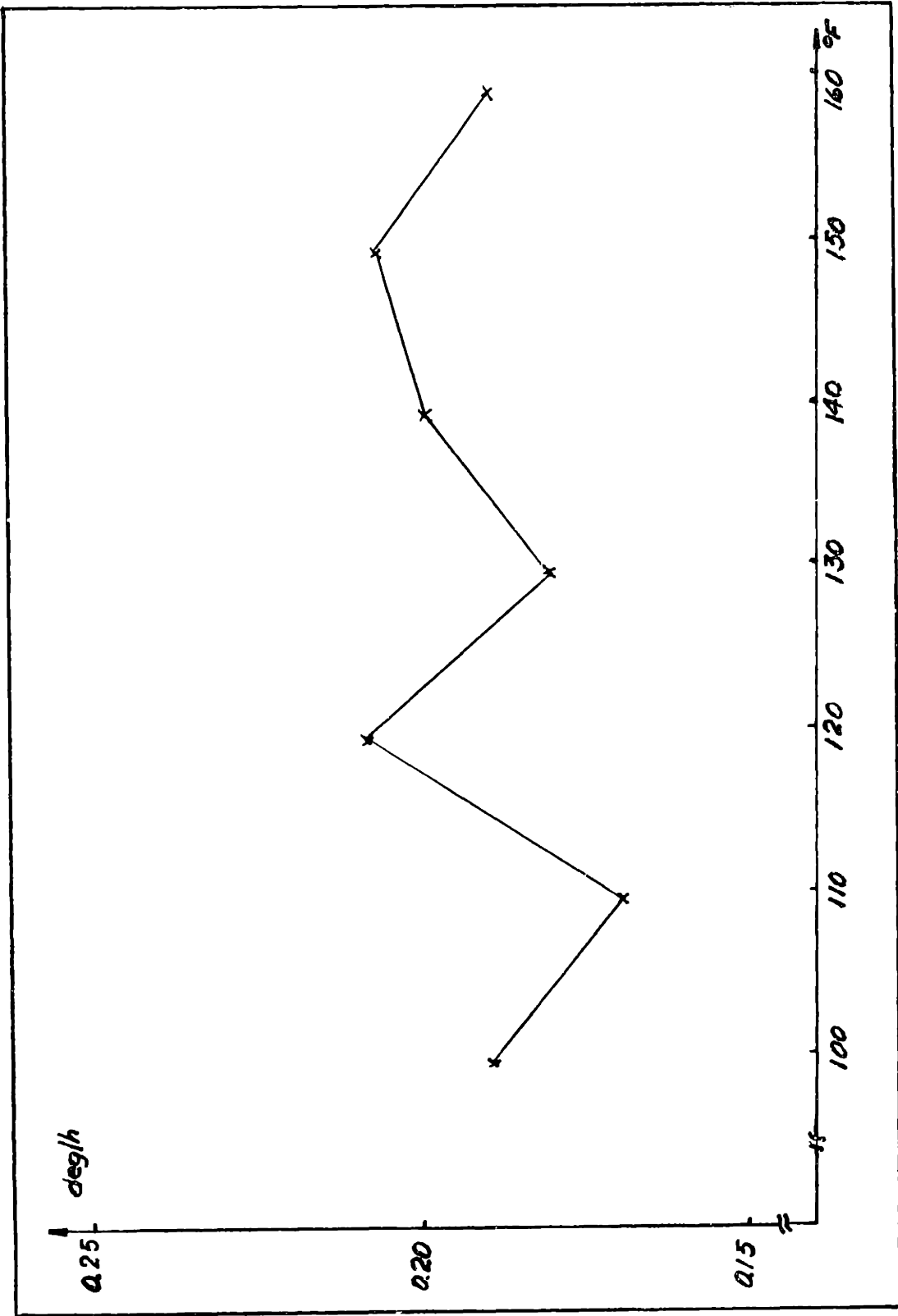


Fig. 5-4-1 Mini RIG-30 ADOA vs. Temperature

CONCLUSIONS AND RECOMMENDATIONS

6-1 Conclusions

a) The average drift coefficient magnitude for this unit was:

$$|BD|_{AVE} = 37.59 \text{ deg/h}$$

$$|ADIA|_{AVE} = 70.40 \text{ deg/h/g}$$

$$|ADSRA|_{AVE} = 7.27 \text{ deg/h/g}$$

$$|ADOA|_{AVE} = 0.19 \text{ deg/h/g}$$

b) The average drift performance for this unit in long and short term continuous operation, with temperature control showed a point-to-point stability of approximately 0.6 deg/h.

c) The acceleration insensitive term (BD) and the acceleration sensitive term (ADSRA) showed a shift in average magnitude of approximately 2 deg/h and 2 deg/h/g, respectively, when comparing the results obtained in the multiple revolution tests and the results obtained in the cardinal position tumbling test. This shift is believed to be a result of a cooldown sensitivity/hysteresis or due to a readout data acquisition problem.

d) The acceleration insensitive drift (BD) and the acceleration sensitive drift (ADSRA) changed linearly by + 0.6 deg/h and +0.27 deg/h/g, respectively, with a linear increase in unit operating temperature of 60°F

$$(m_{BD} \cong 0.01 \text{ deg/h/}^{\circ}\text{F} , m_{ADSRA} \cong 0.005 \text{ deg/h/g/}^{\circ}\text{F} )$$



where:

m is defined here to be the slope of the curve

e) ADOA showed no apparent operating temperature sensitivity (ie, ADOA showed no apparent change in magnitude for a  $\Delta T$  of  $60^{\circ}\text{F}$ .)

f) ADIA showed a change of 2.91 deg/h/g for a  $\Delta T$  of  $60^{\circ}\text{F}$  ( ie,  $m_{\text{ADIA}} \approx 0.005 \text{ deg/h/g/}^{\circ}\text{F}$ ).

#### 6-2 Recommendations

An extension of this tests may include:

- a) Drift coefficient vs. cool down
- b) Drift coefficient vs. radial thermal gradients
- c) Scale Factor/TG sensitivity vs. operating temperature and radial thermal gradients

GYROSCOPE ERROR MODEL EQUATION

I-1 Vector Representation of the Instrument

This analysis assumes a vector representation of the instrument as shown in Fig.I-1-1

The wheel spin reference axis (SRA) is along a radial float axis and therefore perpendicular to the float output axis (OA).

With the spin and output axis thus located by this gyroscope construction the most sensitive axis, the input axis (IA) is the radial axis positioned perpendicular to both spin and output axis.

The direction of SRA,OA and IA is in accordance with a right-handed Cartesian coordinate system.

The spin reference axis is in the direction of the wheel spin vector when the wheel is rotating in its normal direction. In all cases a positive direction may be determined by the right-hand-rule in which the thumb is pointed along the input axis, the first finger aligned parallel with the output axis and the second finger aligned parallel to the spin reference axis, as is shown in Fig I-1-2.

I-2 Background Theory

The steady-state error model equation of a single-degree-of-freedom, floated, integrating gyroscope has the form:

$$\text{Drift} = \pm BD \pm ADIA \pm ADSRA \pm ADOA \pm A^2 D_I \pm A^2 D_S \pm A^2 D_O \pm D_{IS} \pm D_{OS} \pm D_{IO} + \pm(\dots\dots\dots)$$

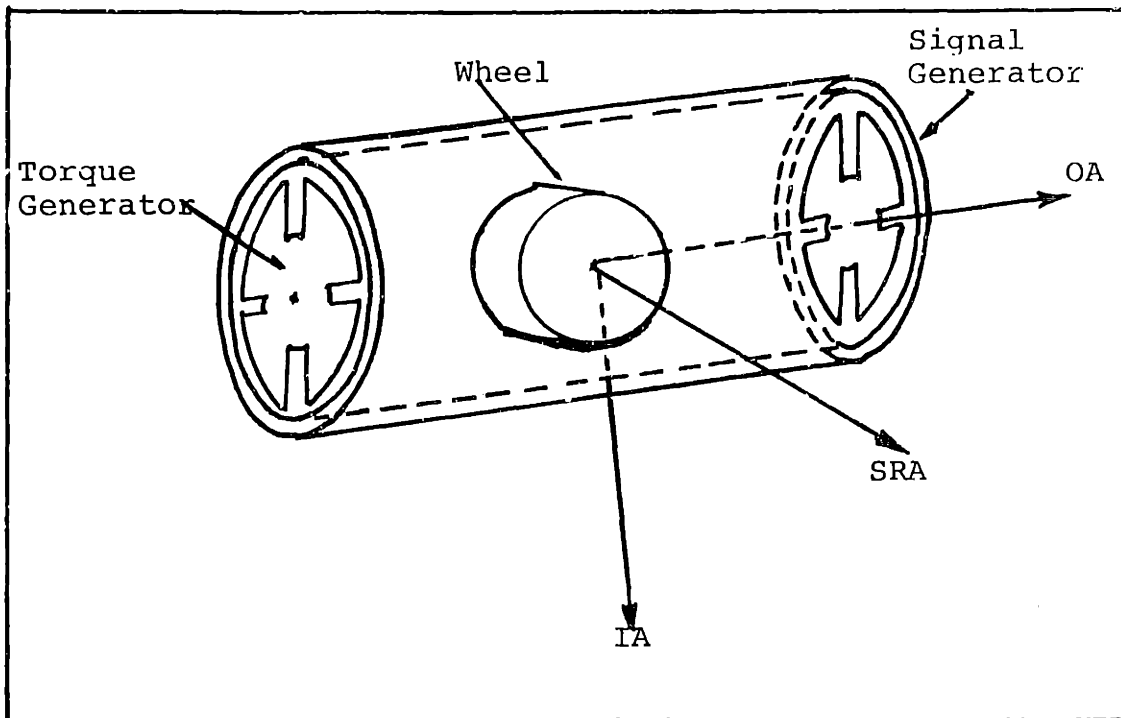


Fig.I-1-1 Vector Representation of the Gyroscope

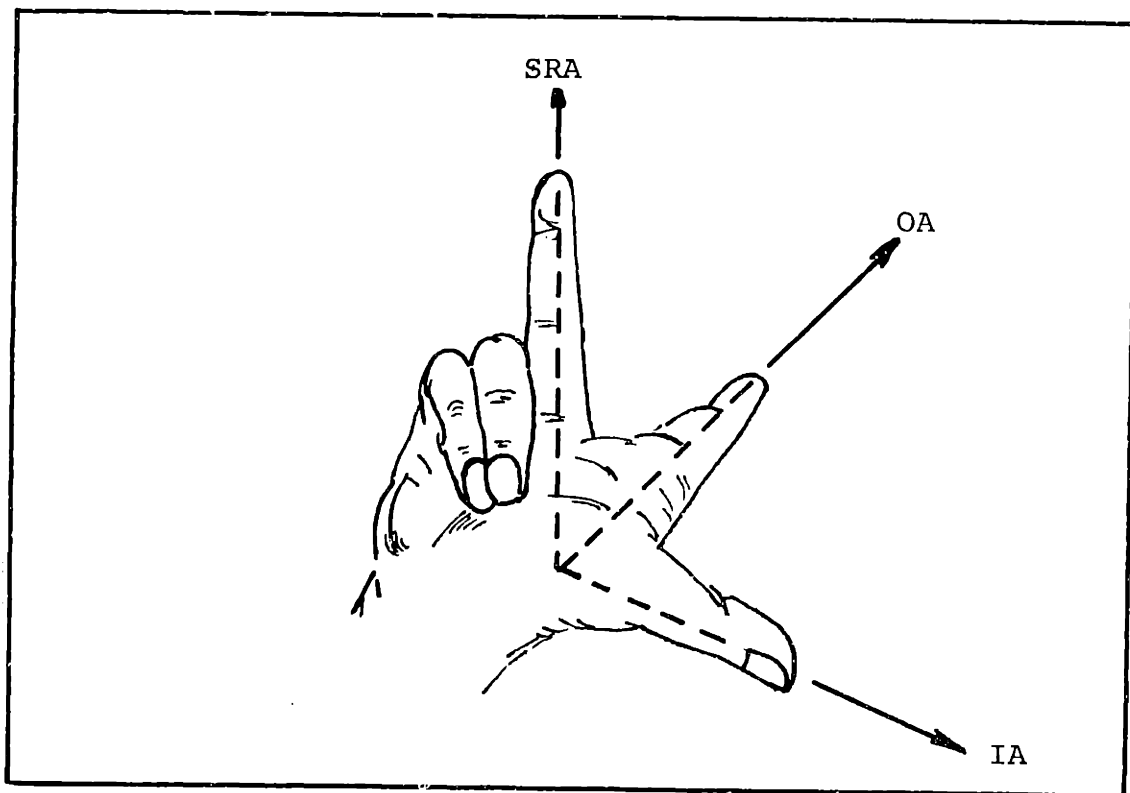


Fig.I-1-2 Right-Hand-Rule for the Gyroscope

where:

BD=gyroscope constant drift rate,non-sensitive to acceleration (deg/h) .

ADIA,ADSRA,ADOA= gyroscope drift that is proportional to the first power of the acceleration along IA,SRA and OA ,respectively (deg/h/g)

$A^2D_I, A^2D_S, A^2D_O$  = gyroscope squared drift rate that is proportional to acceleration squared along IA,SRA and OA ,respectively,also called compliance terms(deg/h/g<sup>2</sup>)

$D_{IS}, D_{OS}, D_{IO}$  = gyroscope drift rate that is proportional to the product of acceleration along IA and SRA;OA and SRA and IA and OA ,respectively (deg/h/g<sup>2</sup>)

Since this particular instrument is of the low to moderate performance type,in the equation it will be assumed:

1) The instrument's spin and spin reference axis are maintained so nearly coincident that cross-coupling effects are negligible.

2) The gyroscope is isolated from linear and angular oscillations so that anisoelastic resonance effects,aniso-inertia,and coning torques are negligible.

3) No terms exist higher than first-order acceleration dependent terms.

4) Gyroscopic torque due to angular rate inputs about IA and command torque generated by the gyroscope torque generator are zero.

The equation then becomes:

$$\text{Drift} = \pm \sum \text{nonacceleration sensitive drifts} \\ \pm \sum \text{acceleration sensitive drifts}$$

### I-3 Analysis of the Error Model Equation

#### I-3-1 Nonacceleration sensitive drift

BD = The fixed bias term, in the error model equation, comprises all the effects that cause gyroscope drift that are nonsensitive to acceleration. These effects include:

- 1) All case-to-float power lead torques.
- 2) Signal-generator reaction torque, which is proportional to signal generator excitation current squared.
- 3) Float torque that are dependent upon temperature changing with time.

For this instrument the nonsensitive drift equation is of the form:

$$BD = CD(1 + \Delta T_b)$$

where:

CD = drift due to terms 1) and 2) (deg/h)

$\Delta T_b$  = gyroscope drift sensitivity to a temperature change 3) (deg/h/ $^{\circ}$ F)

I-3-2 Acceleration sensitive drift

The three acceleration-sensitive coefficients of the error model equation comprise all the effects causing gyroscope drift that are proportional to the first-power of acceleration. These include:

- 1) Mass unbalance torque
- 2) Mass unbalance torque change with time
- 3) Torque due to temperature gradients across the gyroscope. This torque is made up of fluid torque, torque due to float center-of-buoyancy shift and torque due to float center-of-mass shift.
- 4) Torque due to average gyroscope unit temperature change
- 5) Torque due to temperature gradient changing with time
- 6) Torque due to wheel power dissipation change

Since it is possible to change the operating temperature of this instrument from 0 to 180°F it is expected that effects of torque due to 4) will appear. Also since gradient tests were not performed and since that the wheel power is constant, the effects of 3), 5) and 6) can be neglected.

The acceleration sensitive drifts can be expressed in equation form as:

$$ADIA = AD_I (1 + \Delta T_I)$$

$$ADSRA = AD_S (1 + \Delta T_S)$$

$$ADOA = AD_O (1 + \Delta T_O)$$

where:

$AD_I$  = acceleration sensitive term along IA  
due to 1) and 2) (deg/h/g)

$AD_S$  = acceleration sensitive term along SRA  
due to 1) and 2) (deg/h/g)

$AD_O$  = acceleration sensitive term along OA  
due to 1) and 2) (deg/h/g)

$\Delta T_I, \Delta T_S, \Delta T_O$  = gyroscope sensitivity to  
a temperature change along  
IA, SRA and OA respectively  
due to 4) (deg/h/g/°F)

#### I-4 Gyroscope Error Model Equation

Rewriting the error model equation:

$$\text{Drift} = \pm CD \pm CD \cdot \Delta T_b \pm AD \pm AD \cdot \Delta T_I \pm AD \pm AD \cdot \Delta T_S \pm AD + \pm AD \cdot \Delta T_O$$

The algebraic signs of each term will be obtained  
from the following definitions:

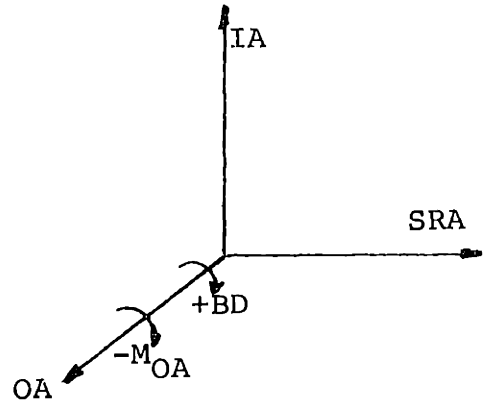
$ADIA$  is equivalent to  $MUSRA$  = Mass unbalance along SRA

$ADSRA$  is equivalent to  $-MUIA$  = Mass unbalance along IA

$M_{OA}$  = Torque about output axis (OA)

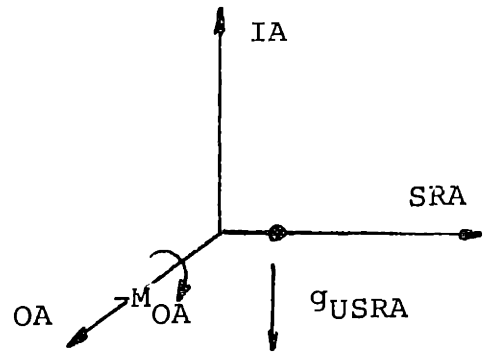
I-4-1

+BD causes  $-M_{OA}$



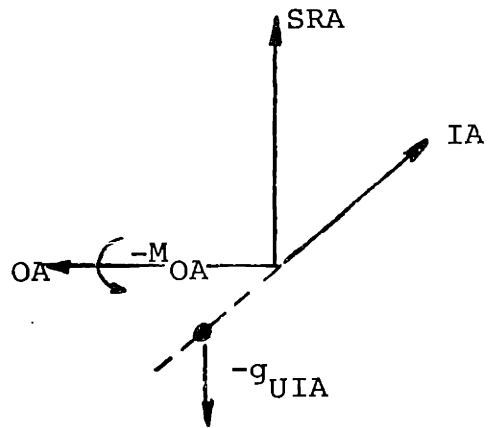
I-4-2

+ADIA causes  $-M_{OA}$



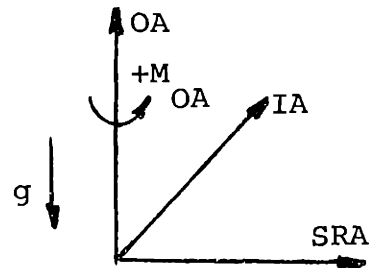
I-4-3

+ADSRA causes  $-M_{OA}$



I-4-4

+ ADOA causes  $+M_{OA}$





The final forms of the gyroscope error model equation, which is dependent upon gyroscope orientation in the gravity field are:

$$\text{Drift} = \pm \text{BD} \pm \text{ADIA}$$

$$\text{Drift} = \pm \text{BD} \pm \text{ADSRA}$$

$$\text{Drift} = \pm \text{BD} \pm \text{ADOA}$$

GYROSCOPE TEST

II-1 Purpose

The purpose of these tests was to show that the bias drift, as well as the acceleration sensitive drift terms of the previously developed error model equation are a function of the change in operating temperature. The drift as it was defined in equation (6) will change as a function of temperature even when the variation is within the range of the operating temperature given in the specifications.

Preliminary operational tests were conducted to establish a performance baseline to verify overall proper operation of the gyroscope. The tests were then extended to determine the performance dependence upon operating temperature. The following sections give a brief explanation of how these tests were run.

II-2 Preliminary Operational Tests

II-2-1 Temperature Sensor Calibration

Since the measurement of the variation of the drift coefficient parameters was made at different temperatures it was necessary to calibrate the temperature-sensing element in a controlled oil bath.

For these tests a FEN WALL SN-58 sensor was used.

Figs. II-2-1-a, II-2-1-b and II-2-1-c show the temperature calibration charts for this sensor for different sensor currents.

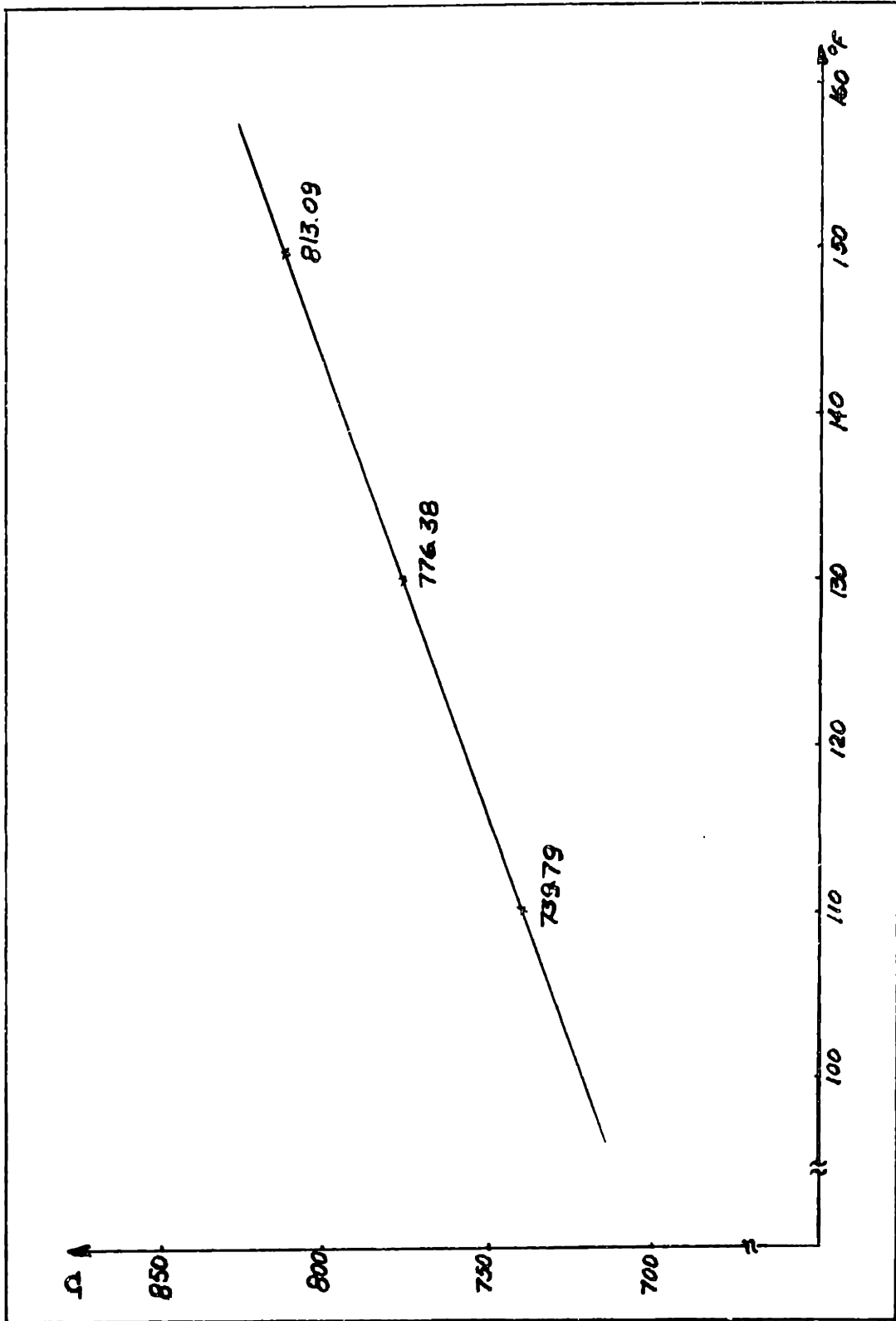


Fig. II-2-1-a Calibration FC-77 FEN WALL SN-58 Sensor Current 1.0 mA

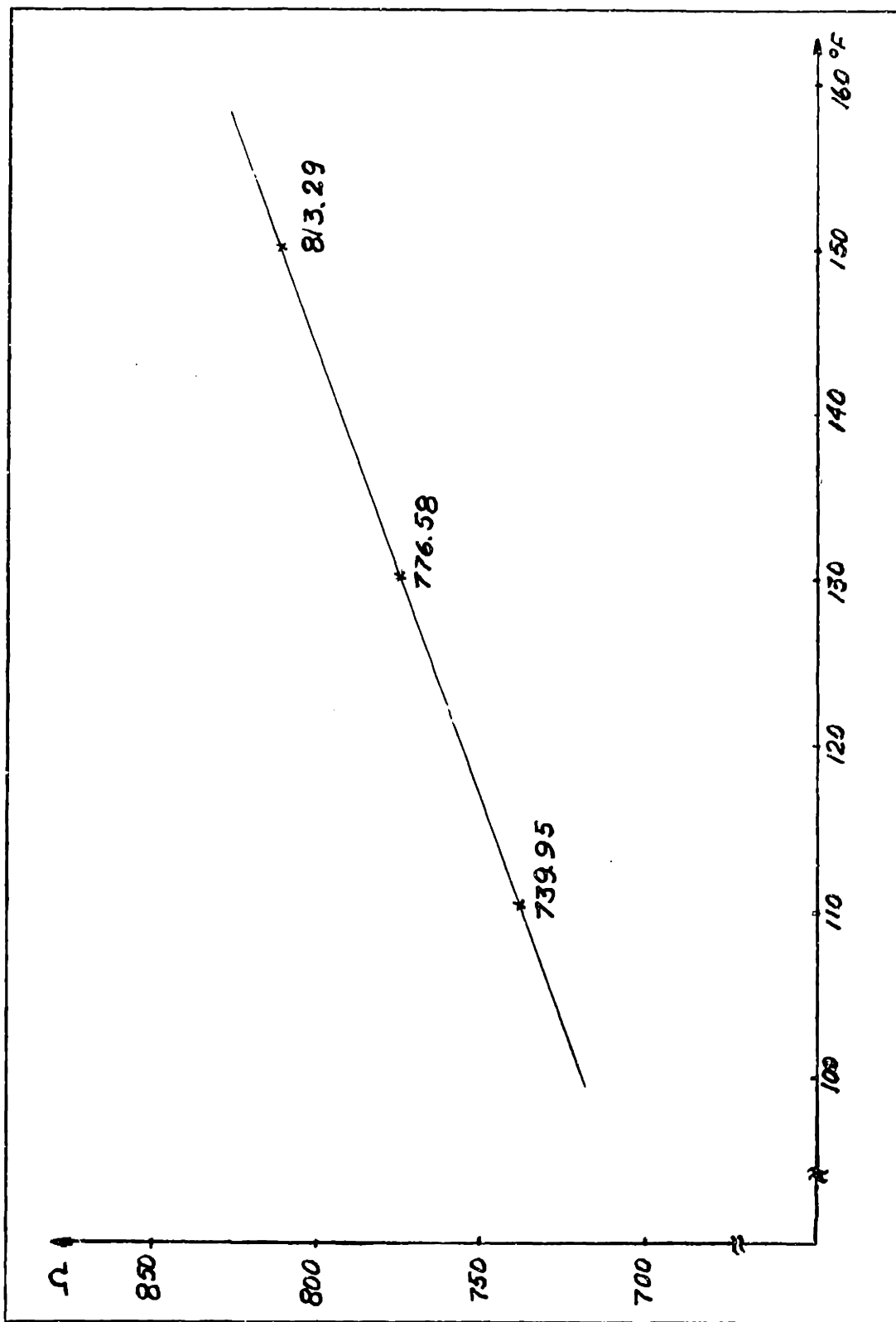


Fig. II-2-1-b Calibration FC-77 FEN WALL SN-58 Sensor Current 2.0 mA

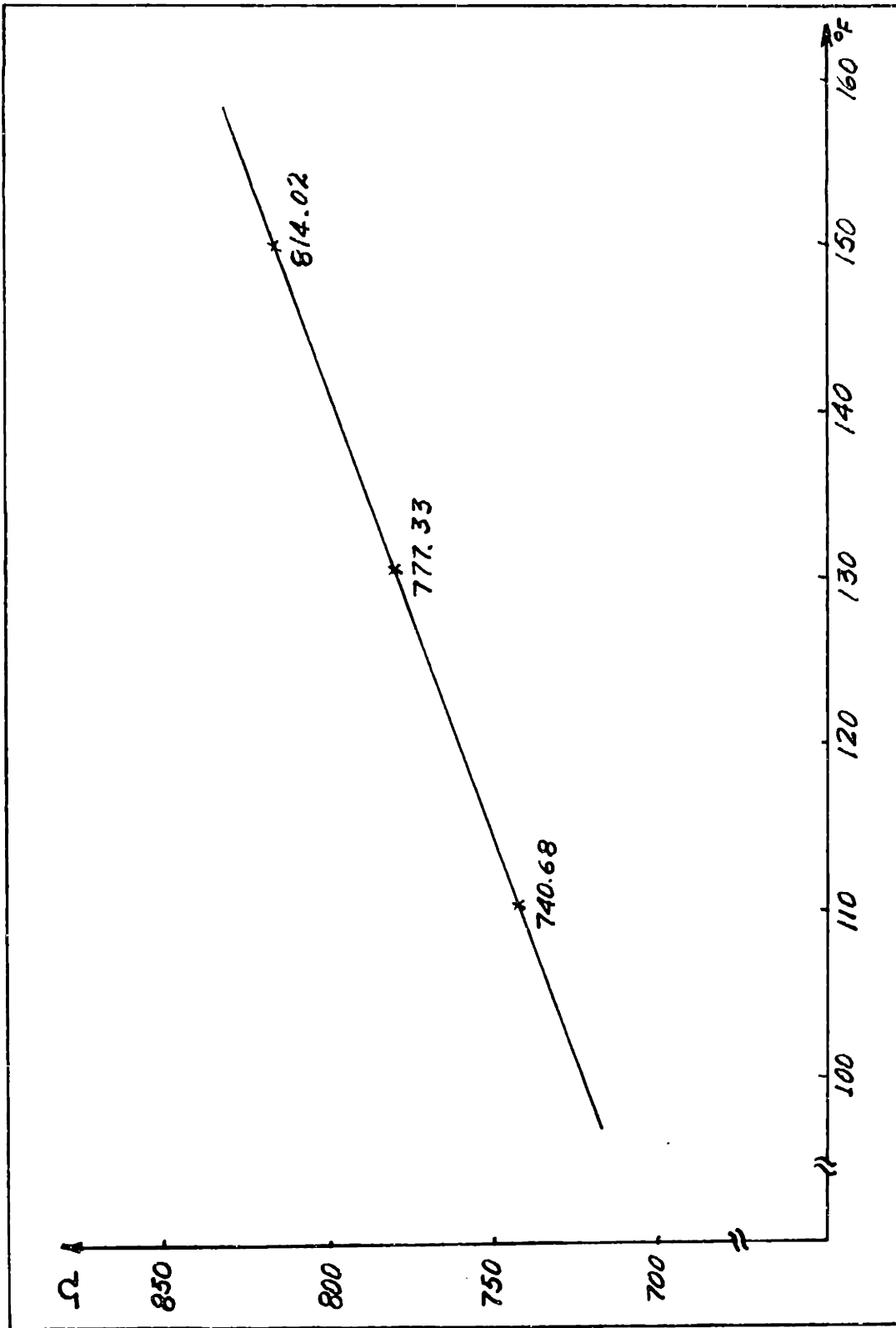


Fig. II-2-1-c Calibration FC-77 FEN WALL SN-58 Sensor Current 4.0 mA

#### II-2-2 Gyroscope Resistance and Continuity Test

The purpose of this test was to verify proper wiring connections within the gyroscope.

The microsyn, wheel and torquer were properly checked out for the correct pin-to-pin, resistance and short circuits to case.

Table II-2-1 shows the results of this test.

#### II-2-3 Test Station Resistance and Continuity Test

The DC resistance and continuity of the interwiring of all connections of and between the Electronics, Test table, and Gyroscope through the breakouts was measured with a volt-ohmmeter or equivalent.

Proper grounding and shielding techniques had to be implemented and verified for low pickup and /or noise.

#### II-2-4 Run Up and Run Down Gyroscope Wheel Tests

The spin motor was excited and a record kept to the time required for the wheel to reach synchronous speed.

From synchronous speed the motor was deenergized and the time required for the wheel to stop was recorded (as noted by oscilloscope indication).

These two checks enabled a tabulated record to kept so that any degradation could be observed in the quality of the wheel ball-bearings.

Table II-2-I

Mini RIG-30 Resistance and Continuity Check

Parameter	Units	Nominal	Measured
$\phi A - \phi B$	ohms	-	220
$\phi A - \phi Com.$	ohms	-	100
$\phi B - \phi Com.$	ohms	-	120
SG Primary	ohms	100	110
SG Secondary	ohms	128	280
Torquer	ohms	355	360

Turn-On and Turn-Off Check out

Parameter	Open Circuit	Gyroscope Load
$\phi A - \phi Com$	26 V(rms)	26 V(rms)
$\phi B - \phi Com$	26 V(rms)	26 V(rms)
SG Primary	10 V(rms)	10 V(rms)

Frequency wheel 800 Hz

Frequency SG 4800 Hz

$\phi A$  Leads  $\phi B$  by 90 deg

II-3 Performance Test

II-3-1 Servo-Turntable Tests

Inertial reference mode tests were performed to check the gyroscope's performance as an angular measurement device, as well as to check the operation of the entire gyroscope test station. Namely, the electronics, test turntable, and gyroscope and their interconnecting interfaces.

The instrument was mounted with IA parallel to the turntable rotary axis, which in turn was parallel to the local vertical.

The gyroscope sensed the vertical component of the earth rate due to the particular location of the test station (ie, latitude angle at M.I.T.), about its IA which causes the float to rotate about OA due to precession. This results in a voltage from the signal generator, which is fed into the servo loop as shown in Fig. II-3-1, which drives a DC motor that rotates the turntable in a direction to cancel the effects of the earth's rotation.

In the ideal case, the turntable rotates cw which is exactly opposite and equal to earth rate (local latitude) and the gyroscope remains fixed with respect to inertial space.

In the real-world case the turntable rotates not only due to the earth's input but also due to gyroscope drift uncertainties.



It is then defined:

$$\omega_T = \text{Turntable rate}$$

$$\omega_{IEV} = \text{Vertical component of earth rate}$$

The Table rate is defined by:

$$(7) \quad \omega_T = \pm \omega_{IEV} \pm \text{Drift}$$

where:

Drift was defined by equation(6)

Since for this particular instrument the turntable rotates ccw, the first approximation that can be made is:

$$(3) \quad \text{Drift} > \omega_{IEV}$$

and:

$\Sigma$  Drift terms cause ccw table rotation (Table top reference)

Therefore equation (7) would result with the following sign designation for lumped drift.

$$(9) \quad \omega_T = +\omega_{IEV} - \Sigma \text{ Drift uncertainties (deg/h)}$$

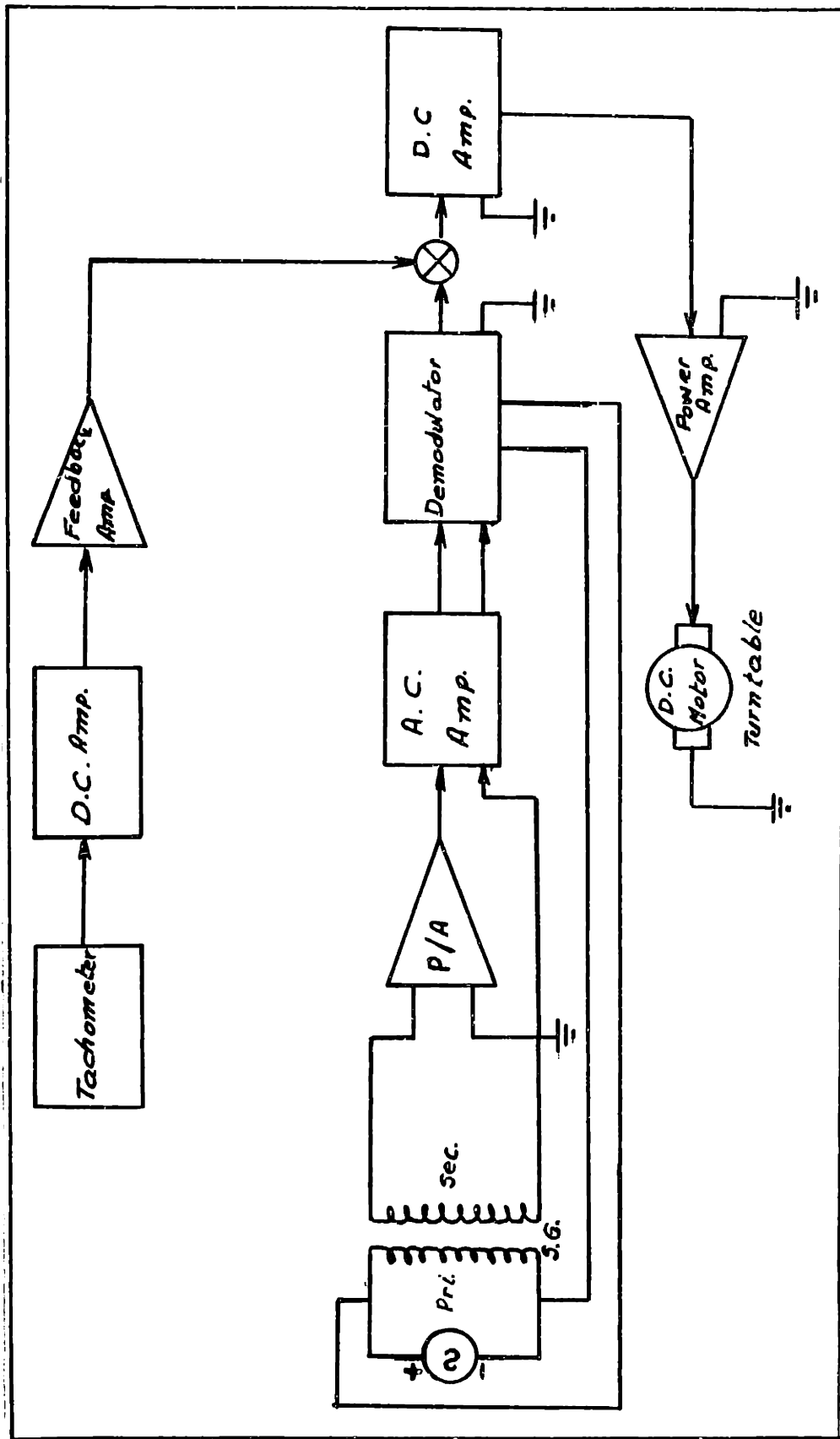


Fig. II-3-1 Mini RIG-30 Servo Loop Block Diagram

II-3-2 Tumbling Tests

The tumbling tests determine the magnitude and direction of torques caused by gravity acting on mass unbalances within the gyroscope (ie,ADIA and ADSRA).The tests also isolate the gravity insensitive term and acceleration sensitive term along OA.These torques are functions of the angle that the unbalance make with the gravity vector (g).

During the test the table is rotated through 360 degrees with IA both vertical and horizontal so that effect of g on the unbalance in various gyroscope orientations can be observed.

II-3-3 Derivation of Drift Coefficients

IA Vertical Down

a) General

Define:

$\omega_{IA}$  = rate about IA

$+\omega_{IA}$  causes  $+M_{OA}$

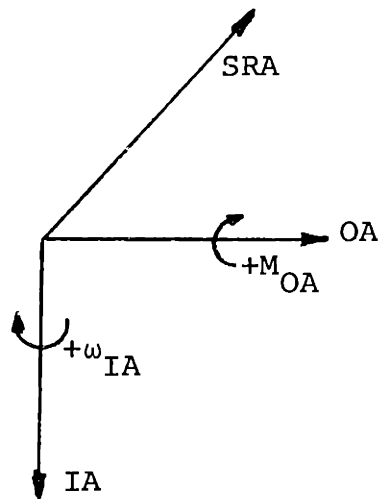


Fig.II-3-2 shows the gyroscope orientation.

Gravity in the OA-IA plane is constant. This orientation is such that no torque about OA due to IA mass unbalance is produced, only mass unbalance along SRA appears in the drift rate equation.

b) Equation Derivation

From definition I-4-2 a mass unbalance along positive SRA produces a negative torque about OA.

The latitude angle at M.I.T. is approximately +42 deg and the earth rotates ccw about its polar axis resulting in a vertical component of earth rate ( $\omega_{IEV}$ ) of positive sense.

From equations (7) and (8) and definitions I-4-1 and I-4-2 the sense of BD is plus and the sense of ADIA is minus (IA vertical down).

This results in:

$$(10) \quad \omega_T = +\omega_{IEV} + BD - ADIA$$

and:

$$(11) \quad \text{Drift} = \omega_{ER} - \omega_T$$

where:

$$\omega_{ER} = \text{appropriate component of the}$$

then: earth rate

$$(12) \quad \text{Drift} = \omega_{IEV} - \omega_T$$

Thus:

$\text{Drift} = -BD + ADIA$
-----------------------------

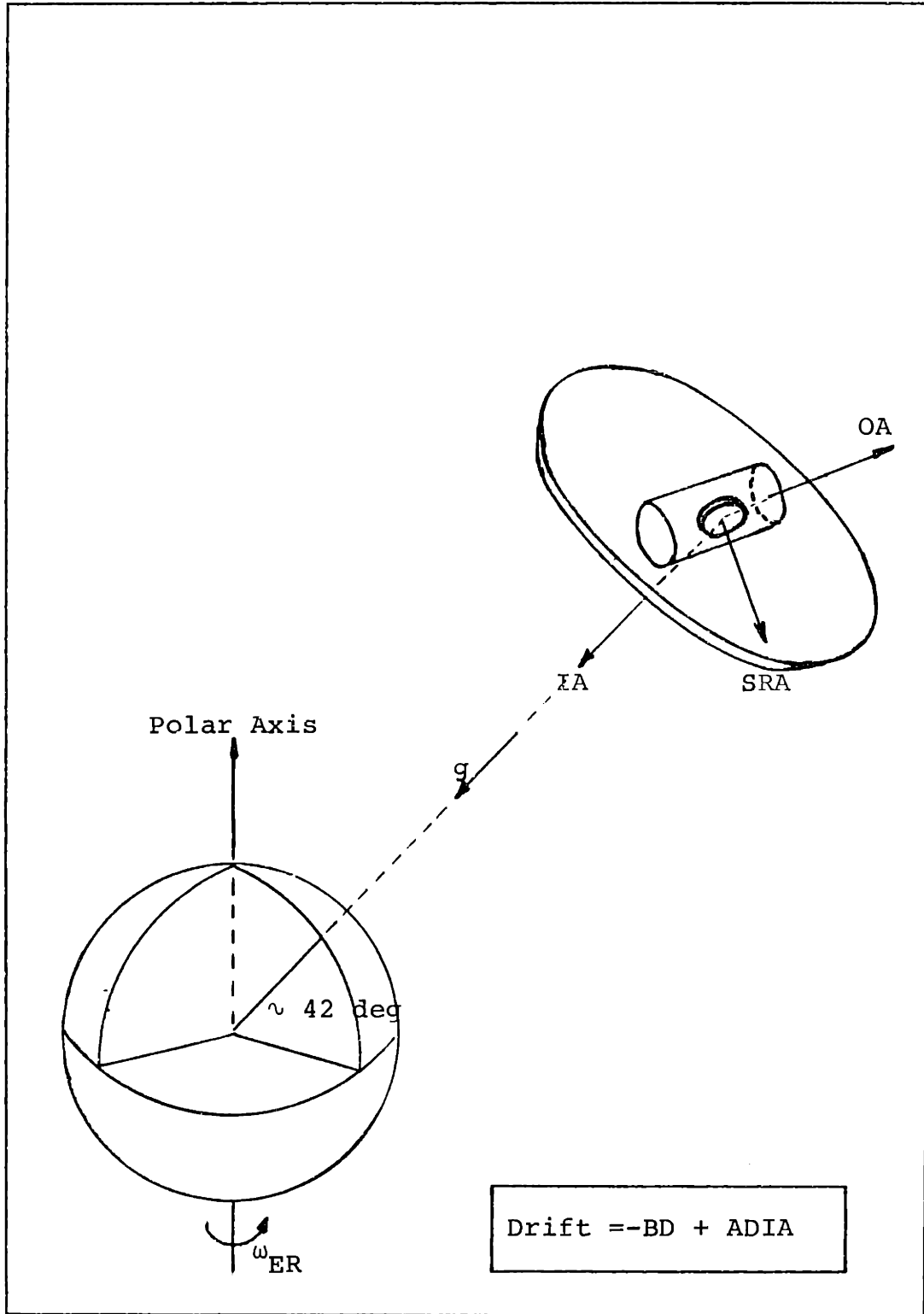


Fig.II-3-2 Gyroscope Orientation IA Vertical Down

a) General

In this position the gravity vector acting perpendicular to the OA-IA plane and on the mass unbalance along IA produces a drift rate which is a function of the table position angle,  $\phi$  or SRA orientation.

b) Equation Derivation

A mass unbalance along the positive IA produces negative torque about OA (See I-4-3) also,  $g$  along -OA causes  $+M_{OA}$ .

The complete drift equation is:

$$\omega_{IEH} - \omega_T = \text{Drift}$$

where:

$\omega_{IEH}$  = Horizontal component of earth rate

Considering the cardinal orientation positions for the gyroscope axes, it is possible to formulate the drift by four different simultaneously equations at specified table angle positions. Namely,

SRA up  $\phi = 0$  deg

SRA down  $\phi = 180$  deg

OA up  $\phi = 90$  deg

OA down  $\phi = 270$  deg

Figs. II-3-3, II-3-4, II-3-5 and II-3-6 shows the four different gyroscope orientations.

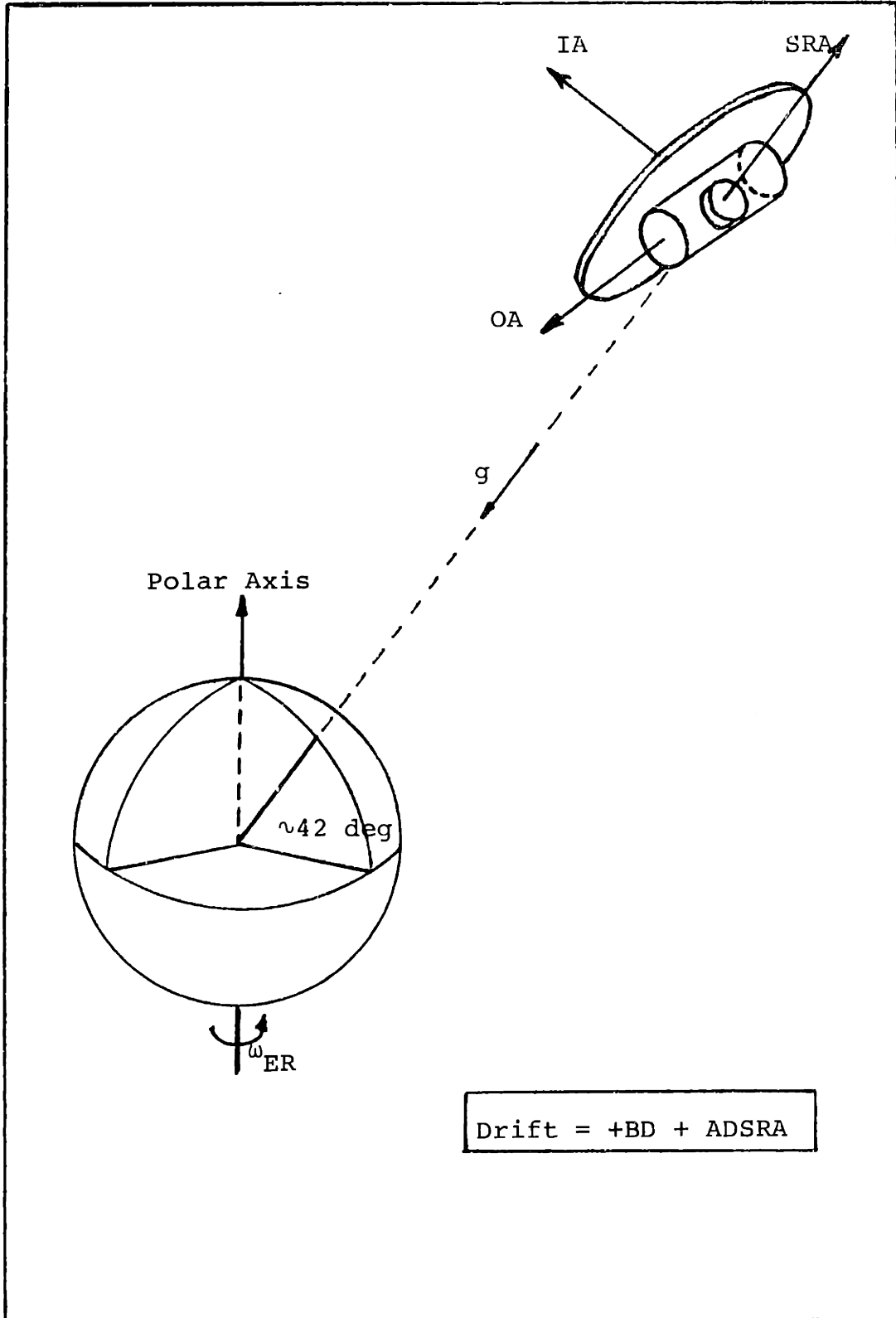


Fig.II-3-3 Gyroscope Orientation IA Horizontal North  
 $\phi = 0 \text{ deg}$

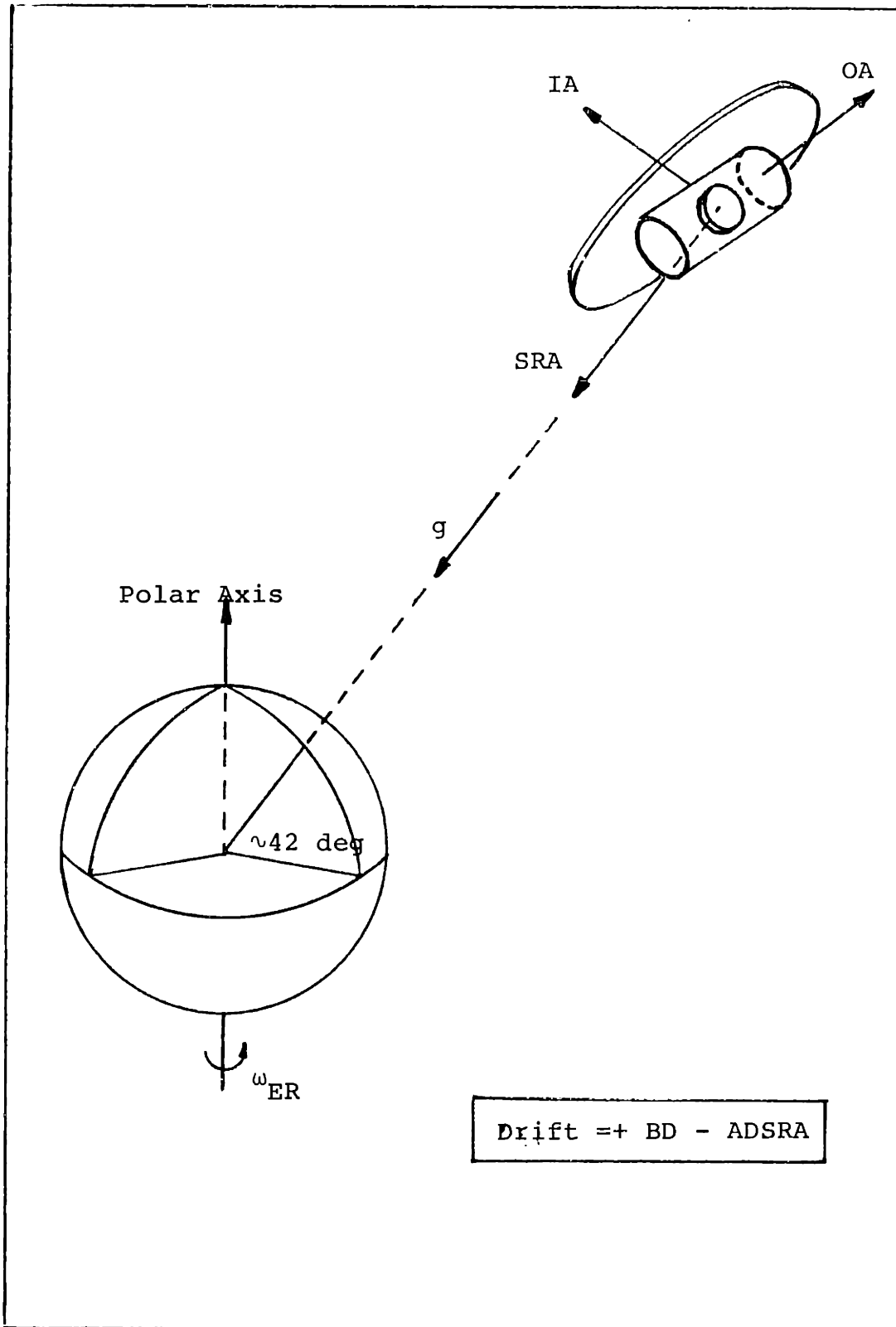


Fig.II-3-4 Gyroscope Orientation IA Horizontal North  
 $\phi=180 \text{ deg}$



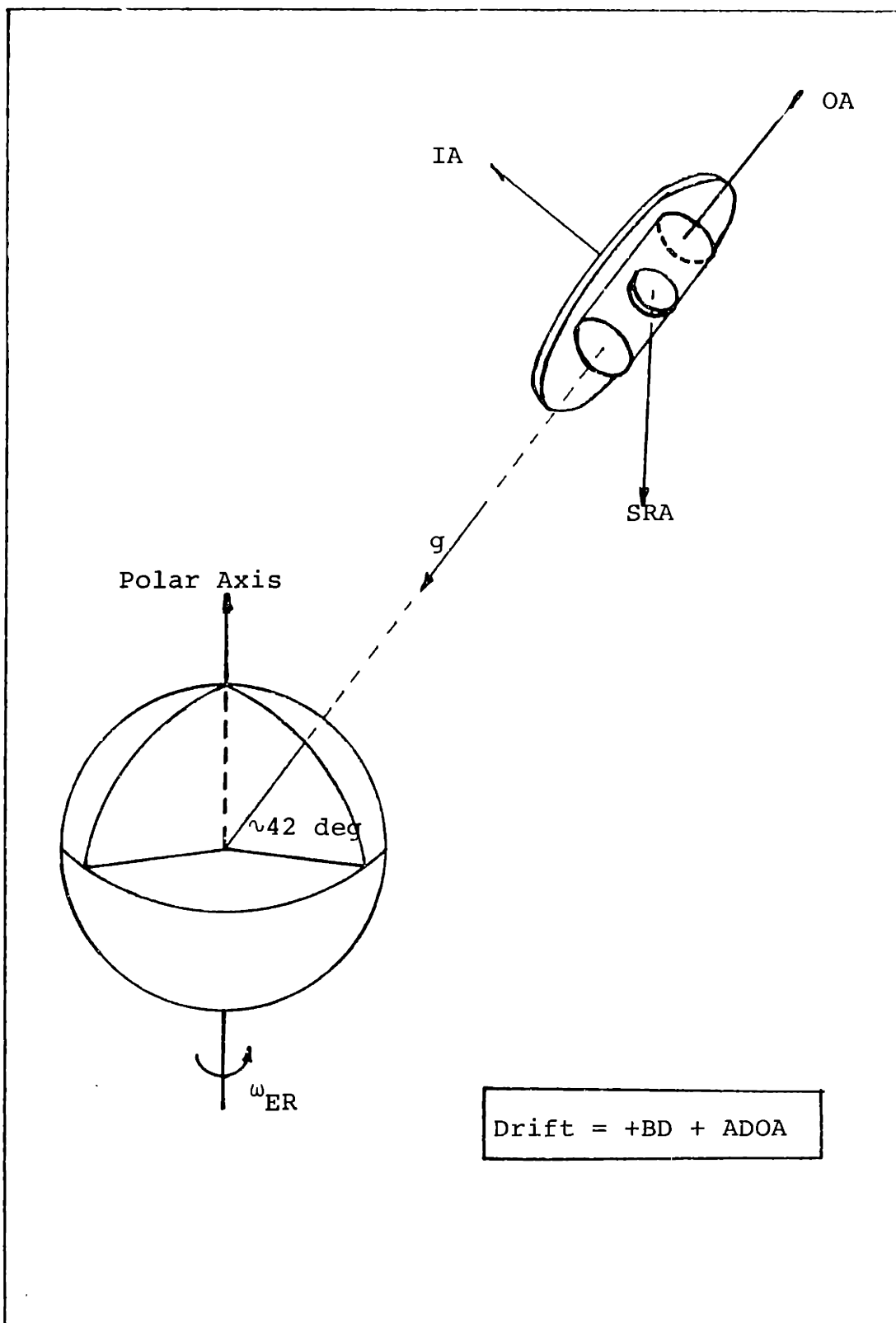


Fig.II-3-5 Gyroscope Orientation IA Horizontal North  
 $\phi = 90 \text{ deg}$

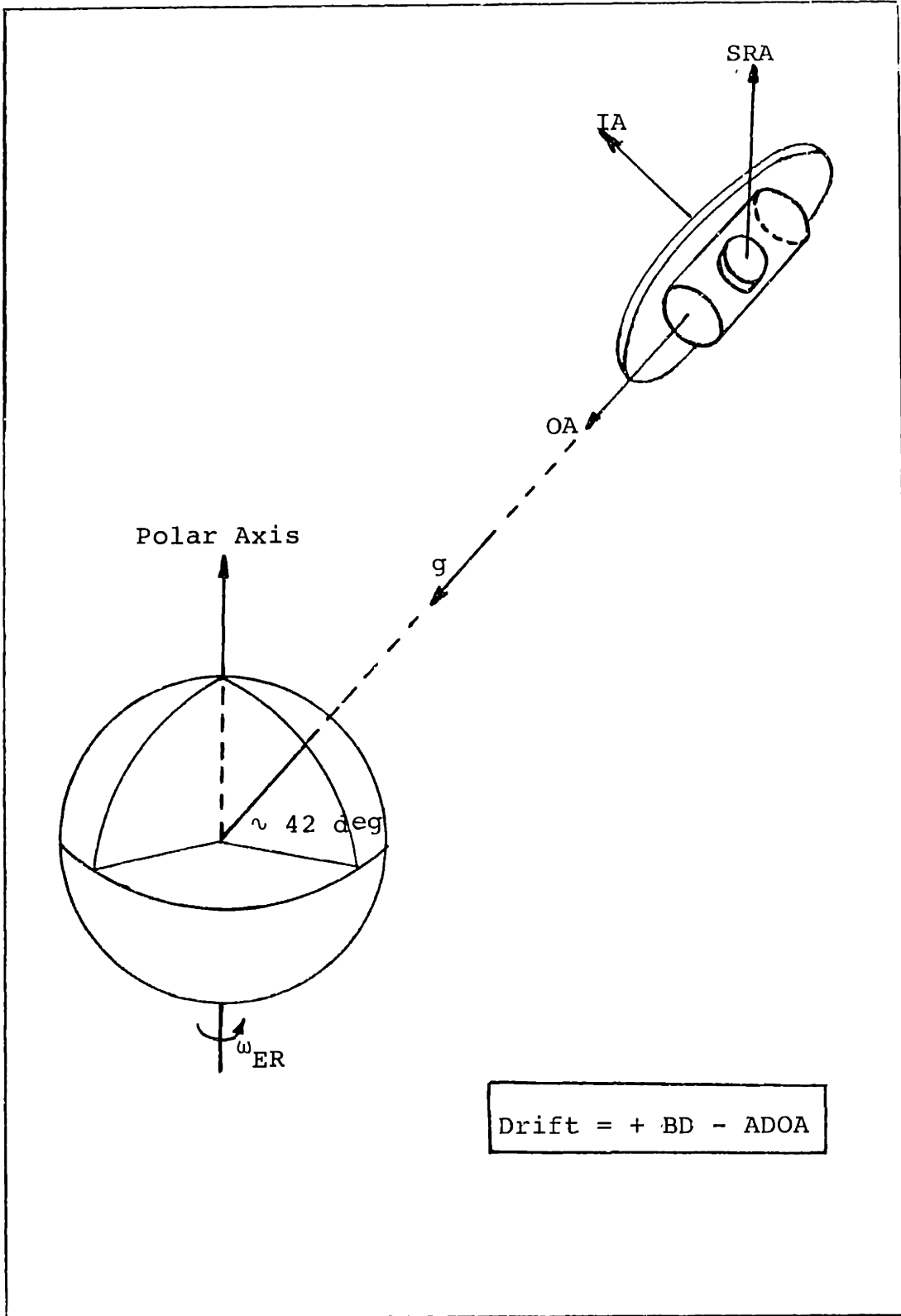


Fig.II-3-6 Gyroscope Orientation IA Horizontal North  
 $\phi = 270 \text{ deg}$

The drift equations are:

For IA Horizontal North

SRA up

$$\text{Drift} = +BD + ADSRA \quad (2)$$

SRA down

$$\text{Drift} = +BD - ADSRA \quad (3)$$

OA up

$$\text{Drift} = +BD + ADOA \quad (4)$$

OA down

$$\text{Drift} = +BD - ADOA \quad (5)$$

Combining with the drift equation for IA vertical  
down:

$$\text{Drift} = -BD + ADIA \quad (1)$$

The individual drift coefficient terms can be  
obtained.

$$ADSRA = \frac{(2) - (3)}{2}$$

Define

$$\text{BD}_{\text{SRA}} = \frac{(2) + (3)}{2} \quad (6)$$

Also

$$\text{ADOA} = \frac{(4) - (5)}{2}$$

Define

$$\text{BD}_{\text{OA}} = \frac{(4) + (5)}{2} \quad (7)$$

From (6) and (7) define

$$\text{BD}_{\text{AVE}} = \frac{(6) + (7)}{2} \quad (8)$$

From (1) and (8)

$$\text{ADIA} = \text{BD}_{\text{AVE}} + \text{Drift \{as calculated in (1)\}}$$

II-3-4 Data Reduction

a) For each position six data samples were taken.

IA vertical down                   (φ from 358° to 2°)

IA horizontal North

SRA up                               (φ from 358° to 2°)

SRA down                           (φ from 177° to 182°)

OA up                               (φ from 88° to 93°)

OA down                           (φ from 267° to 272°)

b) For these positions the readout system generates six (C) numbers.

c) The six numbers are then averaged:

$$C_{AVE} = \sum_{i=1}^6 C_i$$

d) The test station latitude angle is:

42 deg 21 min 39.5 s

$\omega_{IEV}$  = Vertical component of earth rate  
(10.13468 deg/h)

$\omega_{IEH}$  = Horizontal component of earth rate  
(11.11405 deg/h)

e) The drift for each data average, for ccw servo is calculated by:

$$\text{Drift} = \omega_{ER} + \frac{3600 (800)}{C_{AVE}}$$

where:

$\omega_{ER}$  = is the appropriate component of earth rate

f) By simultaneous equations; BD, ADIA, ADSRA and ADOA are calculated.

II-4 Multiple Revolution Tumbling Test

II-4-1 General

For a gyroscope orientation the same as that shown in Fig.II-3-3 the gravity acting perpendicular to the OA-IA plane and on the mass unbalance along IA produces a drift rate which is a function of the table position angle.

The drift rates obtained from multiple revolution testing in this position are evaluated by a Fourier Analysis, the cosine term being ADSRA, and the sine term being ADOA.

It is also possible to evaluate compliance terms through this analysis.

II-4-2 Fourier Analysis

For tumbling tests of one degree table angle increments of data:

Define:

F(φ) = unbalance as a function of table angle φ

F(φ) = A<sub>0</sub> + A<sub>1</sub> cos φ + B<sub>1</sub> sin φ + A<sub>2</sub> cos 2φ + B<sub>2</sub> sin 2φ + R

where:

$$A_0 = \frac{1}{2\pi} \int_0^{2\pi} F(\phi) d\phi = \frac{1}{360} \sum_0^{359} F(\phi)$$

$$A = \frac{1}{\pi} \int_0^{2\pi} F(\phi) \cos\phi d\phi = \frac{1}{180} \sum_0^{359} \{F(\phi) \cos\phi\}$$

$$B_1 = \frac{1}{\pi} \int_0^{2\pi} F(\phi) \sin \phi \, d\phi = \frac{1}{180} \sum_0^{359} \{F(\phi) \sin \phi\}$$

$$A_2 = \frac{1}{\pi} \int_0^{2\pi} F(\phi) \cos 2\phi \, d\phi = \frac{1}{180} \sum \{F(\phi) \cos 2\phi\}$$

$$B_2 = \frac{1}{\pi} \int_0^{2\pi} F(\phi) \sin 2\phi \, d\phi = \frac{1}{180} \sum_0^{359} \{F(\phi) \sin 2\phi\}$$

R=residuals (remainder)

- 1- Denhard,W.G."Inertial Component Testing,Philosophy and Methods" Technivision
- 2- Keysor,J."Introduction to Applied Gyro Theory" A.C. Electronics Division of G.M.C. 1967
- 3- Kerrigan,P.R."Gyro Test Equations" FBM Inertial Components,Instrumentation Lab. 1966
- 4- Sinkiewiz,J.S. Lory,C.B. and Feldman,J."Dynamic Testing of a Single-Degree-of-Freedom Strapdown Gyroscope",C.S.Draper Lab. E-2618,1971
- 5- Sinkiewicz,J.S. Lory,C.B. and Feldman,J."Evaluation of Selected Strapdown Inertial Instruments and Pulse Torque Loops ",C.S.Draper Lab.R\_826,1974
- 6- Slater,J.M."Inertial Guidance Sensors" ,Reinhold Publishing Corporation,N.Y. 1964
- 7- Roberson,R.E.and Farrior,J.S. "Guidance and Control" Progress in Astronautics and Rocketry Vol-8
- 8- Taylor,E.D.and Way,R.L."Gyroscope Fundamentals" A.C.Spark Plug,The Electronics Division of G.M.C. 1962
- 9- Wrigley,W. Hollister,W.M. and Denhard,W.G."Gyroscopic Theory,Design and Instrumentation",M.I.T. Press 1966